Collapse and Resumption of the Thermohaline Circulation during Deglaciation: Insights by Models of Different Complexity

Dissertation
zur Erlangung des Doktorgrades
der Naturwissenschaften im Fachbereich
Geowissenschaften der Universität Hamburg

vorgelegt von

Gregor Knorr

aus

Kühlungsborn

Hamburg

2005

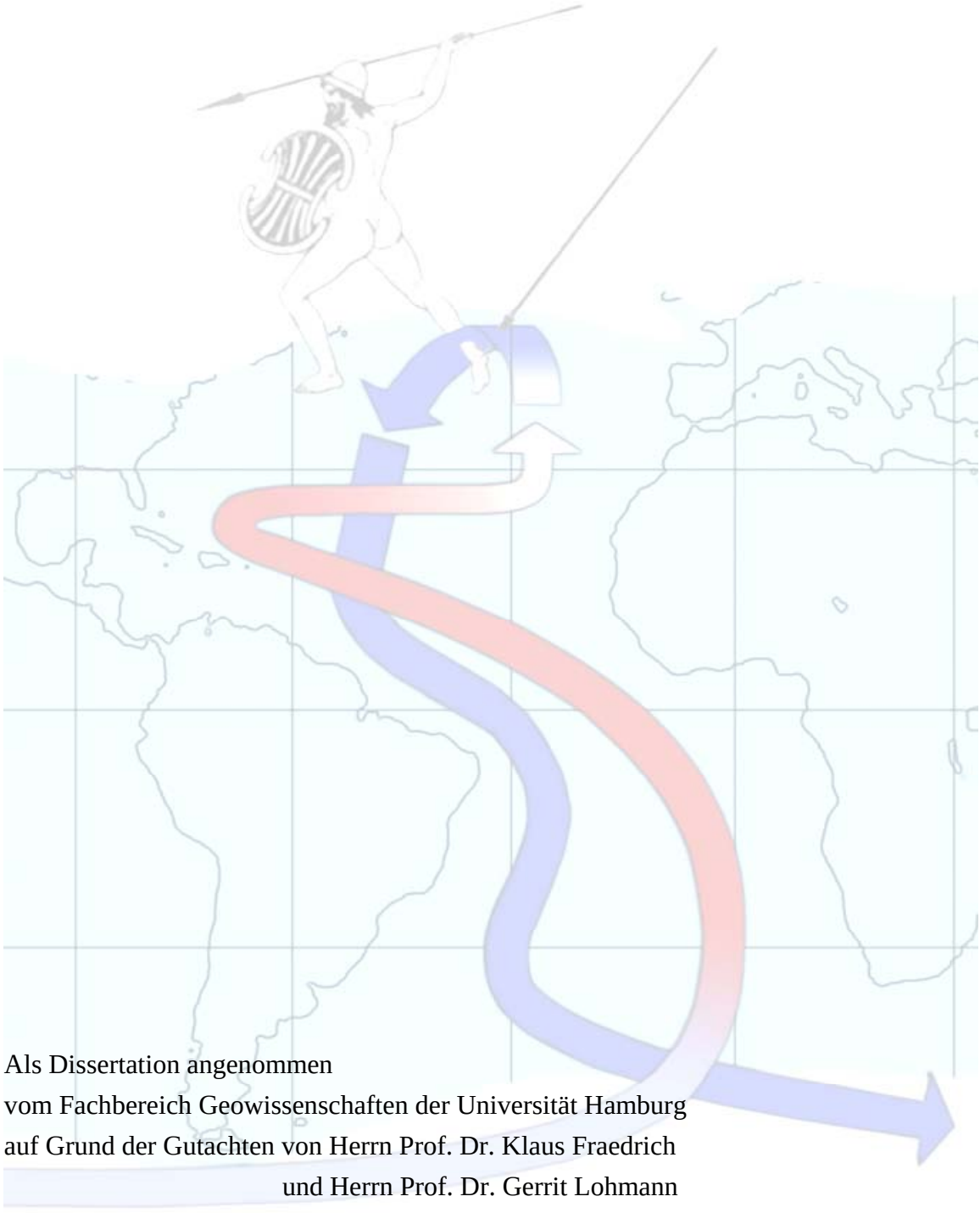

Als Dissertation angenommen
vom Fachbereich Geowissenschaften der Universität Hamburg
auf Grund der Gutachten von Herrn Prof. Dr. Klaus Fraedrich
und Herrn Prof. Dr. Gerrit Lohmann

Hamburg, den 30.6.2005

Prof. Dr. H. Schleicher
Dekan
des Fachbereichs Geowissenschaften

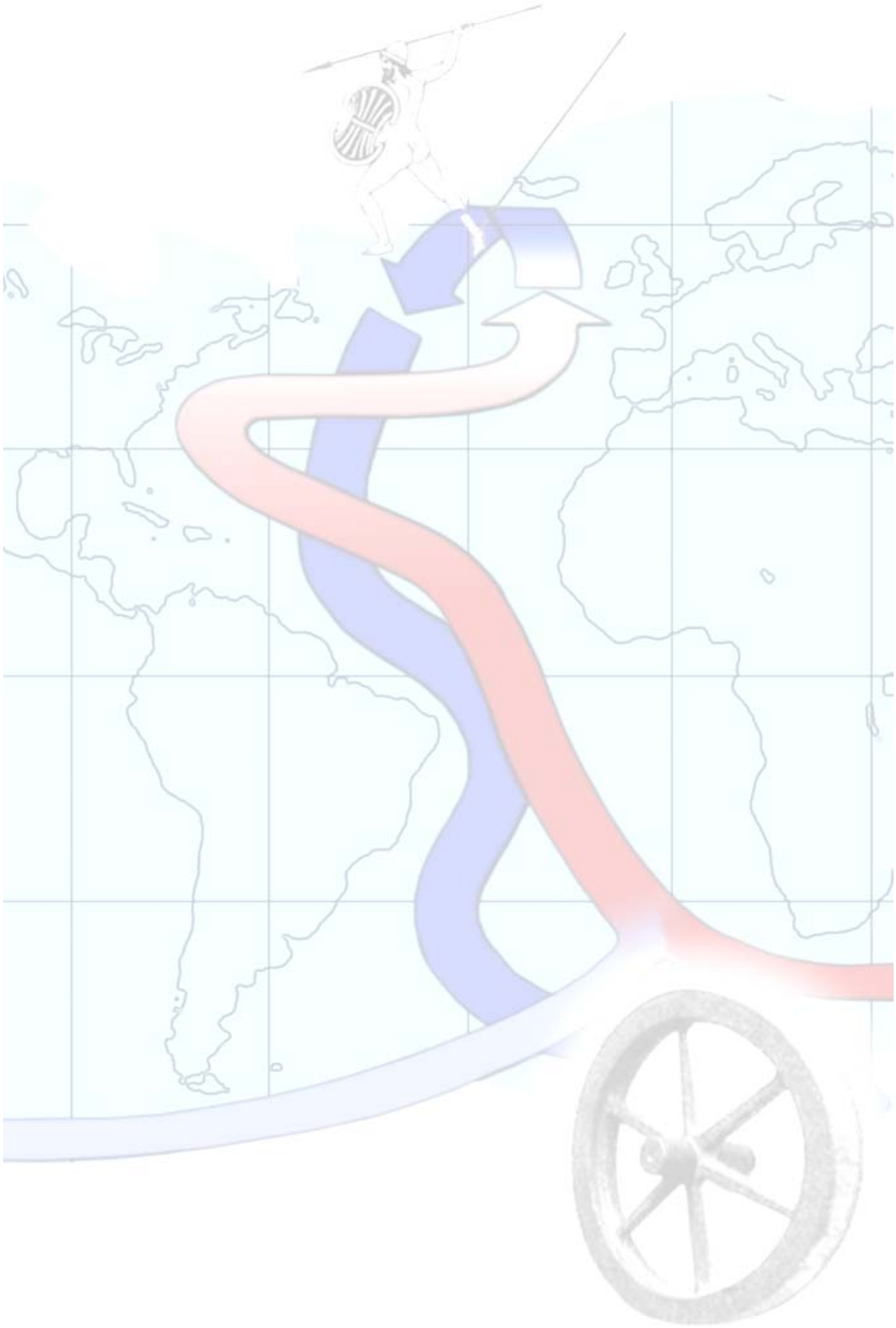

Graphic designed by Lisa Könnecke.

“What has happened can happen again”

Reid A. Bryson
(climate scientist)

Contents

Zusammenfassung

Der Übergang (Deglaziation) vom letzten Glazial (Kaltzeit) zu unserem heutigen Interglazial (Warmzeit) wird zwischen ca. 20000 und 10000 Jahren vor heute datiert, basierend auf Paläodaten von Eisbohrkernen und Ozeansedimentkernen, sowie terrestrischen Klimaarchiven. Diese Daten zeigen, dass während der letzten Deglaziation eine graduelle Erwärmung in der Südhemisphäre einem abrupten Temperaturanstieg in Grönland um mehr als 1000 Jahre vorauslief. Innerhalb der deglazialen Phase kam es außerdem zu abrupten Klimaschwankungen, welche darauf hindeuten, dass massive Änderungen in der thermohalinen Zirkulation (THC) und begleitende Variationen im nordwärts gerichteten Wärmetransport innerhalb des Atlantiks eine Rolle gespielt haben könnten. Bis jetzt war zur Erklärung dieser Phänomene der Blick hauptsächlich auf die nordatlantische Region gerichtet. Dies ist bedingt durch die räumliche Koexistenz von nordatlantischen Tiefenwasserbildungsgebieten, einem empfindlichen Teil der THC, und verschiedenen Quellen von Schmelzwasser, dessen Zustrom in den Nordatlantik die Zirkulation während der Deglaziation abgeschwächt haben könnte.

Mit Hilfe dreidimensionaler Modelle des Ozeans und der Atmosphäre, und eines konzeptionellen Klimamodells, wurden Änderungen der THC in verschiedenen deglazialen Erwärmungs- und Schmelzwasserszenarien analysiert. Die Untersuchungen zeigen, dass eine allmähliche globale oder südhemisphärische Erwärmung eine plötzliche Wiederherstellung der THC bewirkt, während nordhemisphärische Erwärmung nicht ausreicht, um die THC unter dem Einfluss angemessener Schmelzwasserflüsse anzuschalten, nachdem die Zirkulation zum Erliegen gekommen war. Der abrupte Übergang zu einer interglazialen THC wird ausgelöst durch die großräumige Advektion von oberflächennahen salzreichen Wassermassen aus dem Südatlantik/Indischen Ozean und den Tropen zu den Formationsgebieten von nordatlantischem Tiefenwasser, sowie der Wärmeabgabe aus den tieferen Schichten des Nordatlantiks. Dieser Übergang kann mit dem plötzlichen Beginn des Bølling/Allerød Warmintervalls vor 14700 Jahren in Verbindung gebracht werden. Die interglaziale Ozeanzirkulation ist durch eine starke Unempfindlichkeit gegenüber deglazialen Schmelzwasserpulsen gekennzeichnet, besitzt aber gleichzeitig eine ausgeprägte Bistabilität in der Hysterese Kurve für allmählich zunehmende Frischwasserflüsse in den Nordatlantik. Deshalb besitzt die interglaziale THC das Potential für eine verzögerte und auch lang anhaltende Abschwächung als Reaktion auf den starken Schmelzwasserpuls 1A, der ca. 1000 Jahre vor dem Rückfall zu glazialen Klimabedingungen in der Nordhemisphäre auftrat. Diese Jüngere Dryas Kaltphase endete mit einer drastischen Erwärmung vor 11700 Jahren. Das Atmosphärenmodell legt dar, dass die Anfachung der THC die großräumigen atmosphärischen Muster global beeinflusst, mit einer Erwärmung in großen Teilen der Nordhemisphäre und einer Verstärkung des subtropischen Hochs im Nordatlantik. Im Südatlantik entwickeln sich entgegengesetzte Trends. Die umgekehrten Temperatur- und Drucksignaturen ergeben sich als atmosphärische Antwort auf eine Abschwächung der THC durch Schmelzwasser.

Diese Ergebnisse wurden durch Untersuchungen mit einem Boxenmodell einer interhemisphärisch dichtegetriebenen THC bekräftigt. Außerdem wird gezeigt, dass das Zusammenwirken der Wärmetransporte in der Atmosphäre und im Ozean eine effektive interhemisphärische Übertragung einer durch südhemisphärische Erwärmung ausgelösten THC Verstärkung ermöglicht. Eine äquivalente Erwärmung in der Nordhemisphäre führt zu einer wesentlich schwächeren Übertragung in die Südhemisphäre, da eine Abschwächung der THC und großräumiger Auftrieb im globalen Ozean die ozeanische Übertragung abschwächen.

Ein Vergleich der verschiedenen Deglaziationsszenarien mit Klimadaten zeigt, dass eine vorauslaufende deglaziale Erwärmung in der Südhemisphäre, relativ zum Temperaturanstieg in Grönland, durch eine globale Erwärmung und einen überlagerten ozeanischen „Seesaw-Effekt“ durch Schmelzwasserflüsse in den Nordatlantik erklärt werden kann. Die deglaziale Temperaturentwicklung und die Abfolge klimatischer Ereignisse in Paläodaten kann daher durch das Zusammenspiel von Prozessen in beiden Hemisphären, die durch die THC verbunden sind, verstanden werden.

Abstract

The transition between the last glacial (cold) and our modern interglacial (warm) period occurred between about 20,000 and 10,000 years before present, as indicated by proxy data from ice core, ocean sediment and terrestrial records. These data display that deglacial warming over Antarctica preceded a rapid warming in Greenland by more than 1000 years. Furthermore, a series of abrupt climate shifts suggest that massive reorganizations in the thermohaline circulation (THC) and accompanying variations in northward heat transport within the Atlantic have been involved in deglacial climate change. As yet, studies of these phenomena have focused mostly on the North Atlantic region to explain the succession of abrupt climate events. This is because North Atlantic deepwater formation sites, a sensitive key player of the THC, and various sources of freshwater coexist in this realm that perturb the circulation during deglaciation.

Using three-dimensional global models of the ocean and the atmosphere, as well as a conceptual model, THC changes have been analysed that arise in response to different deglacial warming and meltwater scenarios. The results show that gradual global and Southern Hemisphere warming during deglaciation leads to an abrupt resumption of a stalled THC, while Northern Hemisphere warming is not sufficient to trigger an augmentation in presence of reasonable meltwater fluxes to the North Atlantic. The rapid transition to an interglacial THC is linked to large-scale salinity advection of near surface waters from the South Atlantic/Indian Ocean and the tropics to the formation areas of North Atlantic deep water, as well as heat release from the sub-surface North Atlantic. This THC transition can be related to the onset of the Bølling/Allerød warm interval 14,700 years ago. The interglacial circulation mode is characterized by a strong insensitivity to deglacial meltwater pulses, but possesses a distinct bistability in the hysteresis curve for cumulative positive freshwater fluxes to the North Atlantic. Therefore, the restarted THC bears the potential for a delayed long term weakening in response to the large meltwater pulse 1A, which occurred about 1,000 years before climate conditions in the Northern Hemisphere dropped back to glacial conditions during Younger Dryas that ended rapidly 11,700 years ago. The atmosphere model indicates that the resumption of the Atlantic THC influences the large-scale atmospheric pattern globally, with warming in large parts of the Northern Hemisphere and an augmentation of the subtropical high in the North Atlantic. The opposite trends evolve in the South Atlantic. The temperature and pressure signatures in the hemispheres are vice versa in response to a meltwater-induced reduction of the THC. These results are affirmed by low-order model results of an interhemispheric density driven THC. Moreover, it is shown that the coactions of atmosphere and ocean heat transports enable an effective interhemispheric mediation of a Southern Hemisphere warming induced THC amplification. The equivalent warming in the Northern Hemisphere leads to a less effective transmission to the Southern Hemisphere, since a weakening of the THC and broad scale upwelling in the global ocean reduces the contribution of the oceanic mediation.

A comparison of the different deglaciation scenarios with proxy data shows that a lead of increasing Southern Hemisphere temperatures, relatively to the abrupt temperature rise in Greenland, can be reconciled with a gradual global warming trend and a superimposed oceanic “seesaw” response to North Atlantic meltwater pulses. Therefore, the temperature evolution and the succession of climate intervals, as recorded in proxy data can be understood as the interplay of processes in both hemispheres, connected by the THC.

Chapter 1

Introduction

1.1 Motivation and Objectives

The global ocean covers about 71 % of the earth's surface and is a major constituent of the climate system. It influences the system by multiple interactions. As a result of its heat capacity and circulation, the ocean stores and redistributes heat before it is released to the atmosphere, which is in the present state of operation responsible for the relatively mild climate conditions over Europe. As part of the global ocean circulation the buoyancy driven thermohaline circulation (THC) transports heat and salt from the tropics to the northern North Atlantic, where North Atlantic deep-water (NADW) is formed by cooling and sinking (Figure 1.1). There are only two further main locations where deep-water formation occurs, namely in the Ross Sea and the Weddell Sea. Near-surface waters flow towards the deep-water formation regions and recirculate at depth. The system of redistribution of global water masses is commonly known by the "conveyor belt" metaphor [Broecker, 1991] (Figure 1.1), representing an idealised sketch of the global ocean circulation.

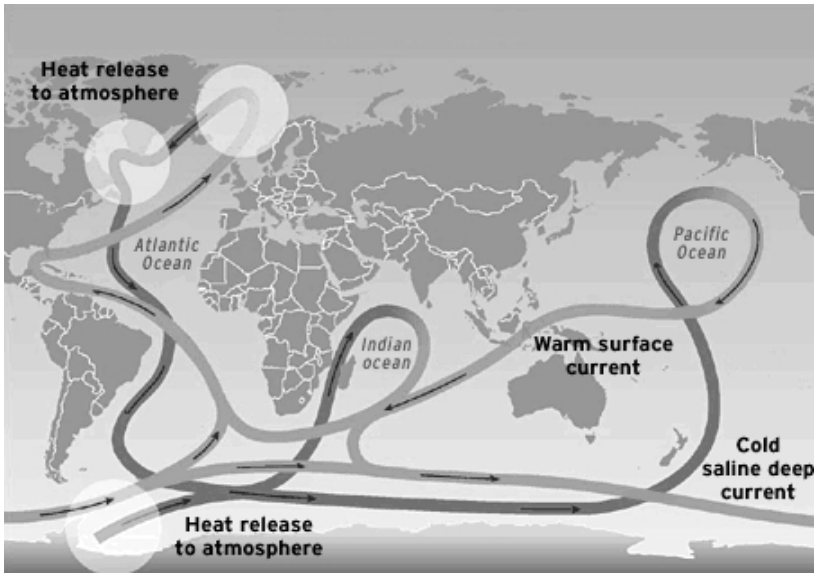

Figure 1.1: Schematic picture of the global ocean circulation as "conveyor belt" [modified version from Broecker, 1991].

The THC and ultimately deep-water formation in the North Atlantic seems to be a sensitive part of the global ocean circulation. During the last decade a possible reduction of the THC has been demonstrated in several atmosphere-ocean model simulations [Manabe and Stouffer, 1993; Stocker and Schmittner, 1997; IPCC, 2001], caused by warming and freshening of high latitude surface water, associated with global warming. Both effects the high latitude warming and enhanced poleward transport of moisture in the atmosphere cause a reduction of the density in the formation regions of NADW [IPCC, 2001]. A less likely, but not impossible, scenario is a complete shut down of the THC after passing a critical threshold, which would have a dramatic effect on the climate of areas surrounding the North Atlantic [IPCC, 2001]. A shut down of the THC might be an irreversible process because of its multiple equilibria, which have been reported by ocean and climate models of different complexity [Stommel, 1961; Bryan, 1986; Marotzke and Willebrand, 1991; Stocker and Wright, 1991].

It is difficult to assess the likelihood of future changes in the THC, due to uncertainties in the response of the climate system to greenhouse warming. In this context the analyses of abrupt changes in the past offers the possibility to form quantitative hypotheses, about the causes, mechanisms and feedbacks of climate changes. In particular the geological epoch of the Quaternary, spanning the last 2 Mio. years is prominent in this respect, since it is characterized by cyclic changes between long glacial (cold) and interglacial (warm) periods. The last ice age (Figure 1.2) came to an end between 20 ka BP (thousand years before present) and 10 ka BP (Figure 1.3).

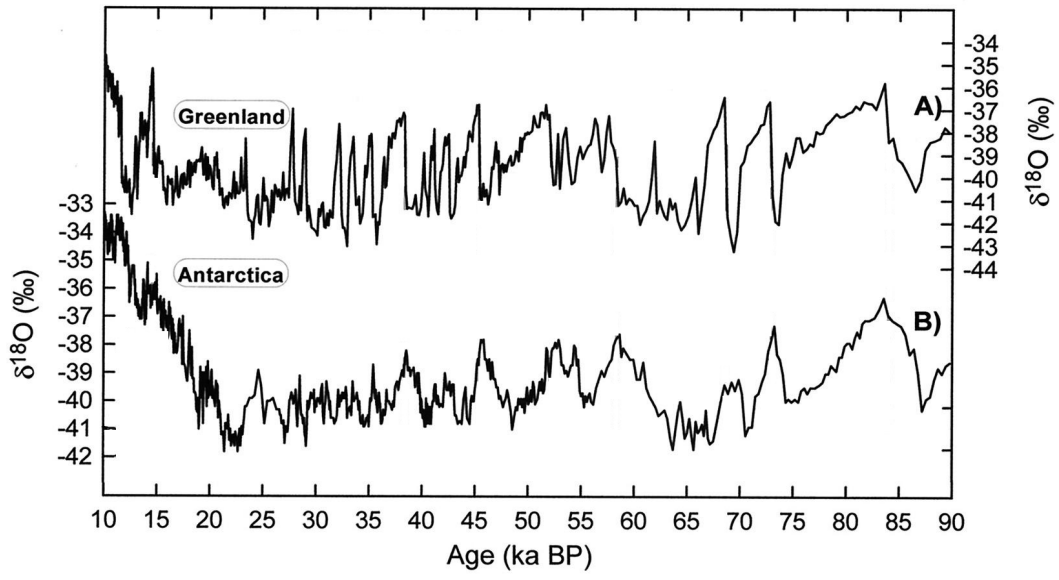

Figure 1.2: Isotopic data from Greenland and Antarctica on the GISP2 time scale. Higher values of $\delta^{18}O_{ice}$ indicate a warmer climate. (a) $\delta^{18}O_{ice}$ from GISP2, Greenland. (b) $\delta^{18}O_{ice}$ from Byrd station, West Antarctica [taken from Blunier and Brook, 2001].

Superposed on a general warming trend, this time span has been punctuated by a series of abrupt climate sequences, which are documented in high resolution paleodata, for example based on ice cores [Dansgaard et al., 1993; Sowers and Bender, 1995; Blunier and Brook, 2001] (Figure 1.2) and marine sediment records [Koc et al., 1993; Sarnthein et al., 1994; Bard et al., 2000; Sachs et al., 2001; Bianchi and Gersonde, 2004]. Analyses of these records also reveal that during the last deglaciation a gradual warming trend in Antarctica preceded a rapid warming in Greenland by more than 1000 years (Figure 1.3) [Sowers and Bender, 1995; Petit et al., 1999]. This transition from the cold Heinrich-I (H1) phase, which is characterised by enhanced abundances of ice-rafted debris and melt water inflow to the North Atlantic [Heinrich, 1988; Bond et al., 1992], to the warm Bølling/Allerød (B/A) interval at 14.7 ka BP (Figure 1.3) is accompanied by an abrupt warming of about 10 ºC as derived from trapped air in polar ice cores [Severinghaus and Brook, 1999]. The largest deglacial discharge of meltwater to the ocean, referred to as MWP-1A [Fairbanks, 1989], escorted the phase to warmer conditions in the North Atlantic. Paradoxically, NADW formation was not stopped immediately and the next significant cooling occurred more than 1000 years later at the onset of the Younger Dryas (YD) [Clark et al., 2002]. At the end of the YD at about 11.5 ka BP the North Atlantic realm again experiences a rapid warming of about 15 °C within a few decades [Severinghaus et al., 1998].

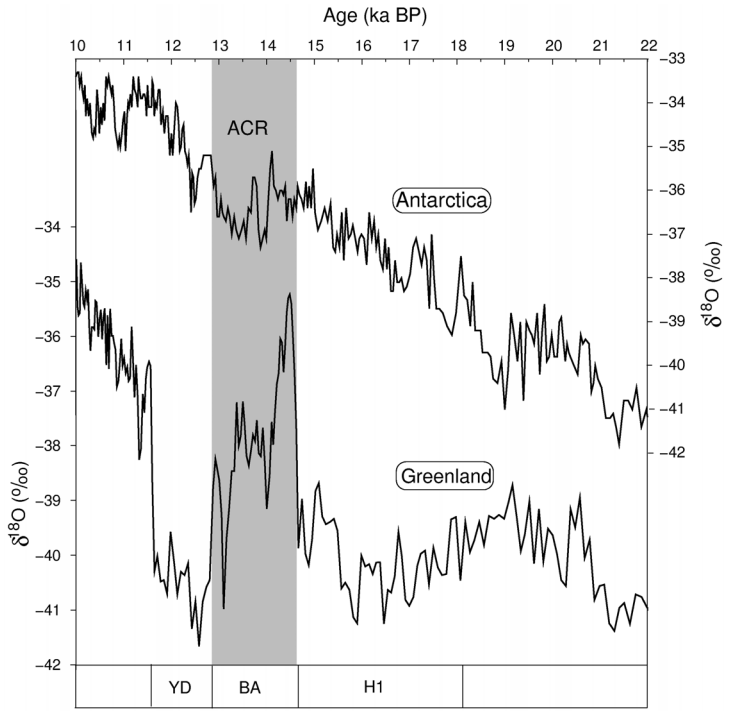

Figure 1.3: Time frame of the last deglaciation based on the same data as the previous figure [data from Blunier and Brook, 2001]. The boundaries of climate intervals are defined as in the GISP2 record: H1, Heinrich 1; B/A, Bølling/Allerød; YD, Younger Dryas. It appears that the warming over Antarctica is interrupted during the Antarctic cold reversal (ACR) at the time of sudden warming over Greenland during the B/A warm period. Subsequently, climate conditions in the north dropped back to glacial conditions during the YD. The end of the YD marks the transition to warm conditions prevailing during the Holocene.

Changes of the oceanic heat transport were suggested as triggers for the ice ages [Flohn, 1974]. This idea has been reviewed and abrupt climate shifts have been attributed to major reorganisations of the THC at a certain threshold [Broecker et al., 1985; Ghil et al., 1987]. Paleoceanographic time-slice reconstructions suggest that the largest changes in North Atlantic climate were associated with transitions among three modes [Sarnthein et al., 1994; Alley and Clark, 1999]: a modern or interstadial warm mode, a glacial or stadial cold mode, and a Heinrich mode commonly known as THC "off"-mode (Figure 1.4). In the modern mode deep-water is formed in the Nordic Seas. Subsequently it flows over the Greenland Scotland ridge [Dickson and Brown, 1994] and recirculates in the Labrador Sea before progressing southward. The glacial mode is characterized by open ocean convection in the subpolar North Atlantic. During the Heinrich mode NADW formation ceased and water of Antarctic origin filled the Atlantic basin to depths as shallow as 1,000 m [Sarnthein et al., 1994].

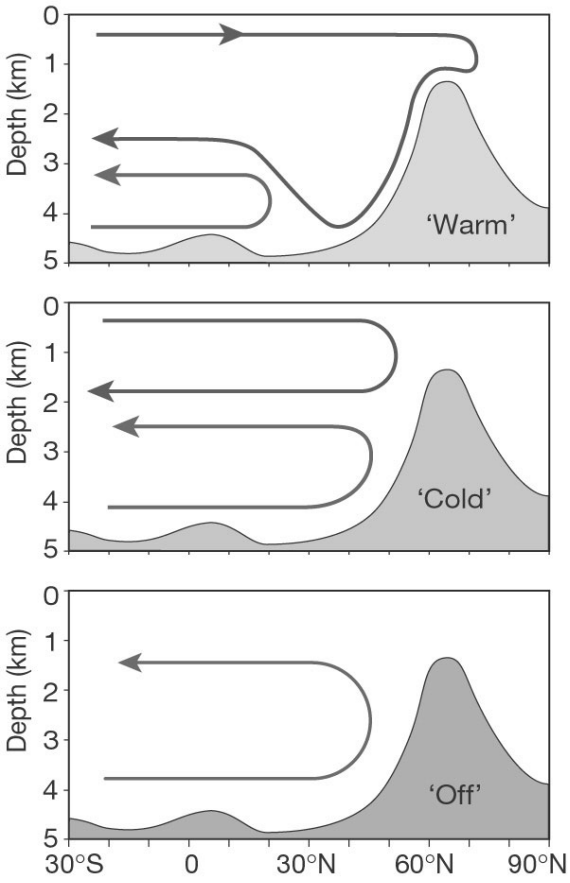

Figure 1.4: Schematic of the three modes of ocean circulation that prevailed during different times of the last glacial period. Shown is a section along the Atlantic; the rise in bottom topography symbolizes the shallow sill between Greenland and Scotland. North Atlantic overturning is shown by the clockwise circulation, Antarctic bottom water by the counter-clockwise circulation [taken from Rahmstorf, 2002].

Switches between the modes are associated with changes in the heat budget of the Atlantic Ocean. A large reduction in THC as during the Heinrich mode causes additional cooling in the North Atlantic [Severinghaus and Brook, 1999], whereas contemporary warming in some locations in the Southern Hemisphere is observed (Figure 1.2) [Hemming et al., 2000; Mix et al., 2001]. This indicates that the reduction of NADW formation decreased meridional heat transport from the South to the North Atlantic realm, leading to the "bipolar seesaw" effect [Crowley, 1992] [Broecker, 1998; Stocker, 1998]. The recovery of the glacial THC after Heinrich events [Sarnthein et al., 1994] raises the question about the transient character of the THC "off-mode" under different climate conditions.

Analogue to the different THC states recorded in paleodata, several ocean and coupled atmosphere-ocean models have found the existence of three distinct modes of the THC in a glacial climate [Ganopolski and Rahmstorf, 2001; Schmittner et al., 2002], which are qualitatively the same as the different states identified by paleodata. These and other model studies have shown that transitions between the distinct modes during the last ice age can be triggered by changes in the freshwater balance of the North Atlantic.

Proxy data time-slice compilations [Sarnthein et al., 1994; Alley and Clark, 1999] also provide evidences that the last deglaciation was characterised by a transition from a weak glacial to a strong interglacial THC, albeit the North Atlantic was exposed to melt water from the continental ice sheets over North America and Scandinavia [Licciardi et al., 1999; Marshall and Clarke, 1999]. This meltwater discharge poses a constant threat to the "Achilles Heel" of the oceanic conveyer belt circulation [Broecker, 1991], which is located in the North Atlantic. Nevertheless, model studies of the modern and the glacial climate also suggest that the glacial THC was weaker than the modern THC [Ganopolski and Rahmstorf, 2001; Prange et al., 2002; Shin et al., 2003].

Based on evidences of a weak glacial conveyor belt it is natural to ask about the "Flywheel" of the ocean circulation, which might have initiated the transition to a strong interglacial ocean circulation during deglaciation, in presence of meltwater discharge to the North Atlantic. This "Flywheel" is not necessarily confined to the North Atlantic realm, where the "Achilles Heel" is located. In this context the Southern Ocean, which is a dynamically active region, comes into focus since it allows the communication between the different ocean basins and influences the salt balance of the Atlantic [de Ruijter et al., 1999]. Furthermore, it represents a barrier to the southern polar-regions (Figure 1.1, Figure 1.5). The most prominent feature in the Southern Ocean is the Antarctic circumpolar current (ACC), representing the strongest circulation system in the global ocean. The communication between the Southern Ocean and the Atlantic occurs mostly in two very energetic frontal regions, namely the Brazil/Malvinas Confluence and the Agulhas Current and its retroflection along with the upwelling area of the Benguela Current (Figure 1.5). These exchanges are linked with the cold (Pacific Ocean) and warm (Indian ocean) water routes of the global ocean circulation [Gordon, 1986].

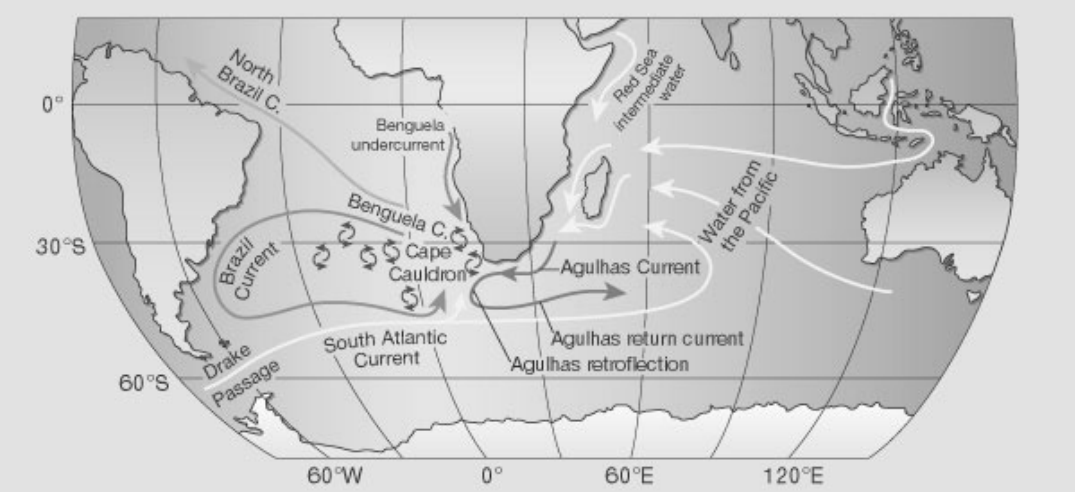

Figure 1.5: The Agulhas system and associated flow patterns. The Agulhas Current draws water from the Pacific Ocean through the Indonesian throughflow and Drake Passage, and from the Tasman Sea. It abruptly turns back towards the Indian Ocean near 20° E. Here, at the Agulhas retroflection, 'leakage' of water occurs within an array of cyclonic (clockwise) and anticyclonic (anticlockwise) eddies that are injected into the vigorous stirring and mixing environment of the Cape Basin (the 'Cape Cauldron'). The South Atlantic Current adds water to the cauldron, as does the subsurface flow of the Benguela undercurrent along the west coast of Africa, and salty Red Sea water along the east coast. A blend of these waters spreads into the Brazil and North Brazil currents. The latter is part of the large-scale 'overturning circulation' induced by the formation of North Atlantic Deep Water [taken from Gordon, 2003].

Oceanographic data [Gordon et al., 1992] and model studies [Weijer et al., 2002] suggest that the thermohaline properties of the upper branch of the overturning circulation in the Atlantic control the buoyancy flux and eventually the NADW formation. Therefore, the relative contributions of cold and warm water routes are important for the THC and its variation may exert a substantial influence on the entire climate system.

While most studies investigate processes responsible for a cessation of the THC, this study is aimed to explore the question of how the global ocean circulation gets restarted after a glacial mode with weak overturning in the Atlantic. Therefore, the effect of different deglacial warming scenarios and meltwater pulses on the THC are examined, using three-dimensional models of the ocean and the atmosphere, as well as a conceptual model of the THC. Moreover, this Ph.D. thesis is aimed to obtain a better quantitative and process-based understanding of transitions in the THC and their global climatic impacts as detected in the geological record during deglaciation. One further aspect is the evaluation of changes in the atmospheric dynamics as response to deglacial shifts in the THC. As a result of the previous considerations four central-questions have been defined that motivated the present work:

(1) What is the reason that gradual deglacial warming over Antarctica preceded a rapid temperature increase in Greenland at the onset of the B/A by more than 1000 years?

(2) What caused the abrupt warming in the north at the onset of the B/A that involved a transition from a weak glacial to a strong interglacial THC in presence of deglacial meltwater discharge to the North Atlantic, characterising the H1 cold sequence?

(3) How is it possible that the largest deglacial meltwater pulse 1A (MWP-1A) occurs more than 1,000 years before the next significant change in the THC associated with the Younger Dryas cold interval?

(4) Where are the centres of activity responsible for the abrupt deglacial changes and shifts in the THC?

1.2 Methods and Design

The overall objective of this thesis is to examine the interactions between deglacial climate change and the THC. One way to investigate the underlying climate dynamics is by numerical modelling, if possible with models of different complexity. Over the past decades a variety of different modelling approaches have been proposed that are capable to reproduce abrupt changes in the THC, ranging from simple low order models [Stommel, 1961; Stocker and Wright, 1991], uncoupled ocean general circulation models (OGCMs) [Bryan, 1986; Marotzke and Willebrand, 1991; Maier-Reimer et al., 1993] to fully coupled atmosphere-ocean general circulation models [e.g. Manabe and Stouffer, 1988].

The present study is mainly based on model simulations, using an improved version of the Large Scale Geostrophic ocean model (LSG) [Maier-Reimer et al., 1993; Lohmann et al., 2003]. This ocean model uses an approach, which allows an adjustment of surface temperatures to changes in the ocean circulation, based on an atmospheric energy balance model with lateral heat diffusion [Prange et al., 2003]. This model approach has the advantage that the hydrological balance is known, since the background climate state is based on atmospheric general circulation model (AGCM) simulations for the modern and the glacial climate, with explicitly resolved hydrological cycle [Lohmann and Lorenz, 2000]. The ocean model is efficient for investigating processes associated with deep-ocean circulation changes and their long adjustment time. It allows to perform multiple experimental setups, due to relatively low computational costs compared to fully coupled atmosphere-ocean circulation models. Nevertheless, the used model approach has some limitations. Because atmosphere dynamics are neglected, changes of ocean circulation patterns and their effect on atmosphere-ocean heat exchange and the freshwater balance through the

hydrological cycle cannot be accounted for. Thus, essential atmosphere-ocean feedbacks are disregarded, which might attenuate or amplify the deglacial processes. To address the respective shortcomings, the Portable University Model of the Atmosphere (PUMA) [Fraedrich et al., 1998; Fraedrich et al., 2003; Fraedrich et al., 2005], which is based on the Reading multi-level spectral Simple Global Circulation Model (SGCM) [Hoskins and Simmons, 1975], is applied to estimate basic atmospheric responses and feedbacks associated with deglacial changes in the THC. To test and deepen the physical understanding evolving from these ocean and atmosphere model simulations, a conceptual model of the Atlantic THC has been designed that allows the consideration of the essential physics of an interhemispheric density driven THC. In order to study the stability and variability of the Atlantic THC under different climate conditions radiation changes are applied that may stem e.g. from different CO_2 concentration in the atmosphere.

The structure of this thesis work reflects the application of the different model types. Chapter 2 is aimed to investigate the effect of deglacial Southern Ocean warming on the THC, and includes stability analyses for different states of the THC with respect to North Atlantic meltwater discharge. In Chapter 3 the influence of deglacial global warming is explored to better understand the evolution of interhemispheric temperature records during deglaciation. Focus is given to a succession of meltwater pulses that influence the THC and their expression in spatial and temporal temperature patterns. The ideas outlined in Chapter 2 and 3 are tested in Chapter 4. Here, a comparison of different warming scenarios is given that is based on the analyses of time dependent model responses in a three-dimensional and a conceptual ocean model. Subsequently, in Chapter 5 focus is given to atmospheric responses, which are related to a meltwater induced reduction of the THC, as well as its abrupt amplification. Conclusions and a comprehensive summary are given in Chapter 6.

1.3 Publications

Chapter 2 to Chapter 6 are based on manuscripts, which are either published, in press, submitted or in preparation for publication. The Chapters 2 to 5 have been written as stand-alone scientific papers. Chapter 6 is partly based on two further publications.

Chapter 2:

Knorr, G., and G. Lohmann (2003), Southern Ocean origin for the resumption of Atlantic thermohaline circulation during deglaciation, *Nature*, 424, 532-536.

Chapter 3:

Knorr, G., and G. Lohmann (2005), Transitions in the Atlantic thermohaline circulation by global deglacial warming and meltwater pulses, *Paleoceanography*, in revision.

Chapter 4:

Knorr, G., G. Lohmann, and M. Prange (2005), Interhemispheric teleconnections of the Atlantic thermohaline circulation: views obtained from conceptual and ocean general circulation models, *Climate Dynamics*, in preparation.

Chapter 5:

Knorr, G., K. Grosfeld, G. Lohmann, F. Lunkeit, and K. Fraedrich (2005), Atmospheric responses to abrupt changes in the thermohaline circulation during deglaciation, *Geochemistry Geophysics Geosystems*, in revision.

Chapter 6:

Knorr, G., and G. Lohmann (2003), Interhemisphärische Telekonnektionen der atlantischen thermohalinen Zirkulation: Evidenzen von Daten und Ozeanmodellen, *Terra Nostra*, 2003/6, 250-254.

Knorr, G., and G. Lohmann (2004), The Southern Ocean as the Flywheel of the Oceanic Conveyor Belt Circulation, *Pages News*, 12, 11-13.

References:

Alley, R. B., and P. U. Clark (1999), The deglaciation of the northern hemisphere: A global perspective, *Annual Review of Earth and Planetary Sciences*, 27, 149-182.

Bard, E., F. Rostek, J. L. Turon, and S. Gendreau (2000), Hydrological impact of Heinrich events in the subtropical northeast Atlantic, *Science*, 289, 1321-1324.

Bianchi, C., and R. Gersonde (2004), Climate evolution at the last deglaciation: the role of the Southern Ocean, *Earth and Planetary Science Letters*, 228, 407-424.

Blunier, T., and E. J. Brook (2001), Timing of millennial-scale climate change in Antarctica and Greenland during the last glacial period, *Science*, 291, 109-112.

Bond, G., H. Heinrich, W. Broecker, L. Labeyrie, J. McManus, J. Andrews, S. Huon, R. Jantschik, S. Clasen, C. Simet, K. Tedesco, M. Klas, G. Bonani, and S. Ivy (1992), Evidence for massive discharges of icebergs into the North Atlantic ocean during the last glacial period, *Nature*, 360, 245-249.

Broecker, W. S., D. M. Peteet, and D. Rind (1985), Does the ocean-atmosphere system have more than one stable mode of operation?, *Nature*, 315, 21-25.

Broecker, W. S. (1991), The great ocean conveyor, *Oceanography*, 4, 79-89.

Broecker, W. S. (1998), Paleocean circulation during the last deglaciation: a bipolar seesaw?, *Paleoceanography.*, 13, 119-121.

Bryan, F. (1986), High-latitude salinity effects and interhemispheric thermohaline circulations, *Nature*, 323, 301-304.

Clark, P. U., N. G. Pisias, T. F. Stocker, and A. J. Weaver (2002), The role of the thermohaline circulation in abrupt climate change, *Nature*, 415, 863-869.

Crowley, T. J. (1992), North Atlantic deep water cools the southern hemisphere, *Paleoceanography*, 7, 489-497.

Dansgaard, W., S. J. Johnsen, H. B. Clausen, D. Dahl-Jensen, N. S. Gundestrup, C. U. Hammer, C. S. Hvidberg, J. P. Steffensen, A. E. Sveinbjörnsdottir, J. Jouzel, and G. Bond (1993), Evidence for general instability of past climate from a 250-kyr ice-core record, *Nature*, 364, 218-220.

de Ruijter, W. P. M., A. Biastoch, S. S. Drijfhout, J. R. E. Lutjeharms, R. P. Matano, T. Pichevin, P. J. van Leeuwen, and W. Weijer (1999), Indian-Atlantic interocean exchange: dynamics, estimation and transport, *Journal of Geophysical Research*, 104, 20885-20910.

Dickson, R., and J. Brown (1994), The production of North Atlantic Deep Water: Sources, rates and pathways, *Journal of Geophysical Research*, 99, 12319-12342.

Fairbanks, R. G. (1989), A 17,000-year glacio-eustatic sea-level record - Influence of glacial melting rates on the Younger Dryas event and deep-ocean circulation, *Nature*, 342, 637-642.

Flohn, H. (1974), Background of a geophysical model of the initiation of the next glaciation, *Quaternary Research*, 4, 385-404.

Fraedrich, K., E. Kirk, and F. Lunkeit (1998), Portable University Model of the Atmosphere. Deutsches Klimarechenzentrum, *Technical Report*, 16, 37 pp.

Fraedrich, K., E. Kirk, U. Luksch, and F. Lunkeit (2003), Ein Zirkulationsmodell für Forschung und Lehre, *Promet*, 29, 34-48.

Fraedrich, K., H. Jansen, E. Kirk, A. Kleidon, U. Luksch, and F. Lunkeit (2005), The Planet Simulator: Model description and application, *Meteorologische Zeitschrift*, submitted.

Ganopolski, A., and S. Rahmstorf (2001), Rapid changes of glacial climate simulated in a coupled climate model, *Nature*, 409, 153-158.

Ghil, M., A. Mullhaupt, and P. Pestiaux (1987), Deep water formation and Quaternary glaciations., *Climate Dynamics*, 2, 1-10.

Gordon, A. L. (1986), Interocean exchange of thermocline water, *Journal of Geophysical Research*, 91, 5037-5046.

Gordon, A. L., R. F. Weiss, W. M. Smethie, and M. J. Warner (1992), Thermocline and Intermediate Water Communication between the South-Atlantic and Indian Oceans, *Journal of Geophysical Research-Oceans*, 97, 7223-7240.

Gordon, A. L. (2003), Oceanography - The brawniest retroflection, *Nature*, 421, 904-905.

Heinrich, H. (1988), Origin and consequences of cyclic ice rafting in the northeast Atlantic-Ocean during the past 130,000 Years, *Quaternary Research*, 29, 142-152.

Hemming, S. R., G. Bond, W. Broecker, W. D. Sharp, and M. Klas-Mendelson (2000), Evidence from Ar-40/Ar-39 ages of individual hornblende grains for varying Laurentide sources of icebergs discharges 22,000 to 10,500 yr BP, *Quaternary Research*, 54, 372-383.

Hoskins, B. J., and A. J. Simmons (1975), A multi-layer spectral model and the semi-implicit method, *Quarterly Journal of the Royal Meteorological Society*, 101, 637-655.

IPCC. in *Climate Change 2001: The Scientific Basis. Contribution of Working Group I to the Third Assessment Report of the Intergovernmental Panel on Climate Change*, edited by Houghton, J. T., Y. Ding, D. J. Griggs, M. Noguer, P. J. v. d. Linden, X. Dai, et al., pp. 881, Cambridge University Press, Cambridge, United Kingdom and New York, NY, USA, 2001.

Koc, N., E. Jansen, and H. Haflidason (1993), Paleoceanographic Reconstructions of surface ocean conditions in the Greenland, Iceland and Norwegian Seas through the last 14-ka based on diatoms, *Quaternary Science Reviews*, 12, 115-140.

Licciardi, J. M., J. T. Teller, and P. U. Clark (1999), Freshwater routing by the Laurentide ice sheet during the last deglaciation, *Mechanisms of Millenial-Scale Global Climate Change*, 112, 177-201.

Lohmann, G., and S. Lorenz (2000), On the hydrological cycle under paleoclimatic conditions as derived from AGCM simulations, *Journal of Geophysical Research-Atmospheres*, 105, 17417-17436.

Lohmann, G., M. Butzin, K. Grosfeld, G. Knorr, A. Paul, M. Prange, V. Romanova, and S. Schubert (2003), The Bremen Earth System Model of Intermediate Complexity (BREMIC) designed for long-term climate studies, Model description, climatology, and applications, *Technical Report*, University Bremen, Germany.

Maier-Reimer, E., U. Mikolajewicz, and K. Hasselmann (1993), Mean circulation of the Hamburg LSG OGCM and its sensitivity to the thermohaline surface forcing, *Journal of Physical Oceanography*, 23, 731-757.

Manabe, S., and R. J. Stouffer (1988), Two stable equilibria of a coupled ocean atmosphere model, *Journal of Climate*, 1, 841-866.

Manabe, S., and R. J. Stouffer (1993), Century-scale effects of increased atmospheric CO_2 on the ocean-atmosphere system, *Nature*, 364, 215-218.

Marotzke, J., and J. Willebrand (1991), Multiple equilibria of the global thermohaline circulation, *Journal of Physical Oceanography*, 21, 1372-1385.

Marshall, S. J., and G. K. C. Clarke (1999), Modeling North Atlantic freshwater runoff through the last glacial cycle, *Quaternary Research*, 52, 300-315.

Mix, A. C., E. Bard, and R. Schneider (2001), Environmental processes of the ice age: land, oceans, glaciers (EPILOG), *Quaternary Science Reviews*, 20, 627-657.

Petit, J. R., J. Jouzel, D. Raynaud, N. I. Barkov, J. M. Barnola, I. Basile, M. Bender, J. Chappellaz, M. Davis, G. Delaygue, M. Delmotte, V. M. Kotlyakov, M. Legrand, V. Y. Lipenkov, C. Lorius, L. Pepin, C. Ritz, E. Saltzman, and M. Stievenard (1999), Climate and atmospheric history of the past 420,000 years from the Vostok ice core, Antarctica, *Nature*, 399, 429-436.

Prange, M., V. Romanova, and G. Lohmann (2002), The glacial thermohaline circulation: Stable or unstable?, *Geophysical Research Letters*, 29, 2028, doi:2010.1029/2002LH015337.

Prange, M., G. Lohmann, and A. Paul (2003), Influence of vertical mixing on the thermohaline hysteresis: Analyses of an OGCM, *Journal of Physical Oceanography*, 33, 1707-1721.

Rahmstorf, S. (2002), Ocean circulation and climate during the past 120,000 years, *Nature*, 419, 207-214.

Sachs, J. P., R. F. Anderson, and S. J. Lehman (2001), Glacial surface temperatures of the southeast Atlantic Ocean, *Science*, 293, 2077-2079.

Sarnthein, M., K. Winn, S. J. A. Jung, J. C. Duplessy, L. Labeyrie, H. Erlenkeuser, and G. Ganssen (1994), Changes in East Atlantic Deep-Water Circulation over the Last 30,000 Years - 8 Time Slice Reconstructions, *Paleoceanography*, 9, 209-267.

Schmittner, A., M. Yoshimori, and A. J. Weaver (2002), Instability of glacial climate in a model of the ocean- atmosphere-cryosphere system, *Science*, 295, 1489-1493.

Severinghaus, J. P., T. Sowers, E. J. Brook, R. B. Alley, and M. L. Bender (1998), Timing of abrupt climate change at the end of the Younger Dryas interval from thermally fractionated gases in polar ice, *Nature*, 391, 141-146.

Severinghaus, J. P., and E. J. Brook (1999), Abrupt climate change at the end of the last glacial period inferred from trapped air in polar ice, *Science*, 286, 930-934.

Shin, S. I., B. Otto-Bliesner, E. C. Brady, J. Kutzbach, and S. P. Harrison (2003), A simulation of the last glacial maximum climate using the NCAR-CCSM, *Climate Dynamics*, 20, 127-151.

Sowers, T., and M. Bender (1995), Climate Records Covering the Last Deglaciation, *Science*, 269, 210-214.

Stocker, T. F., and D. G. Wright (1991), Rapid transitions of the ocean's deep circulation induced by changes in surface water fluxes, *Nature*, 351, 729-732.

Stocker, T. F., and A. Schmittner (1997), Influence of CO_2 emission rates on the stability of the thermohaline circulation, *Nature*, 388, 862-865.

Stocker, T. F. (1998), The seesaw effect, *Science*, 282, 61-62.

Stommel, H. (1961), Thermohaline convection with two stable regimes of flow, *Tellus*, 13, 224-230.

Weijer, W., W. de Ruijter, A. Sterl, and S. Drijfhout (2002), Response of the Atlantic overturning circulation to South Atlantic sources of buoyancy, *Global Planetary Change*, 34, 293-311.

Chapter 2

Southern Ocean origin for the resumption of Atlantic thermohaline circulation during deglaciation

Abstract

During the last two deglaciations, the Southern Hemisphere warmed before Greenland. At the same time the northern Atlantic was exposed to meltwater discharge, which is generally assumed to reduce the formation of North Atlantic Deep Water. Yet during deglaciation, the Atlantic thermohaline circulation became more vigorous, in the transition from a weak glacial to a strong interglacial mode. Here we utilize a three-dimensional ocean circulation model to investigate the impact of Southern Ocean warming and the associated sea-ice retreat on the Atlantic thermohaline circulation. We find that a gradual warming in the Southern Ocean induces an abrupt resumption of the interglacial mode of thermohaline circulation, triggered by increased mass transport into the Atlantic Ocean via the warm (Indian Ocean) and cold (Pacific Ocean) water route of the global ocean circulation. This effect prevails over the destabilizing effect of deglacial meltwater discharge, which would oppose a strengthening of the thermohaline circulation. A Southern Ocean trigger for the transition into an interglacial mode of circulation provides a consistent picture of Southern and Northern hemispheric climate change at times of deglaciation, in agreement with the available proxy records.

2.1 Introduction

Ice-core and ocean-sediment records reveal that during the last deglaciation the onset of warming in the Southern Hemisphere preceded Greenland warming by more than 1000 years [Sowers and Bender, 1995], a time lag that has been even longer for the penultimate deglaciation [Petit et al., 1999]. One candidate for an interhemispheric teleconnection is provided by the oceanic thermohaline circulation (THC). Proxy data [Sarnthein et al., 1994] and modelling studies [Ganopolski and Rahmstorf, 2001; Prange et al., 2002; Shin et al., 2003] indicate that the last

deglaciation is characterized by a transition from a weak glacial to a strong interglacial Atlantic THC. During the Bølling-Allerød (B/A) warm period the sea surface temperatures (SSTs) in the North Atlantic almost reached interglacial values, consistent with active deep water formation, corroborated by benthic $\delta^{13}C$ data [Sarnthein et al., 1994]. While most studies investigate processes responsible for a shut down of the THC, we pose the question how the conveyor gets restarted after a glacial mode with weak overturning, utilizing a numerical model for interglacial and glacial background conditions.

2.2 Methodology

2.2.1 The ocean model

The ocean model is based on the three-dimensional Large Scale Geostrophic model LSG [Maier-Reimer et al., 1993]. It includes a simple thermodynamic sea-ice model, an enhanced advection scheme for temperature and salinity, and a parameterisation of overflow [Lohmann, 1998]. The horizontal resolution is 3.5° on a semi-staggered grid (type 'E') with 11 levels in the vertical. For glacial conditions the storage of water in inland ice sheets is taken into account by setting all ocean points with present-day water depth less than 120 m to land. This causes the Bering Strait to be closed and several shallow areas like the Arctic shelves to become land. To drive the ocean, monthly fields of wind stress, surface air temperature and freshwater flux are taken from a present-day and Last Glacial Maximum (LGM) simulation of the atmospheric general circulation model ECHAM3/T42 [Roeckner et al., 1992; Lohmann and Lorenz, 2000]. We employ a hybrid coupled modelling approach, which allows an adjustment of surface temperatures and salinity to changes in the ocean circulation, based on an atmospheric energy balance model [Rahmstorf and Willebrand, 1995]. The applied heat flux parameterisation has shown to be a suitable choice, allowing the simulation of observed SSTs and the maintenance of large-scale temperature anomalies in perturbation experiments [Prange et al., 2003].

For the present-day state, we obtain an Atlantic Ocean circulation with export of 14 Sv (1 Sv = 10^6 m^3 s^{-1}) at 30°S and maximum heat transport of 1.1 PW, which is in the range of observations [Macdonald and Wunsch, 1996]. For the Last Glacial Maximum, our modelled ocean circulation is characterized by a weaker circulation of about 8.5 Sv (Figure 2.1a) and southward shifted convection sites (Figure 2.1b), compared to present-day sites. North Atlantic deep water (NADW) is formed in the subpolar North Atlantic and the North Atlantic Current flows in zonal direction along the horizontal isopycnals, consistent with reconstructions [Sarnthein et al., 1994].

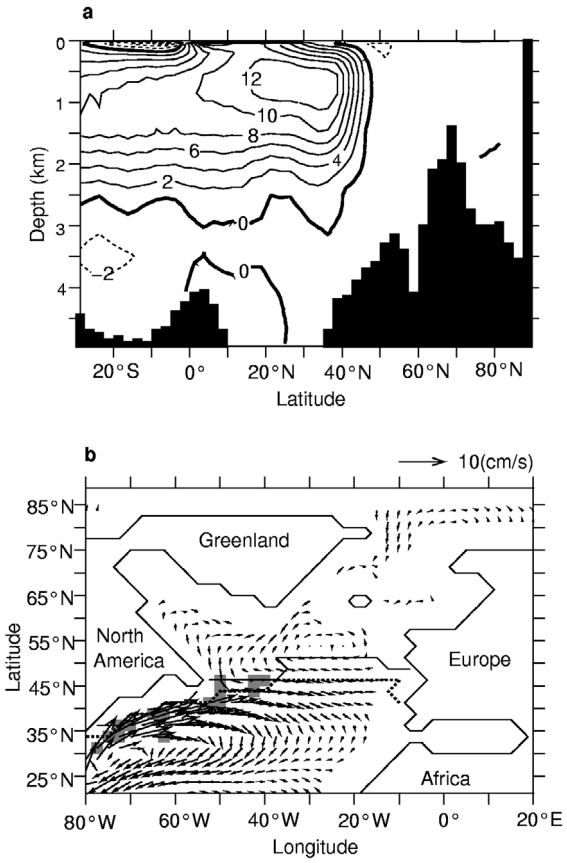

Figure 2.1: Modelled overturning streamfunction, as well as NADW convection sites and horizontal surface velocities in the Atlantic for the glacial control climate (LGM_CTRL). (a) Meridional streamfunction (Sv); warm surface water flows northward to the subpolar regions, sinks, and flows southward as NADW, represented by the solid lines; (b) Horizontal velocity (cm s^{-1}) in the upper 50 m of the North Atlantic. Major NADW convection sites are represented by the shaded area; summer and winter sea-ice margins are indicated by the solid and the dashed line, respectively.

2.2.2 Experimental design

To simulate the resumption of the Atlantic THC during deglaciation, we assume a linear transition from glacial to interglacial values in Southern Ocean temperature, sea-ice and wind stress over 1,500 years, consistent with a deglacial sea-ice retreat within 1,000 years in the Southern Ocean south of the present-day polar front [Shemesh et al., 2002]. Each experiment is started from the glacial equilibrium climate and is integrated until a quasi steady state is reached. All experimental time series are smoothed by a one-year boxcar-average. In the stability analysis of the THC, we

apply a slowly varying freshwater anomaly with a rate of 5 x 10^{-5} Sv yr^{-1} (1 x 10^{-6} Sv yr^{-1} at the transition of the hysteresis curve that starts from LGM_100) uniformly between 20°N and 50°N to the Atlantic Ocean. Integration starts at the upper branches with zero freshwater forcing, which is then increased up to 0.2 Sv and 0.32 Sv for LGM_CTRL and LGM_100, respectively. The integration proceeds on the lower branch until the respective negative freshwater input is reached. Subsequently the freshwater increases again to close the loops. Owing, to the slowly varying nature of the surface forcing the model is in quasi-equilibrium during the integration.

2.3 Results

Caused by Southern Ocean warming and accompanying sea-ice retreat, a strong increase in overturning circulation is detected in experiment LGM_100 (Figure 2.2). The warming generates a negative density anomaly in the Southern Ocean, inducing anomalous westward velocities between 30°S and 50°S, consistent with geostrophic balance (Figure 2.3a). Off the Brazilian coast the anomalous flow is transported along with pressure gradients to the north. Part of the relatively warm and salty water originating from the Indian Ocean is directly injected into the subtropical South Atlantic via the eastern boundary current off the Namibian coast (Figure 2.3). The thermal anomaly is attenuated along the northward conveyor route but the saline characteristics of the warm water route persist [Weijer et al., 2002] (Figure 2.2b). The salinity increase in the upper layer of the North Atlantic preconditions NADW formation comparable to a mechanism proposed by Gordon et al. [1992] that gradually intensifies convection during the first 1,000 years (Figure 2.2b). The mechanism involves a positive feedback of THC, owing to salinity advection [Stommel, 1961]. Furthermore, sea-ice retreat in the Southern Ocean increases volume transport through the Drake Passage (25 Sv to 54 Sv) and the Atlantic import at 30°S of relatively cold and fresh water between 10°W and 50°W (Figure 2.3).

Along with increased Atlantic overturning, the meridional heat transport warms the surface water of the North Atlantic, triggering an abrupt sea-ice retreat after 1,000 years. Besides the advective feedback, a convective feedback contributes to the resumption of the THC. Once convection is initiated in parts of the formerly ice covered North Atlantic, the relatively warm and saline water masses from deeper layers coming up to the surface lose their heat readily, but keep their salt and thus reinforce the starting process of convection (Figure 2.2b). As a result, the mean convection depth in the Atlantic between 50°N and 60°N increases abruptly from 0 to 140 m. The convection in large parts of the Labrador Sea is only temporarily active, whereas the convection sites south of Iceland remain in operation (see the animations at http://www.nature.com). The maximum heat transport in the Atlantic Ocean increases from 0.8 PW to 1.6 PW after 3000 model years, causing an SST rise of more than 6 K in the North Atlantic (Figure 2.3b).

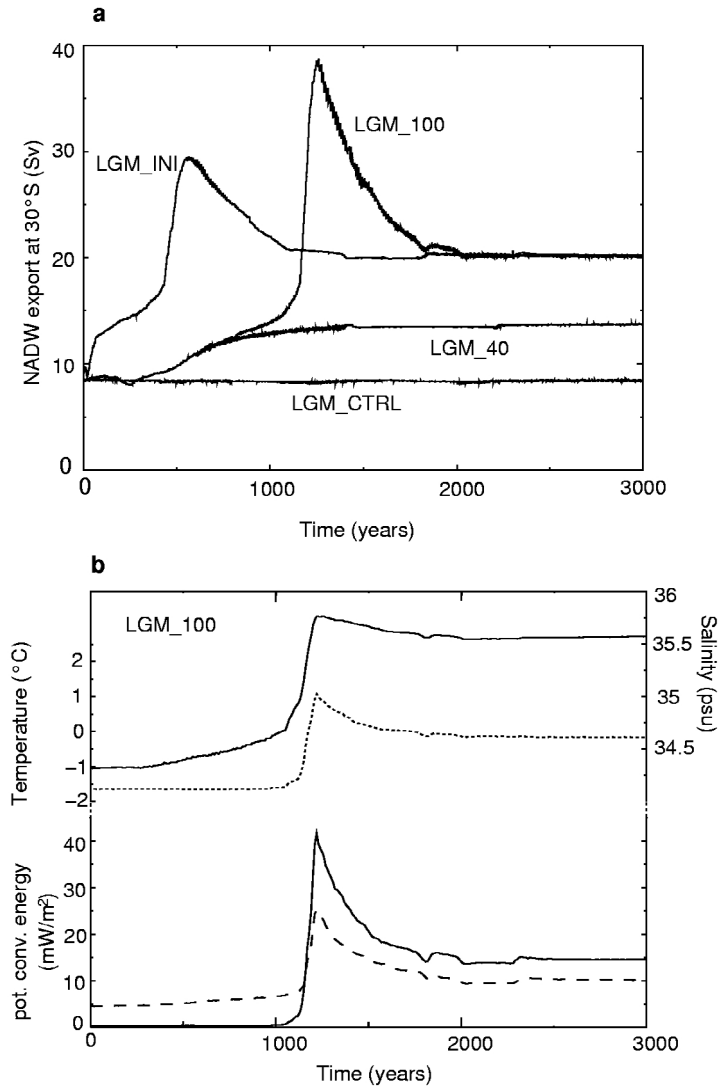

Figure 2.2: Temporal changes of NADW export at 30°S, North Atlantic temperature, salinity and convection energy loss, respectively. (a) In LGM_100, glacial conditions in the Southern Ocean (south of 30°S) are gradually replaced by interglacial conditions within 1500 years. In LGM_40 gradual changes to interglacial conditions as in LGM_100 are assessed, but the transition terminates after 600 years, equivalent to a sea-ice retreat of 40%. Experiment LGM_INI represents instantaneously applied interglacial conditions of temperature, sea-ice and wind stress. The black curve (LGM_CTRL) shows the glacial control run; (b) LGM_100 time series of sea surface temperature (°C), (dotted curve), salinity (psu), (solid curve) and potential energy loss by convection (mW/m^2) in the North Atlantic averaged between 55°N and 65°N (solid curve) and between 40°N and 55°N (dashed curve).

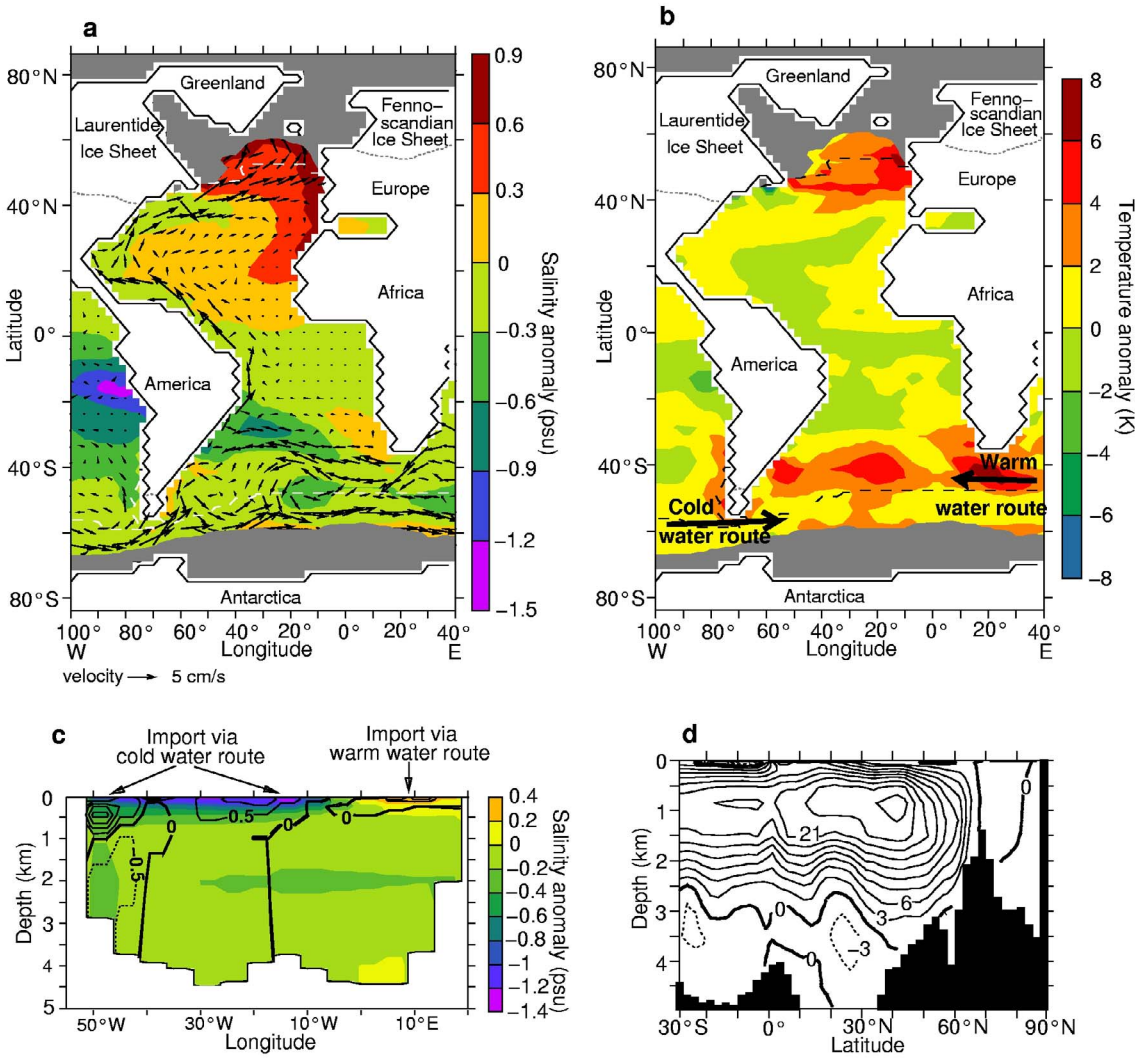

Figure 2.3: Differences between LGM_100 and LGM_CTRL (panels a, b, c) and meridional overturning streamfunction in LGM_100 after 3000 model years. (a) Annual mean salinity (psu) and horizontal velocity (cm s^{-1}) anomalies averaged over the upper 800 m. The grey shaded area and the dashed line show the annual mean 2 m height ice extent in experiment LGM_100 and LGM_CTRL, respectively. The maximum glacial continental ice margins are represented by the dotted lines. (b) Annual mean temperature anomaly (K) averaged over the upper 50 m; schematically overlaid with the main pathways of water import to the Atlantic Ocean. Sea-ice margins and continental ice sheets as in panel a. (c) Annual mean salinity anomaly (psu) and anomaly of the meridional velocity component (cm s^{-1}) at 30°S. Solid lines indicate northward flow, dashed lines represent southward flow. (d) Meridional overturning streamfunction (Sv) in the Atlantic in LGM_100 after 3000 model years.

To investigate the abrupt warming in more detail, we have run experiment LGM_INI where background conditions in the Southern Ocean are instantaneously switched from glacial to interglacial ones. The model response (Figure 2.2a) is similar to LGM_100, indicating that the abrupt warming is independent on the timescale of sea-ice margin retreat in the Southern Ocean. In order to estimate the threshold for the nonlinear transition shown in Figure 2.2a, a series of experiments with different sea-ice retreat scenarios in the Southern Ocean were performed, showing that ~50% sea-ice margin retreat from glacial to interglacial conditions is sufficient to cause the abrupt model response. Experiment LGM_40 with 40% sea-ice margin retreat is representative of the experiments with linear model response (Figure 2.2a). Despite enhanced NADW formation in this experiment, the sea-ice margin in the North Atlantic is almost unaffected and the feedback loop for the nonlinear resumption of the THC described above is not active, suggesting that the abrupt sea-ice retreat in the northern North Atlantic is governed by the level of Southern Ocean warming.

Furthermore, model simulations with alternated wind and temperature forcing reveal that imposed temperature and sea-ice changes in the Southern Hemisphere have a strong influence on THC strength compared to locally alternated wind fields. A further experiment yielded that Northern Hemisphere warming has much less influence on NADW overturning strength than Southern Hemisphere warming (Figure 2.4).

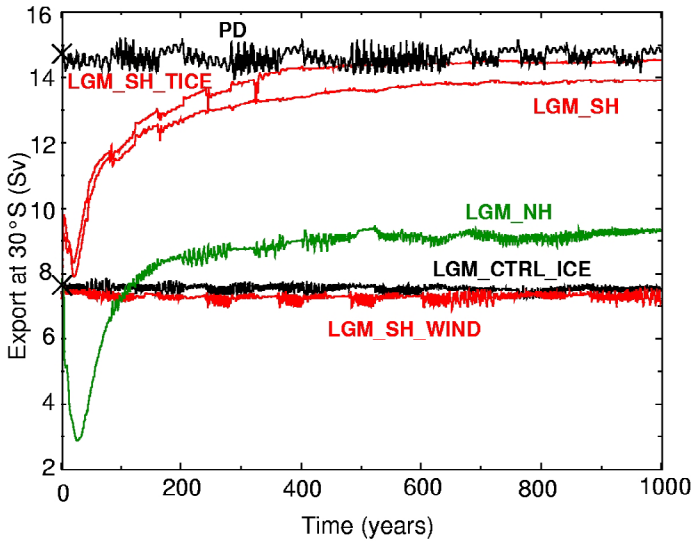

Figure 2.4: Time series of NADW export at 30°S for our deglaciation scenarios with alternated wind and temperature forcing. In this set of experiments, the sea-ice cover has globally been prescribed and the change to interglacial conditions has been applied instantaneously. LGM_SH – changed temperature, sea-ice and wind stress; LGM_SH_TICE – changed temperature and sea-ice; LGM_SH_WIND – changed wind stress. The experiments with Southern Ocean warming south of 30°S are represented by the red curves. In experiment LGM_NH (green curve), interglacial values in temperature, sea-ice and wind stress is applied north of 30°N. The glacial (LGM_CTRL_ICE) and interglacial (PD) reference states are indicated by the black curves and crosses.

2. DEGLACIAL SOUTHERN OCEAN WARMING & THC

In addition we looked at the deglacial Heinrich sequence that is characterized by meltwater discharge to the North Atlantic [Marshall and Clarke, 1999], whose destabilizing impact on THC has been proposed to suppress warming in the North [Stocker, 2000]. Our glacial reference state (LGM_CTRL) is monostable with respect to transient North Atlantic freshwater pulses [Ganopolski and Rahmstorf, 2001; Prange et al., 2002] as revealed by experiment LGM_CTRL_H500 (Figure 2.5). This explains the observed recovery of the reduced glacial THC after Heinrich events. Different experiments with transient (LGM_SH_H500) and permanent (LGM_SH_Hperm) freshwater flow to the North Atlantic (Figure 2.5a) show that the abrupt resumption of Atlantic THC via Southern Ocean warming prevails over the destabilizing impact of meltwater discharge during the Heinrich sequence. Compared to LGM_100, the overturning response in LGM_SH_H500 and LGM_SH_Hperm is damped in magnitude and delayed in time.

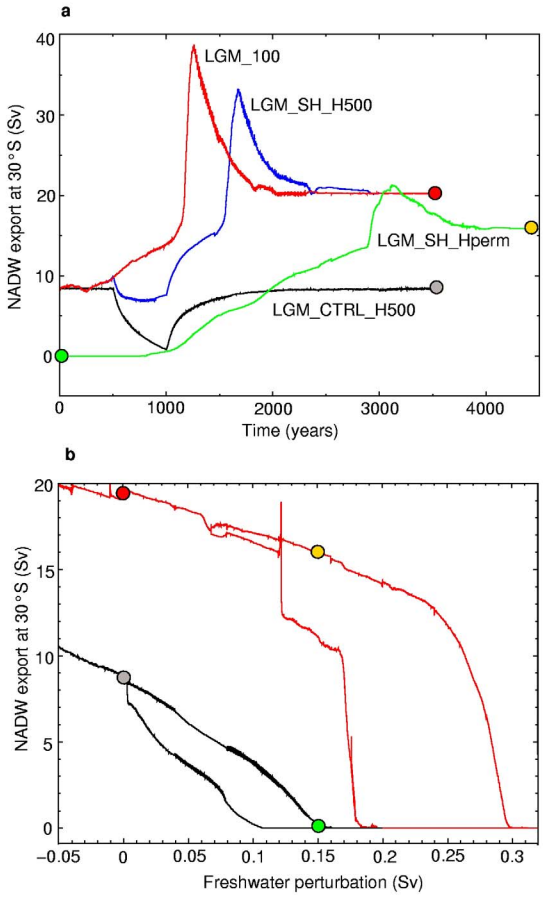

Figure 2.5: Atlantic NADW export at 30°S for the different freshwater pulse experiments and stability diagrams for the Atlantic THC. (a) In LGM_CTRL_H500 and LGM_SH_H500 a transient freshwater pulse to the North Atlantic has been simulated between model year 500 and 1000. In LGM_SH_perm the freshwater input persists. Southern Ocean warming is applied in LGM_SH_H500 and LGM_SH_perm (also see method section). The coloured points indicate the different equilibrium climate states.(b) The stability diagram (procedure explained in method section) of the glacial ocean circulation (black curve) differs substantially from that of LGM_100 (red curve). The restarted Atlantic THC exhibits a pronounced bistability for anomalous freshwater fluxes between +0.12 Sv and +0.3 Sv. The glacial THC shows a monostable behaviour at zero freshwater perturbation and only weak bistability in the area of positive freshwater input. The location of climate states from panel (a) are displayed by the coloured points.

So far our investigations reveal that Southern Ocean warming and associated sea-ice retreat enhances the transport via warm and cold water routes, causing a THC flow regime that is stronger and bistable (Figure 2.5b). The bistable flow regime is driven by heat loss, whereas freshwater tends to reduce overturning strength [Stommel, 1961].

2.4 Discussion and Conclusions

The restarted Atlantic THC bears the potential to react to deglacial meltwater input to the North Atlantic in accordance with the Younger Dryas cold sequence [Stocker and Wright, 1991; Rühlemann et al., 1999] (Figure 2.5b). As a result of the restarted conveyor circulation (Figure 2.3d) the maximum heat transport and the temperature in the North Atlantic increase dramatically, consistent with a temperature rise of more than 6 K for the B/A warm transition [Bard et al., 2000]. At the same time, temperatures in the tropical [Rühlemann et al., 1999] and South Atlantic [Sachs et al., 2001] decrease (Figure 2.3b) in accordance with the oceanic interhemispheric teleconnection that increased THC cools the Southern Hemisphere [Crowley, 1992]. In our model simulations Southern Hemisphere cooling, as a response to a resumption of the THC in the North Atlantic, is inhibited by the experimental design. On the basis of the present investigation, the Antarctic Cold Reversal can be associated with an abrupt transition from a glacial to an interglacial ocean circulation mode that effectively transported heat to the North Atlantic. The corresponding B/A warm phase occurs only after a certain amount of heat has been transported to the North Atlantic, triggering a northern sea-ice retreat, which is then abruptly amplified by convective processes. We speculate that in conjunction with other effects [Stephens and Keeling, 2000; Toggweiler, 1999], the increase in northward oceanic heat transport can contribute to the reduction of the great Northern Hemisphere ice sheets over North America and Scandinavia. The respective meltwater input weakens but does not stop NADW formation [Lohmann and Schulz, 2000]. The involved mechanism is consistent with the phase offsets between Southern and Northern Hemisphere climate change on Milankovitch time scales [Sowers and Bender, 1995; Petit et al., 1999] and provides a possible explanation for the onset of the B/A. This mechanism represents an alternative explanation to the proposal that meltwater from Antarctica retracts Antarctic Bottom Water formation, leading to a switch-on of THC at a critical threshold [Stocker, 2000], an effect that would amplify the mechanism proposed here.

Our study suggests that the “Achilles Heel” [Broecker, 1991] and the “Flywheel” of the Atlantic overturning circulation are located at the North Atlantic and the Southern Ocean, respectively. Interestingly, the tropical foraminifer *G. menardii* is re-seeded in the Atlantic Ocean at the last glacial-interglacial transition [Schott, 1935]. The only way to re-seed *G. menardii* in the Atlantic is around the Cape of Good Hope, leading to speculation [Berger and Wefer, 1996] that the reopening of the Agulhas gap at the end of the last ice age may have played a role in restarting the Atlantic THC. Southern Ocean warming and associated sea-ice retreat might be the response to

local Milankovitch forcing on the precessional period [Kim et al., 1998] or the result of tropical SST anomalies that transmitted from the tropical Pacific to the Antarctic region [Koutavas et al., 2002]. Since the South Atlantic is characterized by a number of unique dynamical features, such as the large Agulhas Rings that form a key link in the THC [Gordon et al., 1992] it is of interest to investigate the mechanism proposed here, using high-resolution models of the South Atlantic region to obtain a more detailed view in this region. More well-dated high-resolution records from terrestrial and marine sites in the Southern Hemisphere will be needed to decipher these additional pathways. They seem to be necessary for the prediction of future climate scenarios with respect to rising atmospheric CO_2 concentration and its impact on the Atlantic overturning circulation.

2.5 Appendix

Alternative deglacial scenarios starting from the THC "off-mode"

This additional part of the chapter is aimed to provide a deeper insight into the dynamics of the deglacial THC resumption from the "off-mode". This mode of ocean circulation possibly prevailed during the phase prior to the resumption of a stronger ocean circulation, which is associated with the onset of the B/A [Sarnthein et al., 1994].

The "off-mode" is established in the same way as in experiment LGM_SH_Hperm. Beside the permanent meltwater inflow of 0.15 Sv into the North Atlantic, the background climate is changed globally in experiment LGM_glob, while in LGM_NH the respective climate forcing fields of surface air temperature, sea-ice and wind stress are changed north of 30°N. Experiment LGM_wind is conducted in the same way as the global warming scenario, however the wind fields remain in glacial conditions.

The model simulations show that gradual global, Southern Ocean, and North Atlantic warming cause different responses of the modelled THC strength (Figure 2.6). An amplification of the THC is detected in the global and Southern Ocean warming scenario, while Northern Hemisphere warming does not generate a substantial change of the prevailing THC "off-mode". In LGM_SH_Hperm, the transition to the stronger interglacial ocean circulation can be characterised by two phases, a 2000 years lasting gradual phase that is followed by an abrupt augmentation of the THC.

The gradual first phase is linked to enhanced volume transport into the South Atlantic via the warm and cold water route of the global ocean circulation, affecting the salt balance in the

Atlantic. Phase two, after about 3000 years, is associated with a massive sea-ice margin retreat and the generation of NADW formation sites in the formerly ice covered parts of the North Atlantic, temporarily reinforced by a convective feedback, owing to vertical heat transfer. The energy required to trigger the abrupt sea-ice retreat in the northern North Atlantic that commences phase two is provided by the northward oceanic heat transport and the heat stored in the relatively warm subsurface layers of the northern North Atlantic (Figure 2.7a), since the background climate in the Northern Hemisphere remains in cold glacial conditions.

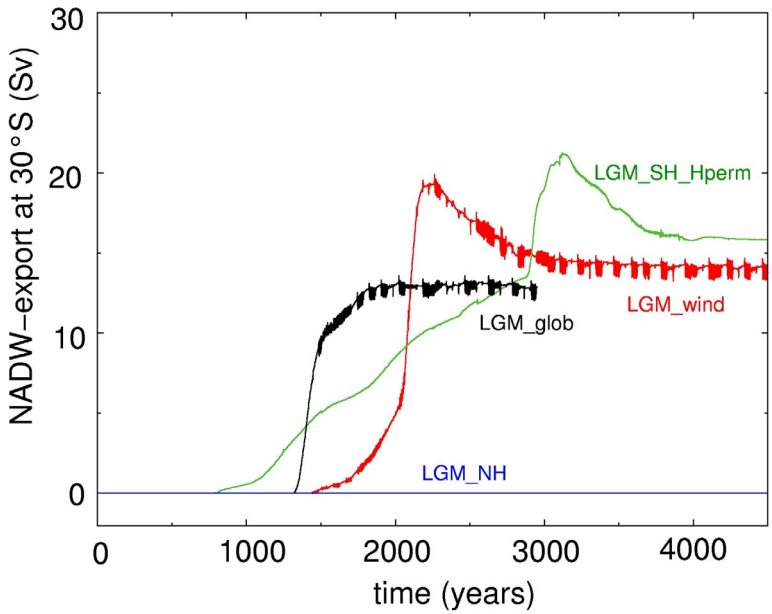

Figure 2.6: Temporal changes of the NADW export at 30°S in the different degalcaial warming scenarios LGM_glob (black), LGM_wind (red), LGM_SH_Hperm (green) and LGM_NH (blue). All deglaciation experiments are started from the THC "off-mode" and the North Atlantic is exposed to a permanent melt-water flow of 0.15 Sv.

The THC amplification in experiment LGM_glob via global warming can be characterised by a one-step strengthening of the THC starting from the THC "off-mode". The reactivation of NADW formation is associated with the activation of stable convection sites in the Nordic Seas and the Labrador Sea. The THC intensification is not contemporaneous to the sea-ice retreat in the North Atlantic, since warming in the North Atlantic and the simultaneous meltwater discharge inhibits the initiation of NADW formation in response to a sea-ice retreat. Consequently, the sea-ice retreat is chiefly governed by advanced atmospheric warming and the subsurface temperatures increase in large parts of the North Atlantic at the resumption of a stronger THC (Figure 2.7b). The northward sea-ice margin retreat modifies the wind driven circulation in the North Atlantic. The deglacial reduction of the catabatically induced southward wind component in the northern North Atlantic and the formation of a cyclonic wind driven gyre results in a surface salinity maximum at about 60°N (Figure 2.7c). This surface maximum south west of Iceland is associated with a doming of isopycnals, which favours convective activity (Figure 2.7c). Once convection is initiated, the THC

is amplified by the positive feedback between northward salt transport and overturning strength, which activates additional convection sites in the Norwegian and Labrador Sea, respectively. This generates an interhemispheric overturning cell in the Atlantic, and NADW export at 30°S is detected in LGM_glob after about 1300 model years (Figure 2.6). Moreover, the wind driven component of the merdional overturning circulation is important, since the main portion of freshwater export from the North Atlantic is assigned to the anticyclonic North Atlantic gyre circulation that causes a relatively low salinity branch off the north west coast of Africa (Figure 2.7c). Compared to LGM_glob, the alternated wind find fields in LGM_wind lead to relatively low surface salinities in the Labrador Sea in LGM_wind (Figure 2.7d) and the signature of the THC amplification in LGM_wind is characterised by a gradual phase between model year 1500 and 2000. During this time span convection occurs along the sea-ice margin in the Nordic Seas. Subsequently, convection is initiated in the Labrador Sea (not shown).

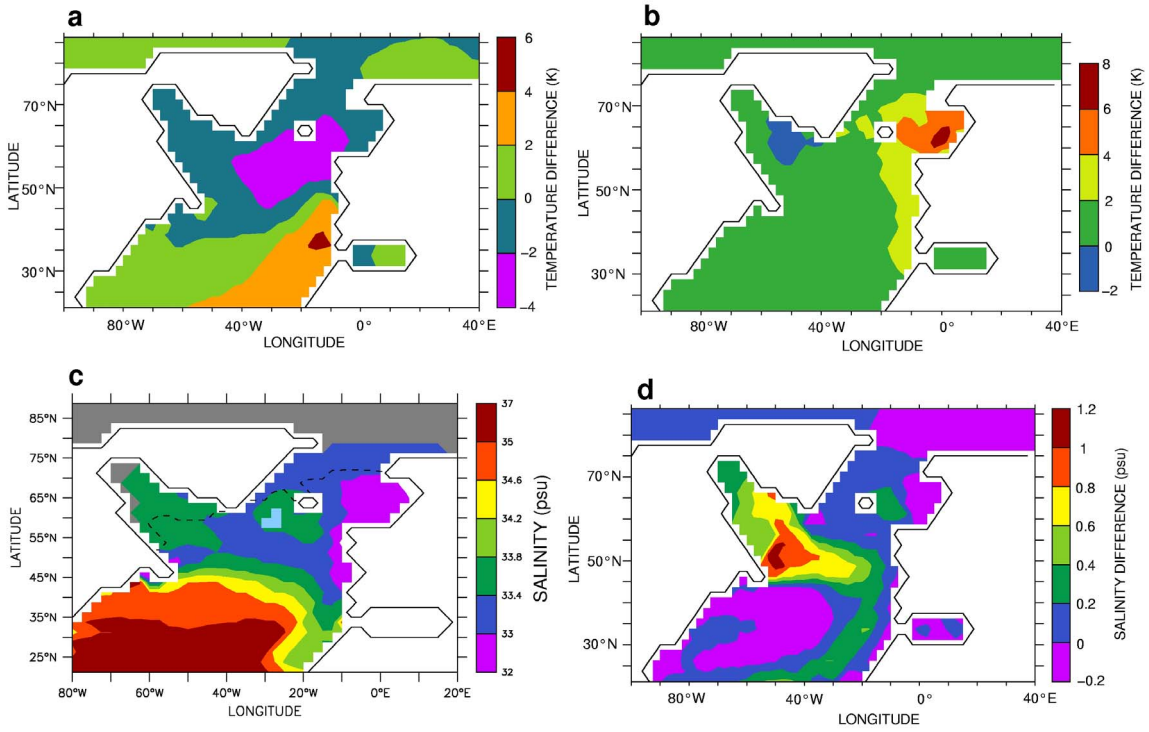

Figure 2.7: North Atlantic temperature and salinities in different deglaciation scenarios. (a) Temperature difference (K) averaged between 200-500 m in LGM_SH_Hperm between model year 1550 and 2850, as well as in LGM_glob (b) between 1300 and 1650 years. Panel (c) shows the surface salinity (psu) in LGM_glob after 1300 years overlaid with the initial convection sites (light blue), the winter sea-ice cover (grey shaded), and the summer sea-ice margin (dashed line); and (d) the surface salinity differences between experiment LGM_glob and LGM_wind for model year 1300.

The warming of the northern high latitudes in experiment LGM_NH is not sufficient to cause an amplification of the THC from the “off-mode” (Figure 2.6), since local warming and melt-water inflow to the North Atlantic cause a density reduction in the formation regions of NADW. The persistent glacial conditions in the Southern Ocean inhibit an enhanced inter-ocean basin exchange

of the Atlantic with the Indian and the Pacific Ocean, respectively. Therefore, the import characteristic to the Atlantic remains in the glacial conditions. This shows the importance of warming conditional processes in the Southern Ocean that precondition NADW formation and lead to a THC intensification, starting from the "off-mode".

Besides the regaining influence of the warm and cold water route, the wind forcing becomes more important with a diminishing overturning circulation, since the density driven component is substantially reduced in the THC "off-mode". Therefore, the oceanic transports of heat and salt are mainly governed by horizontal Ekman-driven transport due to the wind driven circulation [Weaver et al., 1993]. Furthermore, the vertical salinity transport [Oka et al., 2001] and the preconditioning of oceanic convection [Killworth, 1983] due to Ekman pumping in the North Atlantic affect the initiation of an interhemispheric THC during deglaciation. As in experiment LGM_glob, the cyclonic wind driven Ekman pumping has also found to be responsible for the maintenance of a shallow and weak overturning cell in the North Atlantic for the present climate state [Prange et al., 2003]. However, this effect is not an inevitable pre-requisite for the deglacial construction of an interhemispheric overturning cell in the Atlantic as shown in LGM_wind.

Summarising we find in the different warming and meltwater scenarios that gradual deglacial global and Southern Ocean warming lead to an amplification of the THC from the glacial "off-mode". This THC intensification can be associated with a transition from the Heinrich I event [Heinrich, 1988], to a stronger interstadial ocean circulation in the Atlantic during the B/A [Sarnthein et al., 1994; Alley and Clark, 1999]. Contrary, local warming in the North Atlantic is not sufficient to cause a THC amplification, in presence of reasonable meltwater fluxes to the North Atlantic. This highlights the key role of warming conditioned import changes to the South Atlantic via an enhanced warm and cold water route that compensates deglacial meltwater discharge to the North Atlantic.

References:

Alley, R. B., and P. U. Clark (1999), The deglaciation of the northern hemisphere: A global perspective, *Annual Review of Earth and Planetary Sciences*, 27, 149-182.

Bard, E., F. Rostek, J. L. Turon, and S. Gendreau (2000), Hydrological impact of Heinrich events in the subtropical northeast Atlantic, *Science*, 289, 1321-1324.

Berger, W. H., and G. Wefer (1996), *Expeditions into the Past: Paleoceanographic Studies in the South Atlantic*, 644 pp., Springer-Verlag, Berlin Heidelberg.

Broecker, W. S. (1991), The great ocean conveyor, *Oceanography*, 4, 79-89.

Crowley, T. J. (1992), North Atlantic deep water cools the southern hemisphere, *Paleoceanography*, 7, 489-497.

Ganopolski, A., and S. Rahmstorf (2001), Rapid changes of glacial climate simulated in a coupled climate model, *Nature*, 409, 153-158.

Gordon, A. L., R. F. Weiss, W. M. Smethie, and M. J. Warner (1992), Thermocline and Intermediate Water Communication between the South-Atlantic and Indian Oceans, *Journal of Geophysical Research-Oceans*, 97, 7223-7240.

Heinrich, H. (1988), Origin and Consequences of Cyclic Ice Rafting in the Northeast Atlantic-Ocean During the Past 130,000 Years, *Quaternary Research*, 29, 142-152.

Killworth, P. D. (1983), Deep convection in the world ocean, *Reviews of Geophysics Space Physics*, 21, 1-26.

Kim, S. J., T. J. Crowley, and A. Stössel (1998), Local orbital forcing of Antarctic climate change during the last interglacial, *Science*, 280, 728-730.

Koutavas, A., J. Lynch-Stieglitz, T. M. Marchitto, and J. P. Sachs (2002), El Ninio-like pattern in ice age tropical Pacific sea surface temperature, *Science*, 297, 226-230.

Lohmann, G. (1998), The influence of a near-bottom transport parameterization on the sensitivity of the thermohaline circulation, *Journal of Physical Oceanography*, 28, 2095-2103.

Lohmann, G., and S. Lorenz (2000), On the hydrological cycle under paleoclimatic conditions as derived from AGCM simulations, *Journal of Geophysical Research-Atmospheres*, 105, 17417-17436.

Lohmann, G., and M. Schulz (2000), Reconciling Bølling warmth with peak deglacial meltwater discharge, *Paleoceanography*, 15, 537-540.

Macdonald, A. M., and C. Wunsch (1996), An estimate of global ocean circulation and heat fluxes, *Nature*, 382, 436-439.

Maier-Reimer, E., U. Mikolajewicz, and K. Hasselmann (1993), Mean Circulation of the Hamburg LSG OGCM and its Sensitivity to the Thermohaline Surface Forcing, *Journal of Physical Oceanography*, 23, 731-757.

Marshall, S. J., and G. K. C. Clarke (1999), Modeling North Atlantic freshwater runoff through the last glacial cycle, *Quaternary Research*, 52, 300-315.

Oka, A., H. Hasumi, and N. Suginohara (2001), Stabilization of thermohaline circulation by wind-driven and vertical diffusive salt transport, *Climate Dynamics*, 18, 71-83.

Petit, J. R., J. Jouzel, D. Raynaud, N. I. Barkov, J. M. Barnola, I. Basile, M. Bender, J. Chappellaz, M. Davis, G. Delaygue, M. Delmotte, V. M. Kotlyakov, M. Legrand, V. Y. Lipenkov, C. Lorius, L. Pepin, C. Ritz, E. Saltzman, and M. Stievenard (1999), Climate and atmospheric history of the past 420,000 years from the Vostok ice core, Antarctica, *Nature*, 399, 429-436.

Prange, M., V. Romanova, and G. Lohmann (2002), The glacial thermohaline circulation: Stable or unstable?, *Geophysical Research Letters*, 29, 2028, doi:2010.1029/2002LH015337.

Prange, M., G. Lohmann, and A. Paul (2003), Influence of vertical mixing on the thermohaline hysteresis: Analyses of an OGCM, *Journal of Physical Oceanography*, 33, 1707-1721.

Rahmstorf, S., and J. Willebrand (1995), The role of temperature feedback in stabilising the thermohaline circulation, *Journal of Physical Oceanography*, 25, 787-805.

Roeckner, E., K. Arpe, L. Bengtsson, S. Brinkop, L. Dümenil, M. Esch, E. Kirk, F. Lunkeit, M. Ponater, B. Rockel, R. Sausen, U. Schlese, S. Schubert, and M. Windelband (1992), Simulation of present-day climate with the ECHAM model: Impact of model physics and resolution. MPI Report No. 93, ISSN 0937-1060, Max-Planck-Institut für Meteorologie, Hamburg, Germany, 171 pp.

Rühlemann, C., S. Mulitza, P. J. Müller, G. Wefer, and R. Zahn (1999), Warming of the tropical Atlantic Ocean and slowdown of thermohaline circulation during the last deglaciation, *Nature*, 402, 511-514.

Sachs, J. P., R. F. Anderson, and S. J. Lehman (2001), Glacial surface temperatures of the southeast Atlantic Ocean, *Science*, 293, 2077-2079.

Sarnthein, M., K. Winn, S. J. A. Jung, J. C. Duplessy, L. Labeyrie, H. Erlenkeuser, and G. Ganssen (1994), Changes in East Atlantic Deep-Water Circulation over the Last 30,000 Years - 8 Time Slice Reconstructions, *Paleoceanography*, 9, 209-267.

Schott, W. (1935), Die Foraminiferen in dem äquatorialen Teil des Atlantischen Ozeans, *Wissenschaftliche Ergebnisse der deutschen Atlantik Expedition mit der Meteor*, 1925-1927, 43-134.

Shemesh, A., D. Hodell, X. Crosta, S. Kanfoush, C. Charles, and T. Guilderson (2002), Sequence of events during the last deglaciation in Southern Ocean sediments and Antarctic ice cores, *Paleoceanography*, 17.

Shin, S. I., B. Otto-Bliesner, E. C. Brady, J. Kutzbach, and S. P. Harrison (2003), A simulation of the last glacial maximum climate using the NCAR-CCSM, *Climate Dynamics*, 20, 127-151.

Sowers, T., and M. Bender (1995), Climate Records Covering the Last Deglaciation, *Science*, 269, 210-214.

Stephens, B. B., and R. F. Keeling (2000) The influence of Antarctic sea ice on glacial-interglacial CO_2 variations, *Nature*, 404, 171-174.

Stocker, T. F. The Role of Simple Models in Understanding Climate Change. In: *Continuum Mechanics and Applications in Geophysics and the Environment.* Straugham, B., Greeve, R., Ehrentraut, H. & Wang, Y. (eds.), Springer Verlag, 337-367 (2001).

Stocker, T. F., and D. G. Wright (1991), Rapid transitions of the ocean's deep circulation induced by changes in surface water fluxes, *Nature*, 351, 729-732.

Stommel, H. (1961), Thermohaline convection with two stable regimes of flow, *Tellus*, 13, 224-230.

Toggweiler, J. R. (1999), Variation of atmospheric CO_2 by ventilation of the ocean's deepest water, *Paleoceanography*, 14, 571-588.

Weaver, A. J., J. Marotzke, P. F. Cummins, and E. S. Sarachik (1993), Stability and variability of the thermohaline circulation, *Journal of Physical Oceanography*, 23, 39-60.

Weijer, W., W. de Ruijter, A. Sterl, and S. Drijfhout (2002), Response of the Atlantic overturning circulation to South Atlantic sources of buoyancy, *Global Planetary Change*, 34, 293-311.

Chapter 3

Transitions in the Atlantic thermohaline circulation by global deglacial warming and meltwater pulses

Abstract

Modelling results show that gradual global warming during deglaciation leads to an abrupt resumption of the thermohaline circulation (THC) after being stalled. The modelled deglaciation scenarios include a sequence of meltwater pulses at 19 ka BP and Heinrich-I events in the North Atlantic. The resumption of the THC is associated with heat release from the sub-surface ocean in the North Atlantic, as well as large-scale salinity advection of near-surface waters from the South Atlantic/Indian Ocean and the tropics to the formation areas of North Atlantic deep water. The restarted THC possesses a strong insensitivity against deglacial meltwater pulses, and coexistent a distinct bistability in the hysteresis curve for cumulative positive freshwater fluxes to the North Atlantic. Therefore, the restarted ocean circulation bears the potential for a long term weakening of the THC in accordance with the Younger Dryas. A comparison of the presented deglaciation scenarios with proxy data shows that a lead of increasing Southern Hemisphere temperatures, relatively to Greenland temperatures, can be reconciled with a gradual global warming trend and a superimposed oceanic “seesaw” response to meltwater pulses, associated with the Heinrich-I sequence. Therefore, the evolution of deglacial temperature records as recorded in proxy data can be understood as an interplay of processes in both hemispheres, connected by the THC.

3.1 Introduction

Ice core records exhibit that deglacial warming at the transition from the last glacial period to the present interglacial started prior to 20 ka BP (thousand years before present) (Figure 3.1) [Alley et al., 2002; Blunier et al., 1997]. Changes in atmospheric CO_2 and Vostok air temperature occurred nearly coincidentally, whereas ice volume lags these variables as revealed by cross-spectral analyses [Shackleton, 2000]. It has been suggested that increasing atmospheric CO_2 concentration contributed to global deglacial warming [Bender et al., 1997]. Different feedbacks, involving e.g.

ice albedo and greenhouse-gas effects, caused regional to global synchronization of deglaciation [Alley and Clark, 1999]. Superimposed on the general warming trend that characterized the transition from glacial to interglacial conditions, ice core records from Greenland and Antarctica exhibit strong north - south coupling (Figure 3.1) [Bender et al., 1994; Blunier and Brook, 2001; Jouzel et al., 1995; Petit et al., 1999; Sowers and Bender, 1995]. In response to deglacial global warming, freshwater discharge from the great northern ice sheets to the North Atlantic may shut down the thermohaline circulation (THC) [McCabe and Clark, 1998; Stocker and Wright, 1991]. The reduced northward oceanic heat transport maintained cold conditions during Heinrich-1, lasting from about 17.5 ka BP to 14.7 ka BP [Heinrich, 1988; Sarnthein et al., 1994]. In the Southern Hemisphere, reduced oceanic heat transport further enhances warming in the South Atlantic, as documented by alkenone and oxygen isotope based sea surface temperature (SST) records from the Cape Basin [Sachs et al., 2001], as well as of the Brazilian and Namibian coasts [Arz et al., 1999; Kim et al., 2002]. The end of the Heinrich-1 cold sequence is marked by the abrupt transition to the Bølling/Allerød (B/A) warm phase in the North Atlantic realm and the Antarctic cold reversal (ACR) at about 14.5 ka BP. During the B/A, temperatures in the North Atlantic almost reached interglacial values, which are consistent with active North Atlantic deep-water (NADW) formation, as corroborated by benthic $\delta^{13}C$ data [Sarnthein et al., 1994] and $^{231}Pa/^{230}Th$ ratios of bulk sediment [McManus et al., 2004]. A major inflow of meltwater to the ocean, referred to as MWP-1A [Fairbanks, 1989], accompanied the phase to warmer conditions in the North Atlantic. Interestingly, NADW formation was not stopped immediately and the next significant cooling occurred more than 1000 years later at the onset of the Younger Dryas (YD). Finally, the YD ends at about 11.5 ka BP and North Atlantic realm again experiences a strong warming [Severinghaus et al., 1998].

The abrupt B/A warming has raised a debate referring the timing of deglaciation in the Northern and Southern Hemisphere. Some workers [e.g. Petit et al., 1999; Sowers and Bender, 1995] interpreted the B/A as the onset of deglacial warming over Greenland, while reanalysis of ice core data has been interpreted to show a warming of approximately one-third of the total termination-I warming over almost 10 ka prior to the onset of the B/A [Alley et al., 2002]. The correlation between the Byrd and GISP2 ice core chronologies based on the isotopic composition of $\delta^{18}O$ of O_2 in air bubbles also yields a northern lead for the onset of warming [Bender et al., 1999]. The latter interpretation is in accordance with the Milankovitch [Milankovitch, 1941] theory. A key element of this theory is that summer insolation at high latitudes of the Northern Hemisphere determines glacial-interglacial transitions connected with the waxing and waning of large continental ice sheets [e.g. Imbrie and Imbrie, 1980].

A similar temporal shape to the B/A onset is detected at other abrupt stadial (cold) to interstadial (warm) transitions, named Dansgaard-Oeschger (DO) events, of the last glacial period [Dansgaard et al., 1984]. These millennial-time scale variations have been linked to various mechanisms such as a salt oscillator [Broecker et al., 1990], deep-decoupling oscillations [Schulz et al., 2002; Winton, 1993], latitudinal shifts in convection sites associated with THC changes induced by negative freshwater flux perturbations in the North Atlantic [Ganopolski and Rahmstorf, 2001], as

well as a stochastic resonance phenomenon [Ganopolski and Rahmstorf, 2002]. The trigger of these millennial-time scale variations is unknown and there is debate as to whether these fluctuations are regular or stochastic [Rahmstorf, 2003; Schulz, 2002; Wunsch, 2000].

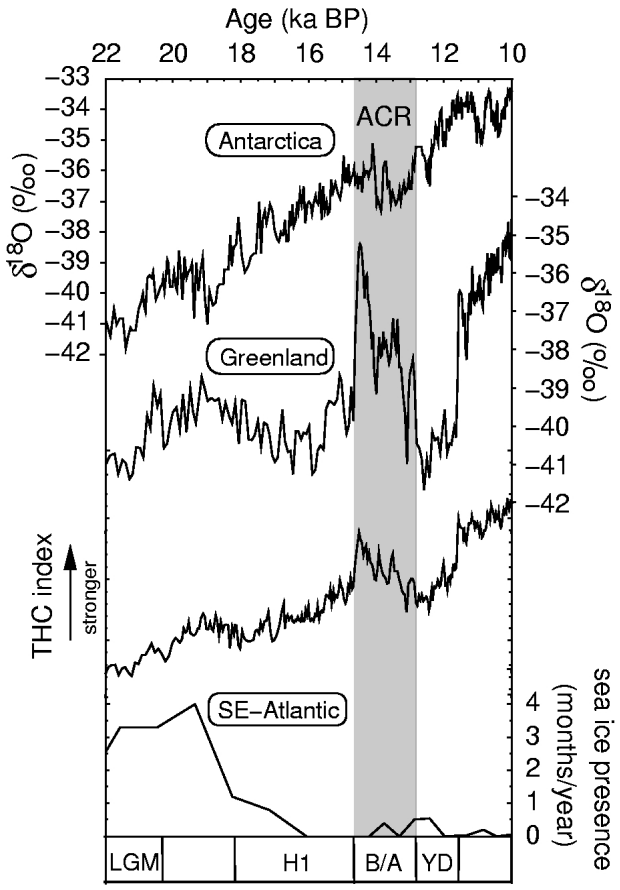

Figure 3.1: Deglacial climate records from ice and ocean sediment cores. High-resolution climate records based on polar ice cores from Antarctica (BYRD), and Greenland (GISP2), during the last deglaciation [Blunier and Brook, 2001] from 22 to 10 ka BP, including a sequence of abrupt climate changes (boundaries of climate intervals, defined as in the GISP2 record: H1, Heinrich 1; B/A, Bølling-Allerød; YD, Younger Dryas. The difference between the $\delta^{18}O_{ice}$ signals from Greenland and Antarctica can be interpreted as an estimate for THC strength, shown as a relative THC index. Deglacial warming in Antarctica commenced between 19 to 17.5 ka BP. At the same time, sea ice in the Southern Ocean diminished to present day assemblages [Shemesh et al., 2002].

Recent modelling investigations have suggested that changes in the Southern Hemisphere are able to trigger a resumption of THC after being stalled. In one scenario gradual warming and receding sea-ice cover around Antarctica leads to an abrupt amplification of the THC [Knorr and Lohmann, 2003], by increasing mass transport into the Atlantic Ocean via the warm and the cold water route [Gordon, 1986] of the ocean conveyor belt circulation [Broecker, 1991]. Additionally, it has been reported that the injection of MWP-1A, possibly originating from Antarctica [Clark et al., 2002]

can increase NADW formation by reducing the density of Antarctic intermediate and bottom water, respectively [Weaver et al., 2003]. These mechanisms illuminate a potential influence of the Southern Ocean for deglacial climate shifts [Stocker, 2003]. On the occasion of the debate of an apparent lead of increasing Southern Hemisphere temperatures, relative to Greenland temperatures during deglaciation, as well as a possible influence of processes in the Southern Ocean for the B/A-onset, we examine the influence of global deglacial warming on the Atlantic THC. With the aid of an ocean general circulation model we simulate the deglacial sequence from the Last Glacial Maximum (LGM) at 20 ka BP until 10 ka BP, containing Heinrich 1, the B/A and the YD. Focus is given to the succession of meltwater pulses that influence the THC during deglaciation and their expression in spatio-temporal temperature pattern. A further aspect is the examination of deglacial changes in the stability behaviour of the THC with respect to meltwater fluxes.

3.2 Methodology

The three-dimensional ocean model is based on the large-scale geostrophic model LSG [Maier-Reimer et al., 1993], which is part of the Bremen Earth system model of intermediate complexity (BREMIC) [Lohmann et al., 2003]. The horizontal resolution is 3.5° on a semi-staggered grid (type 'E') with 11 levels in the vertical. It includes a simple thermodynamic sea ice model, a 3rd order advection scheme for temperature and salinity [Schäfer-Neth and Paul, 2001], and a parameterisation of overflow [Lohmann, 1998]. For glacial conditions the storage of water in inland ice sheets is taken into account by setting all ocean points with present day water depth less than 120 m to land. This causes the Bering Strait to be closed and shallow areas like the Arctic shelves to become land. The ocean is driven by monthly fields of wind stress, surface air temperature and freshwater fluxes, which are taken from a present day and LGM simulation of the atmospheric general circulation model ECHAM3/T42 [Lohmann and Lorenz, 2000; Roeckner et al., 1992]. In order to close the hydrological cycle, a runoff scheme transports freshwater from the continents to the ocean. We employ a modelling approach, which allows an adjustment of surface temperatures and salinity to changes in the ocean circulation, based on an atmospheric energy balance model [Rahmstorf and Willebrand, 1995]. The applied heat flux parameterisation has shown to be a suitable choice, allowing the simulation of observed sea surface temperatures and the maintenance of large-scale temperature anomalies in perturbation experiments [Prange et al., 2003].

For the present day state, we obtain an Atlantic Ocean circulation with an export of 14 Sv (1 Sv = 10^6 m^3 s^{-1}) at 30°S and maximum heat transport of 1.1 PW, which is in the range of observations [Macdonald and Wunsch, 1996]. For the LGM, our modelled ocean circulation is characterized by a weaker circulation of about 8.5 Sv and southward shifted convection sites compared to present day sites [Knorr and Lohmann, 2003; Prange et al., 2002]. The slowdown of the glacial THC is in the range of geological estimates [McManus et al., 2004]. NADW is formed in the sub-polar North

Atlantic and the North Atlantic Current flows in zonal direction along the horizontal density gradients, consistent with reconstructions [Sarnthein et al., 1994]. A detailed description of the modern THC and hydrographic fields can be found elsewhere [Prange et al., 2003; Romanova et al., 2004].

3.2.1 Experimental set-up

The experiments in this study will be consisting of two major parts. In the first part we simulate the deglacial climate sequence between about 20 ka BP and the onset of the B/A warm phase (experiments B1-B4). In the second part attention is paid to investigate the effect of MWP-1A on the THC and to evaluate its impact on the B/A and the YD (experiments MWP1–MWP5). These experiments are completed by a stability analysis of the THC, concerning North Atlantic freshwater perturbations.

Deglacial warming is implemented by a linear transition from glacial to interglacial background climate being accomplished within 15 ka. The background climate is provided by monthly fields of air temperature, sea ice (Southern Hemisphere) and wind stress, linearly interpolated between the LGM conditions at 20 ka BP and present day climatology. All meltwater discharge to the North Atlantic is uniformly applied between 20°N and 50°N, according to deglacial meltwater routes via the Mississippi, St. Lawrence and Hudson River, respectively [Clark et al., 2001].

3.2.2 Last Glacial Maximum, Heinrich-1 and Bølling-Allerød

In the first set of experiments we focus on the transition from the LGM to the B/A and the boundary conditions attained at model year 7000 remain constant in order to obtain an equilibrium climate state (experiments B1-B4). The gradual transition of 7000 years, between glacial and present-day background climate conditions, is related to 13 ka BP on a geological time scale and 7/15 (ca. 47 %) of the total termination-I warming (Figure 3.2a).

Additional to the changed background climate in experiment B1, different freshwater flux perturbations are applied to the North Atlantic (experiments B2, B3 and B4) to mimic the effect of melting ice from the Laurentide and Fennoscandian Ice Sheets. Such meltwater pulses are motivated by geological data at 19 ka BP (19 ka MWP) [Clark et al., 2004], as well as centred at 17.5 ka BP (H1b) and 16 ka BP (H1a) [Bard et al., 2000]. In experiment B2, the 19 ka MWP and the Heinrich-pulses H1a and H1b are induced in the model. The 19 ka MWP is simulated by a freshwater magnitude of 0.25 Sv [Clark et al., 2004] with a duration of 200 years. Both Heinrich spikes H1a and H1b are performed with a 400 year lasting freshwater flux of 0.15 Sv [Chappell, 2002]. In experiment B3, we induce the 19 ka MWP, whereas in B4 the Heinrich events H1a and H1b are considered only. In addition to these freshwater perturbations a deglacial background meltwater discharge of 0.05 Sv is applied at the remaining time of experiment B2, B3 and B4.

3.2.3 Bølling-Allerød, meltwater pulse 1A and Younger Dryas

The second set of experiments is constitutive on experiment B2 after 6000 model years. In these experiments termination-I warming is continued over another 4000 years until the transition reaches 2/3 (ca. 66 %) of the total glacial-interglacial transition. Supplementary, a meltwater pulse is applied that linearly increases to different maxima within 500 years and subsequently decreases with the same gradient to zero (Figure 3.6a). In MWP1 and MWP2 a maximum meltwater injection of 0.55 Sv to the North Atlantic starts after 6000 and 7000 model years, respectively. In experiment MWP3 a meltwater pulse of the same magnitude is released to the South Atlantic south of 60°S, to imitate an Antarctic origin of MWP-1A [Clark et al., 2002]. In experiment MWP4 and MWP5 the maximum meltwater flow amounts to 0.55 Sv and 0.2 Sv, which is uniformly distributed to both, the North and South Atlantic. Furthermore, we examine the stability of the THC in experiment B2 after 7000 model years, with respect to North Atlantic freshwater discharge. We apply a slowly varying freshwater anomaly with a rate of 5×10^{-5} Sv yr^{-1} in the hysteresis analysis. Integration starts with a deglacial background meltwater flux of 0.05 Sv that increases to 0.35 Sv. Subsequently, the freshwater input is decreased until –0.35 Sv, and then again increased to 0.05 Sv to close the loop.

3.3 Results

3.3.1 Last Glacial Maximum, Heinrich-1 and Bølling-Allerød

All experiments clearly exhibit an abrupt transition from a weak glacial to a strong interglacial THC within 7000 years (Figure 3.2b). The simulations reveal that the transition depends on the succession of freshwater pulses to the North Atlantic. Compared to B1, the overturning response in the meltwater pulse experiments (B2, B3, B4) is delayed in time (Figure 3.2b). In experiment B1 and B2 the rapid amplification of the THC occurs after 3000 and 6000 model years, respectively. These time intervals are related to a warming of 1/5 and 2/5 of the total termination-I warming and the respective transitions can occur from the THC “on-mode” and from the THC “off-mode”.

In the phase prior to the rapid amplification of the THC, different effects influence NADW formation. The gradual warming and melting of sea ice reduces the density of the surface waters in the North Atlantic (Figure 3.3a, b) while gradual warming in the Southern Ocean increases the salinities in the South Atlantic (Figure 3.3c), which preconditions NADW formation. These effects counteract each other, resulting in a relatively small NADW export reduction of 2 Sv in B1 during the first 3000 model years (Figure 3.2b). The THC in the meltwater experiments B2, B3 and B4 is dominated by the simulated freshwater pulses, which strongly reduce the surface salinity and hence the density in the deep-water formation regions. Both, warming and freshwater perturbations

destabilize NADW formation and decrease the strength of the Atlantic THC (Figure 3.2b, Figure 3.3a, b).

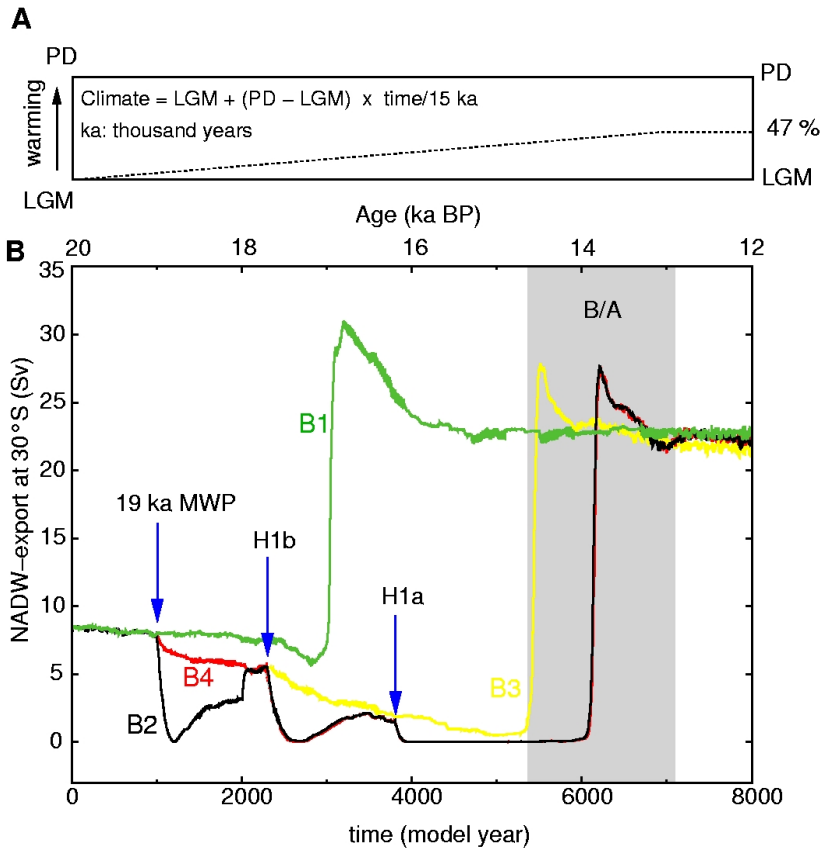

Figure 3.2: Illustration of temporal changes in the global background climate and NADW export at 30°S in the Atlantic Ocean. (a) The background climate conditions are linearly interpolated between glacial (LGM), and modern (PD), conditions. All experiments start from the glacial equilibrium. Gradual warming is stopped after 7000 model years, which is related to 7/15 of the total termination-I warming. (b) The green curve (B1) represents the experiment without any deglacial freshwater pulses to the North Atlantic. The other experiments B2 (yellow curve), B3 (red curve), and B3 (green curve), exhibit different successions of deglacial meltwater pulse scenarios to the North Atlantic. The beginning of the respective freshwater perturbations is indicated by the blue arrows (for further explanation see experimental set-up).

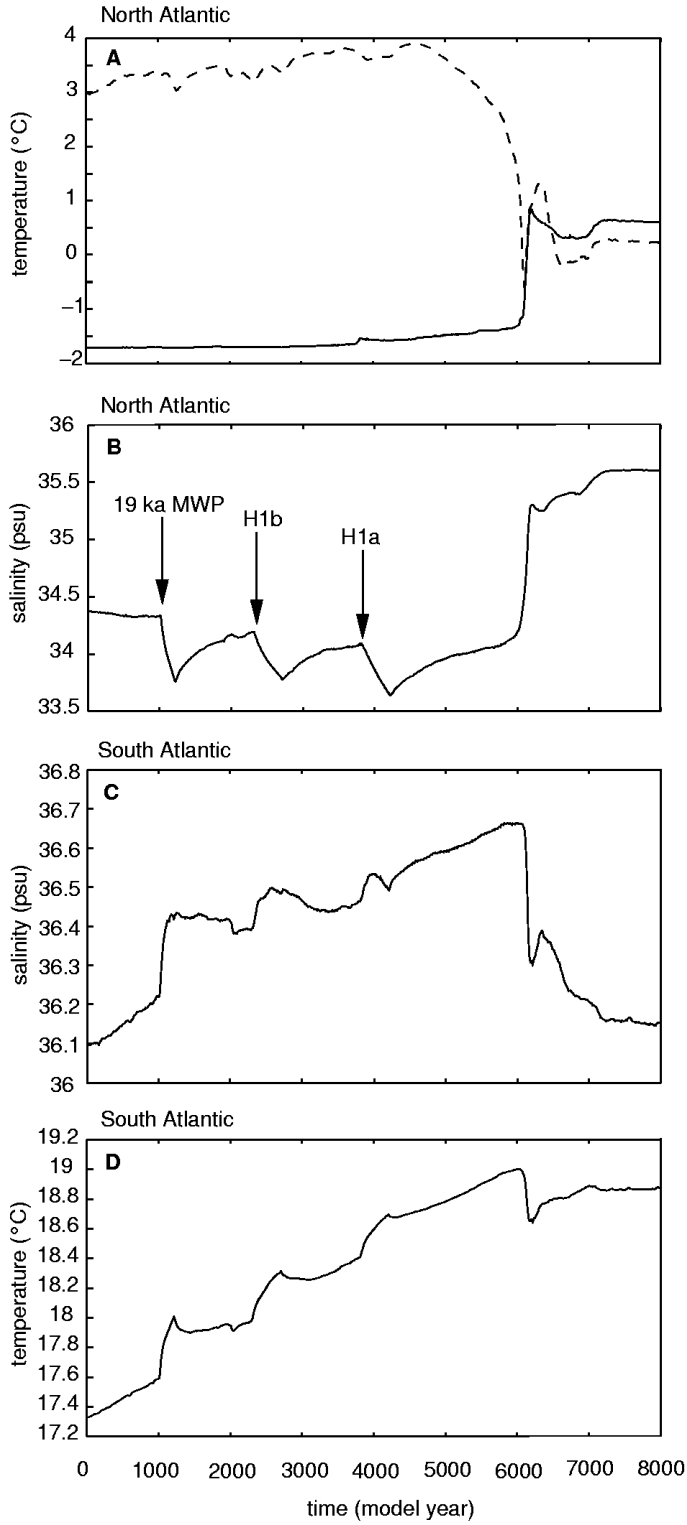

Figure 3.3: Temporal temperature and salinity changes in the Atlantic Ocean in experiment B2. (a) SST (°C), and (b) salinity (psu), at the surface Atlantic are averaged between 65°N - 75°N. The arrows mark the onset of the meltwater pulses. Additionally, the averaged temperature in the North Atlantic between 850 m and 1500 m (dashed curve) is shown. Panels (c) and (d) show the respective changes at the surface South Atlantic averaged between 20°S - 30°S.

In the following, we focus on experiment B2, which includes the simulation of the 19 ka MWP [Clark et al., 2004], as well as the Heinrich meltwater pulses H1a and H1b [Bard et al., 2000]. Details of the model responses are shown in Figures 3.3, 3.4 and 3.5. Figure 3.3 displays temperature and salinity changes in the North and South Atlantic. Figures 3.4 and 3.5 show the spatial temperature signature in response to the 19 ka MWP and the abrupt onset of the B/A flow regime, respectively.

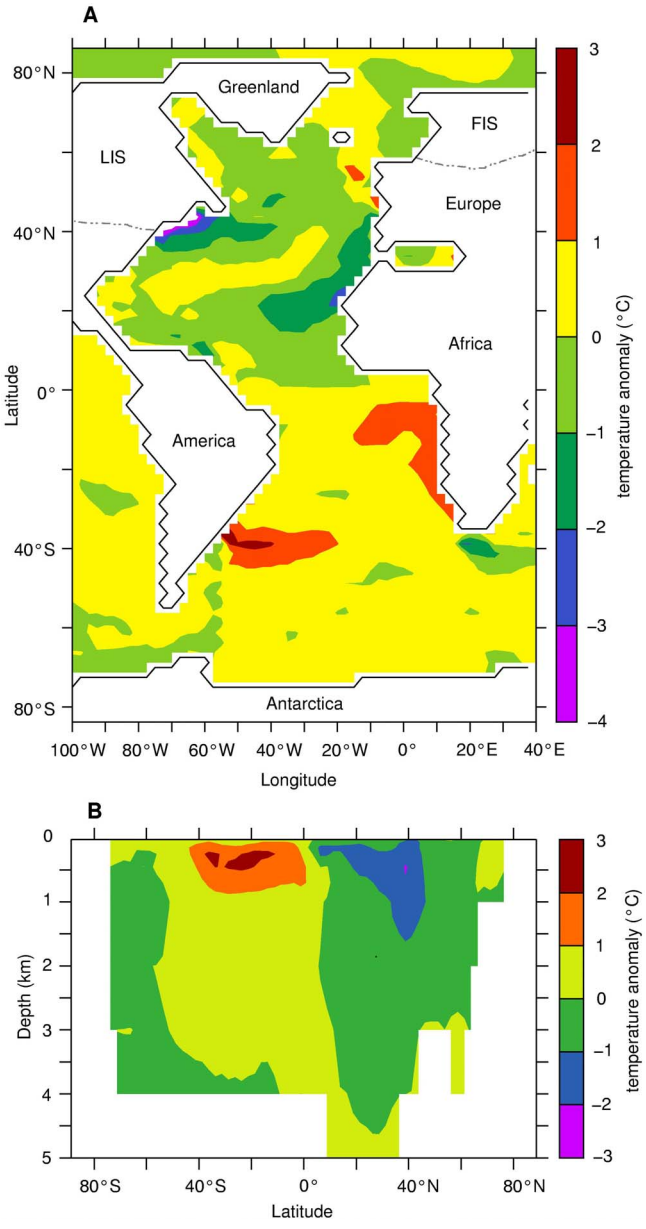

Figure 3.4: Spatial temperature changes in the Atlantic as response to the 19 ka MWP. (a) Annual mean surface temperature (°C) field differences in the Atlantic Ocean in experiment B2 between 1200 and 1000 years as response to the 19 ka MWP; and (b) the respective zonally averaged temperature differences. The gray lines in (a), indicate the LGM extension of the Laurentide (LIS), and Fennoscandian (FIS), Ice Sheets, respectively.

Experiment B2 shows that the NADW formation is significantly reduced immediately in response to the freshwater discharges and its export at 30°S diminishes at all occasions (Figure 3.2b), linked to decreasing salinities and hence density in the near-surface North Atlantic (Figure 3.3b). The 19 ka MWP causes a temporary shut down of the THC. As the meltwater inflow decreases the THC recovers. After the meltwater spikes H1a and H1b the Atlantic overturning circulation remains in the "off-mode" until the resumption of the THC at the onset of the B/A. As response to the 19 ka MWP, the SST decrease 1-2 °C in large parts of the North Atlantic, while South Atlantic SST increase up to 3°C off the Argentinean coast (Figure 3.4a). This seesaw signature is also prominent in the intermediate and deeper layers of the Atlantic Ocean (Figure 3.3a, 4b). The strongly reduced THC decreases the interhemispheric oceanic transport of heat and salt, causing a delayed warming of the surface North Atlantic (Figure 3.3a), as well as additional warming and a salt build up in the near-surface South Atlantic by 0.6 psu during the first 6000 model years (Figure 3.3c, d). The increasing salinities in the South Atlantic are linked to the regaining influence of the warm water route, which enhances the inflow of relatively warm and saline waters from the Indian Ocean to the South Atlantic. The Antarctic Circumpolar Current shifts southward and increases in strength by about 80 % (not shown).

The abrupt amplification of the Atlantic overturning circulation occurs after 6000 model years (Figure 3.2b). It is associated with a strong warming in particular in the Labrador Sea (Figure 3.5a) and an abrupt boost of NADW formation (Figures 3.2b, 3.5c). The regaining influence of the warm water route and the enhanced salt transport to the Atlantic counteracts the meltwater inflow to the North Atlantic. Although, convective activity is considerably reduced in presence of the THC "off-mode", there is still some open ocean convection in the North Atlantic (Figure 3.5c). The wind-driven induced convective activity leads to the maintenance of a weak and shallow overturning cell in the North Atlantic. Moreover, freshwater transports by the horizontal subtropical gyres enable an exchange with tropical water masses. The deglacial reduction of the catabatically induced southward wind component in the high-latitude North Atlantic enhances the near surface transport of relatively saline waters to the northern North Atlantic that explains the strong intensification of convective activity (Figure 3.5c). A detailed description of the THC "off-mode" dynamics of the applied OGCM can be found in [Prange et al., 2003].

Once convection is initiated, the THC is amplified by a positive feedback between northward salt transport and overturning strength. The maximum northward oceanic heat-transport increases from 0.8 PW to 1.6 PW after 8000 model years (not shown). This leads to a rapid increase of North Atlantic SST up to 10°C (Figure 3.5a), while temperatures in the South Atlantic decrease (Figures 3.3d, 3.5b). After the onset of NADW formation in formerly ice covered parts of the Labrador Sea and Nordic Seas, relatively warm and saline waters from deeper layers of the North Atlantic rise to the surface and lose their heat rapidly to the colder overlaying atmosphere (Figure 3.3a). The combined cooling and conservation of salt causes a density increase at the surface North Atlantic, which enhances the generation of NADW and therefore increases the strength of the Atlantic THC (Figure 3.2b).

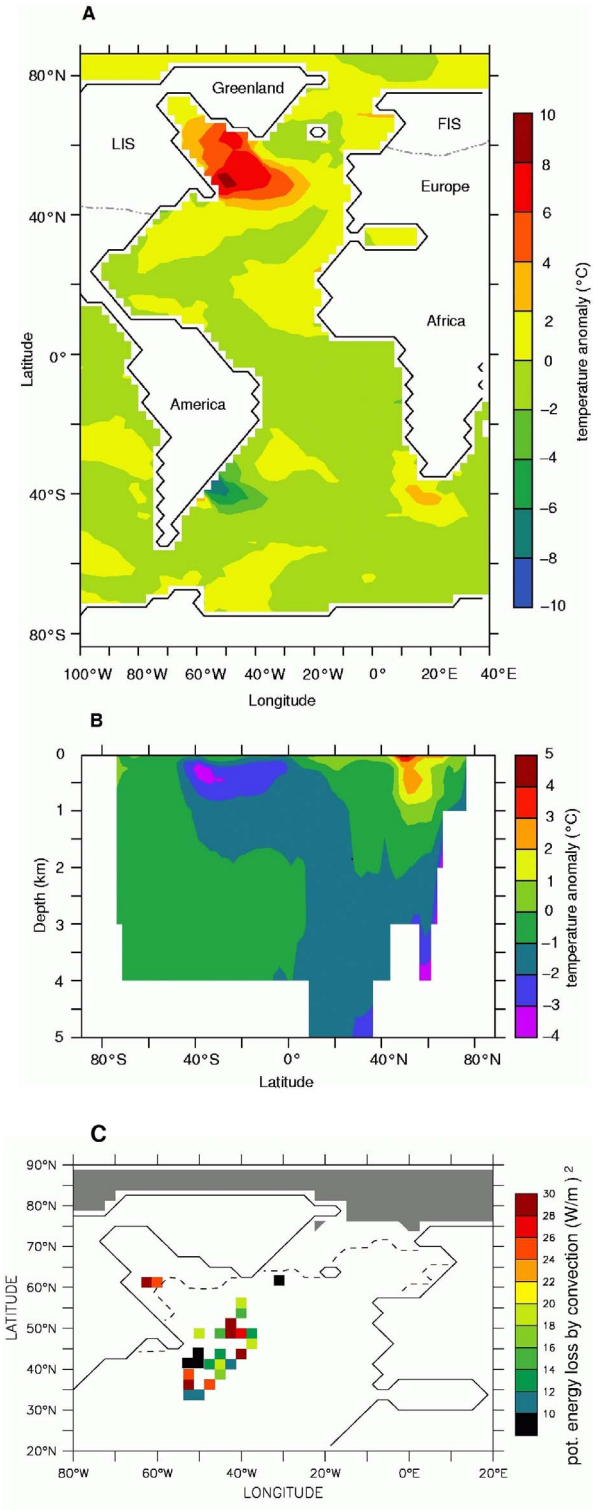

Figure 3.5: Spatial temperature differences in the Atlantic as response to the "kick-start" of the THC, associated with the onset of the B/A. (a) Annual mean surface temperature (°C) field differences in the Atlantic Ocean in B2 between 6200 and 6000 model years, as response to the abrupt resumption of the interglacial Atlantic THC; and (b) the respective zonally averaged temperature changes; the lower panel (c) displays changes in the North Atlantic convective activity (W/m^2), the black marks indicate weak and shallow convection sites prior to the THC amplification. The gray shaded area and the dashed line indicate the annual men sea ice heights of 8 m and 2 m, respectively.

This convective event is only temporarily active until the subsurface-temperatures are relaxed to the abruptly changing surface conditions in the North Atlantic realm (Figure 3.3a). As a result, a cooling of more than 3°C is detected in the intermediate water depths between 850 and 1500 m of the North Atlantic (Figure 3.3a). The temperatures in deeper layers of the North Atlantic below 2000 m decrease by 1-2°C (Figure 3.5b). A convective "flush" generally occurs if deep-water formation is initiated in areas where temperature increases with depth, so that the energy stored in deeper layers of the North Atlantic can be released to the overlaying atmosphere.

At the resumption of the THC, surface salinities in the North Atlantic increase by more than 1 psu (Figure 3.3b), while South Atlantic salinities decrease by 0.4 psu. These changes in the Southern Ocean amplify the advection of excess salt from the tropics to the North Atlantic realm at the resumption of the THC.

3.3.2 Bølling-Allerød, meltwater pulse 1A and Younger Dryas

The first part of the results has presented that global deglacial warming leads to a THC amplification from the "off-mode", leading to an abrupt temperature increase in the North Atlantic by up to 10°C. In the following we try to evaluate the impact of meltwater discharge in the order of MWP-1A on the restart of the THC (Figure 3.6) and analyse the stability behaviour with the aid of a hysteresis diagram (Figure 3.7).

In MWP1, the release of the MPW-1A to the North Atlantic retards the abrupt THC amplification by about one decade and dampens the maximum amplitude by 7 Sv, but does not inhibit the amplification of the THC. The rising freshwater flux of MWP-1A causes a drop back to the THC "off-mode" simultaneously to the maximum meltwater magnitude. The THC remains stalled until the warming proceeds to more than 50 % of the total termination-I warming at 7500 years. After 7500 model years the THC "off-mode" recovers abruptly to a stronger interstadial circulation mode within a century.

In experiment MWP2 the MWP-1A is released 1000 years later than in MWP1 and the THC is also suppressed to the "off-mode", and the recovery to an interstadial THC occurs 500 years after the cessation of MWP-1A within a century. By way of contrast the application of MWP-1A in the Weddel Sea results in a slight increase of the NADW export in experiment MWP3. The division of the meltwater inflow to both, the North Atlantic and the Weddell Sea in MWP4 also ceases NADW export to the South Atlantic for about 1000 years with a minimal retarded model response compared to MWP2. The application of a weaker meltwater pulse than in MWP4 temporarily reduces, but does not shut-down the Atlantic THC in MWP5. Moreover, it is evident in this experiment that the course of NADW intensification is directly aligned to the reduction of the freshwater forcing after the maximum meltwater magnitude has been reached, while the THC recovery from the "off-mode" in MWP1, MWP2, and MWP4 is delayed by about 500 years.

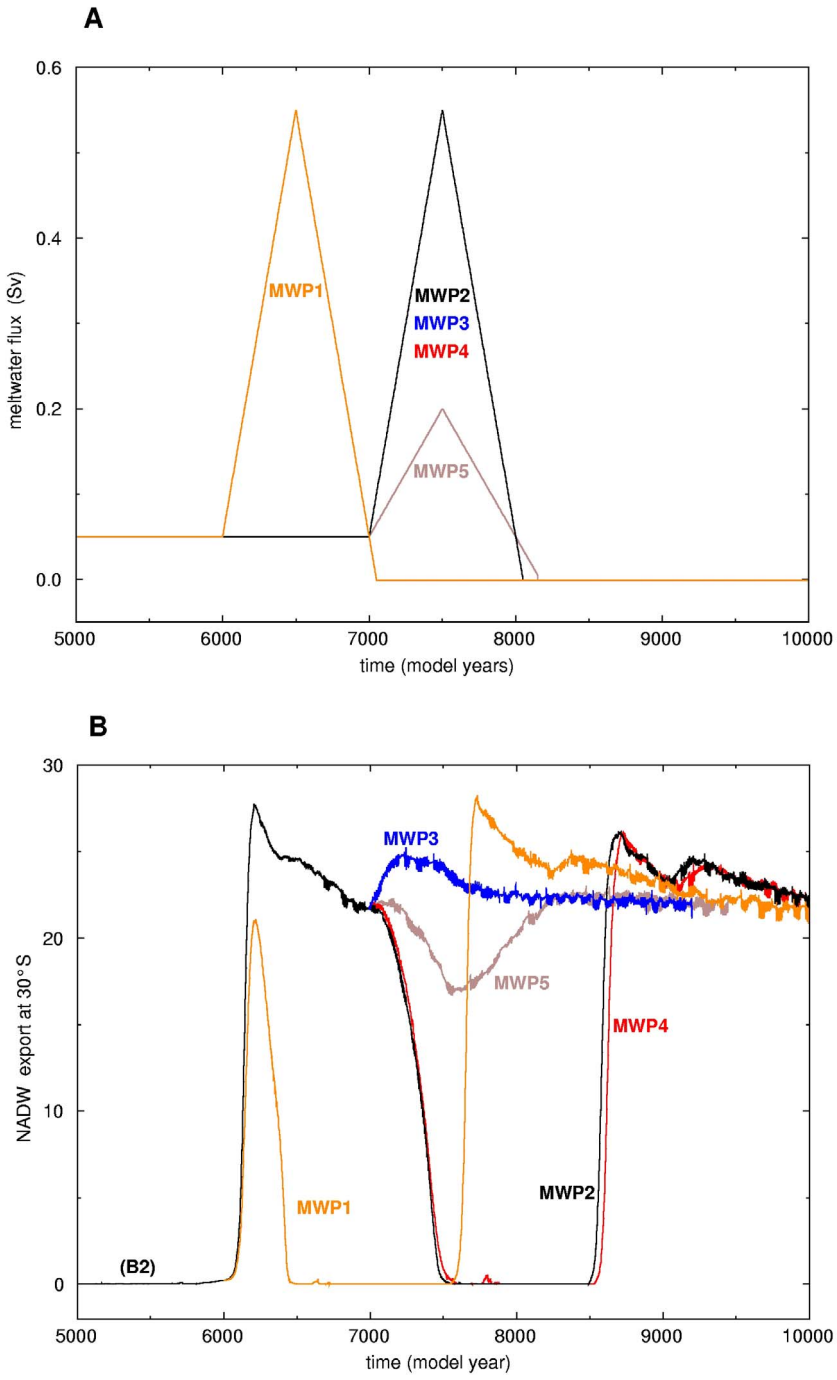

Figure 3.6: Temporal signature of the different meltwater scenarios and accompanying changes in the NADW export at 30°S. (a) The different meltwater fluxes (Sv) are assigned to the different experiments by the respective colours (b) In MWP1 the onset of MWP-1A is after 6000 years prior to the onset of the B/A in B2. In experiments MWP2-MWP5, MWP-1A is discharged after 7000 model years. In MWP2 and MWP3 it is released to the North Atlantic and the Weddell Sea, respectively. In MWP4 and MWP5 the pulses are discharged uniformly to both locations.

The hysteresis curve (Figure 3.7), starting from experiment B2 after 7000 years, exhibits that the restarted THC posses a pronounced bistability for positive freshwater fluxes between about 0.025 Sv and 0.25 Sv. The restarted ocean circulation state is driven by heat loss, while freshwater tends to break the flow. Contrary, the glacial THC shows only a weak bistability in the area of positive freshwater fluxes up to 0.15 Sv. The different hysteresis loops clearly demonstrate the relative insensitivity of the restarted Atlantic THC concerning meltwater pulses of less than 0.25 Sv to the North Atlantic.

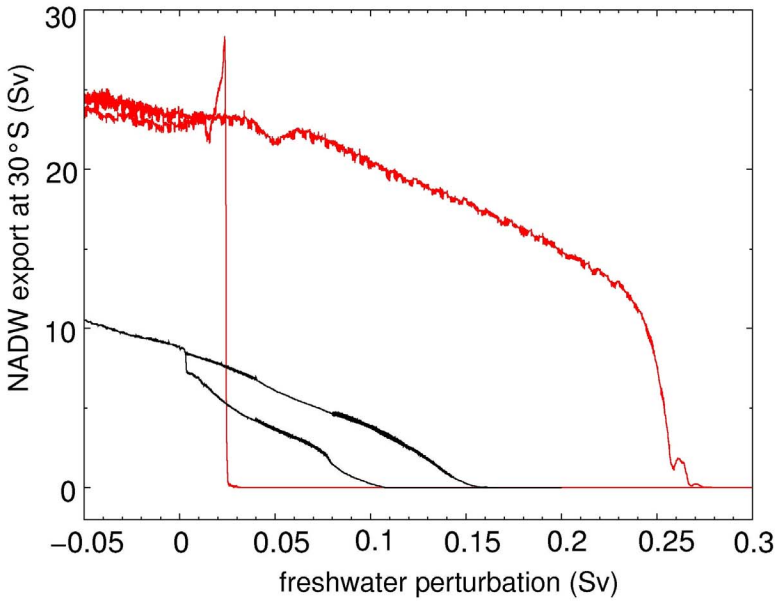

Figure 3.7: Stability diagrams for the glacial and restarted THC constructive on experiment B2. The hysteresis curves for the restarted interstadial ocean circulation (red curve) in experiment B2 after 7000 model years, and the glacial Atlantic THC (black curve) [taken from Knorr and Lohmann, 2003].

3.4 Discussion

3.4.1 Last Glacial Maximum until the Bølling-Allerød

In the first part of this study, we have shown that deglacial global warming leads to an abrupt transition from a stalled THC to a stronger interstadial ocean circulation associated with the B/A onset (Figure 3.2b). In the deglaciation scenarios simulated in B2, B3 and B4 the transition takes place after about 2/5 of the total deglacial warming has been reached. This is in quantitative agreement with the analysis of ice core data, suggesting that about one-third of the total termination-I warming has been achieved before the abrupt warming into the B/A [Alley et al., 2002].

The shift between the THC “off-mode” and the B/A flow-regime is amplified by salinity advection (Figure 3.3c) from the tropics and the South Atlantic (with reopened warm water route). This large-scale salinity advection is in accordance with marine sediment core data that exhibit an abrupt decrease of the surface salinities in the Caribbean Sea at the initiation of the B/A [Schmidt et al., 2004].

The simulated transition between the weak glacial and the stronger interstadial THC can be related to the transition from a weak Heinrich-mode to the more vigorous THC during the B/A [McManus et al., 2004]. The time interval of about 5500 - 6000 years in B2, B3 and B4 (Figure 3.2) corresponds to the deglacial phase beginning at the onset of warming until the transition to the B/A at about 14.7 ka BP documented in ice core records (Figure 3.1) [e.g. Blunier and Brook, 2001; Sowers and Bender, 1995]. The relatively cold conditions in the North Atlantic, as indicated by marine sediment data during Heinrich-I sequence [e.g. Bard et al., 2000], can be attributed to a shut down of the Atlantic meridional overturning circulation and reduced oceanic heat transport, due to freshwater release by melting icebergs (Figure 3.2b). In conjunction with the 19 ka MWP [Clark et al., 2004], the Heinrich-I freshwater discharges contributed to deglacial warming in the Southern Hemisphere (Figures 3.3d, 3.4a, b) superimposed on the general warming trend. The recovery of the THC after the 19 ka MWP indicates that at this point of deglaciation the climate system is still near its glacial state, which has shown to be monostable with respect to freshwater perturbations [Knorr and Lohmann, 2003; Prange et al., 2002]. The spatial pattern of the SST changes in response to meltwater pulses during deglaciation shows that the surface regions off Portugal [Bard et al., 2000] and Namibia [Kim et al., 2002] are particularly sensitive to detect THC weakening and the associated cooling and warming.

Accentuated warming in the Southern Hemisphere and a reduction of sea ice cover to interglacial conditions between 19–18 ka BP, as documented by proxy data from the Southern Ocean [Sachs et al., 2001; Shemesh et al., 2002], can be reconciled with Northern Hemisphere cooling (Figure 3.1), insofar as additional warming in the South Atlantic (Figure 3.3d) is the result of an oceanic “seesaw” response to the 19 ka MWP. At the resumption of the THC, northward oceanic heat transport is reactivated. As a result, temperatures and salinity in the South Atlantic decrease

(Figures 3.3c, d and 3.5a, b) and Southern Hemisphere cooling begins (Figure 3.1), while the temperatures in the North Atlantic realm almost reached interglacial values. The spatial temperature differences in the Atlantic, associated with the resumption of the THC show that the Labrador Sea might be particularly important for deglacial climate change over Greenland (Figure 3.5a), due to the large temperature response of up to 10°C (Figure 3.5a), which is in the range of the temperature increase documented in Greenland ice cores [e.g. Cuffey et al., 1995; Johnsen et al., 1995].

In previous model investigations, the Southern Ocean has been shown to play an active role for the deglacial resumption of the THC at the B/A onset [Knorr and Lohmann, 2003; Weaver et al., 2003]. The simulations presented here exhibit that gradual global warming can trigger an abrupt amplification of the glacial THC. Once NADW generation is initiated, the THC is temporarily reinforced by a convective event in the North Atlantic that is prominent in both scenarios. In case of deglacial global warming, the rapid transition between the glacial and interstadial THC mode can occur from the “on-mode” (experiment B1) and from the “off-mode” (experiment B2 and B4). The resumption of the THC via Southern Ocean warming requires a phase of gradual NADW-intensification that triggers the abrupt sea ice margin retreat in the North Atlantic via increased northward oceanic heat transport. The gradual NADW amplification is linked to advection of salty waters from the tropics and the Indian Ocean to the formation regions of NADW similar to a process described by Gordon et al. [1992]. Additionally, these processes might be amplified by large-scale discharge of meltwater from the Antarctic ice sheet, reducing the density of deep and intermediate waters from Antarctica, which compete with NADW and therefore accelerate the THC [Weaver et al., 2003]. Therefore, it has been proposed that the Southern Ocean might represent a “Flywheel” of the Atlantic overturning circulation on paleoclimatic time scales [Knorr and Lohmann, 2004].

The “kick-start” of the THC at the transition to the B/A in the global warming, as well as in the Southern Hemisphere warming scenario is forced by strong vertical heat release from deeper ocean layers to the surface North Atlantic. This heat transfer might provide large amounts of energy, necessary for deglaciation. The characteristic opposite temperature evolution of the surface and subsurface layers (Figure 3.3a) may be a sensitive indicator for the resumption of THC during deglaciation. This vertical “smoking gun” might also be detectable in proxy data of the North Atlantic. Although no direct estimate of intermediate water temperature variations exists as yet, benthic oxygen-isotope data [Dokken and Jansen, 1999; Rasmussen et al., 2002; van Kreveld et al., 2000] corroborate the inferred subsurface warming prior to or concurrent to DO warmings.

3.4.2 Bølling-Allerød until the Holocene

In the second part of this work it has been reported that the stronger interstadial THC is characterized by a distinctive bistability (Figure 3.7) with respect to positive freshwater fluxes to

the North Atlantic, indicating a thermal flow regime [Rahmstorf, 1996; Stommel, 1961]. This is in accordance with previous modelling work, suggesting that the flow regime of the THC depends sensitively on the background climate [Prange et al., 2002]. The deglacial shift from the monostable glacial to the interstadial bistable flow regime bears the potential for a long-term THC weakening in response to sufficiently large meltwater pulses to the North Atlantic (Figure 3.6). Indeed, the YD has been associated with a THC shut down [e.g. Broecker et al., 1985]. The resulting Northern Hemisphere cold phase has been identified in a broad range of proxy data around the globe, including ice core records [e.g. Blunier and Brook, 2001; Severinghaus and Brook, 1999], ocean sediment cores [e.g. Koc et al., 1993]. Surprisingly, the onset of the YD occurred about 1000 years after MWP-1A, although the THC in current models [Manabe and Stouffer, 1997; Saravanan and McWilliams, 1995; Stocker and Wright, 1991] responds to freshwater forgings in the order of 0.1 Sv without delay. In this context it has been proposed that MWP-1A largely originated from the Antarctic Ice Sheet, where its effect on the THC would be reduced considerably [Clark et al., 2002]. Our results support this explanation, since a reasonable deglacial meltwater spreading to the Northern and Southern Hemisphere [Rohling et al., 2004] would weaken but does not stop NADW formation (Figure 3.6). Even though the MWP-1A did not trigger a THC shut down and the associated YD directly, it probably preconditioned this event by shifting the ocean circulation towards a state in the area of positive freshwater fluxes in the hysteresis curve (Figure 3.7). In this position near the bifurcation point the THC is extremely sensitive and even small freshwater variations within the natural variability are sufficient to cause rapid reduction of the THC strength and accompanying northward oceanic heat transport. This might explain the onset of the YD in absence of any noticeable deglacial meltwater pulses [Fairbanks, 1989]. The non-appearance of a comparable thermally antiphased southern signal at the YD onset suggests that changes in the THC were either too short or to small too be clearly registered in climate records [Clark et al., 2002]. The latter explanation seems to be in accordance with a THC attenuation by cumulative deglacial freshwater fluxes to the North Atlantic that already reduced northward oceanic heat transport prior to the onset of the YD.

Cooler conditions during the YD reduced snow accumulation over Greenland [Kapsner et al., 1995] and deglacial meltwater inflow to the North Atlantic that results in a shift along the lower branch of the hysteresis curve towards zero freshwater perturbation. This shift might have caused a rapid amplification of the THC, resulting in a tremendous temperature increase of about 15°C, as derived from thermally fractionated gases in Greenland ice cores [Severinghaus et al., 1998]. The respective transition at 11.5 ka BP marks the end of the YD [Severinghaus and Brook, 1999] and the transition to relatively warm conditions that are prevailing during the Holocene. A possible sequence of changes in the THC regime and the temporal integration in a deglacial framework is shown in Figure 3.8.

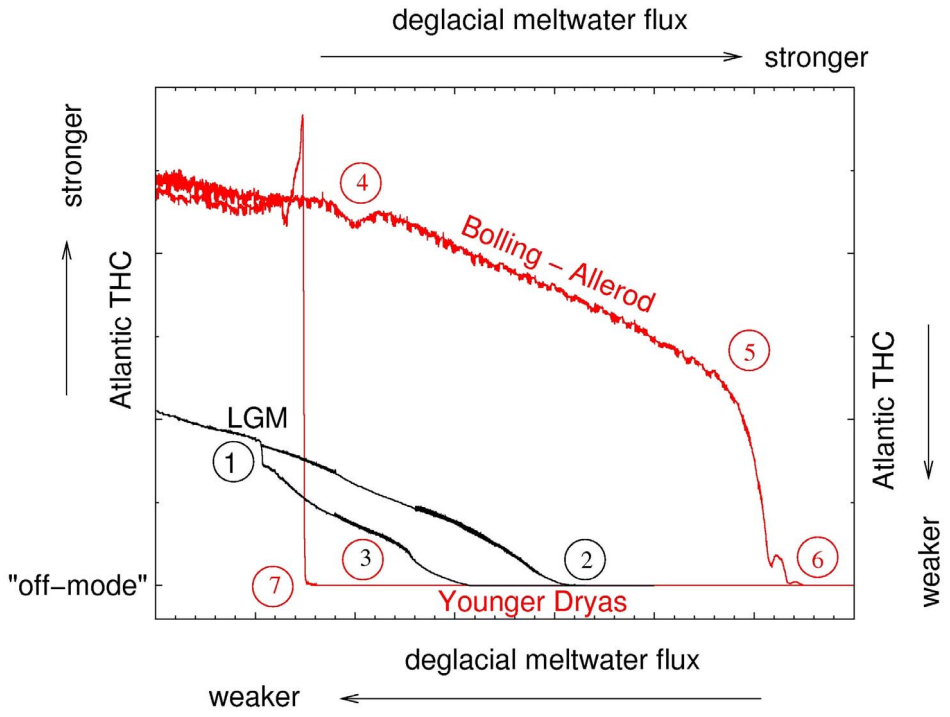

Figure 3.8: Schematic representation of degalcial THC changes within a temporal classification of the deglacial climate sequence. (1) Starting point is the LGM 20,000 years ago that is followed by a transition to the THC “off-mode” (2) associated with the 19 ka MWP and H1. Despite deglacial meltwater fluxes (3) the onset of the B/A is initiated (4). Subsequently, boosted Northern Hemisphere warming during the B/A increases deglacial meltwater discharge (including MWP-1A), which shifts the system near the bifurcation point (5). At this point even small changes in the North Atlantic freshwater budget are sufficient to drop the THC to the “off-mode” that marks the YD onset (6). The resulting Northern Hemisphere cooling reduces the meltwater flux to the North Atlantic and the THC is abruptly restated at the end of the YD (7) that again might increase the meltwater flux leading to MWP-1B [Fairbanks, 1989], which is not strong enough to shut down the THC. The colouring of the numbers relates the position of the climate states to the different hysteresis curves.

3.5 Conclusions

We conclude that the resumption of the Atlantic THC from a strongly reduced THC during deglaciation can be triggered by deglacial global or Southern Hemisphere warming [Knorr and Lohmann, 2003] in presence of meltwater discharge to the North Atlantic. The abrupt augmentation of the THC in the global warming scenario is governed by an abrupt initiation of NADW formation in particular in the Labrador Sea, linked to increasing salinities in the high latitude North Atlantic that increase density, after H1a. The THC is amplified by heat release from the sub-surface ocean in the North Atlantic, as well as large-scale salinity advection from the South Atlantic/Indian Ocean and the tropics to the formation areas of NADW. Superimposed on the deglacial warming trend, freshwater perturbations to the North Atlantic at 19 ka and H1 result in reduced northward heat transport associated with cooling in the north and warming in the south. The THC provides an active link between both hemispheres, by “heat-storage” in the South [Stocker, 1998] during the Heinrich-I sequence or “heat piracy” from the South Atlantic [Crowley, 1992], leading to cold conditions over Antarctica (ACR) at the onset of the B/A. The temporal and spatial pattern of interhemispheric climate changes is in agreement with ice core [e.g. Bender et al., 1994; Petit et al., 1999; Sowers and Bender, 1995] and ocean sediment records [e.g. Bard et al., 2000; Charles et al., 1996; Sarnthein et al., 1994].

Furthermore, it has been shown that the restarted stronger interstadial THC is relatively insensitive, with respect to deglacial meltwater and possesses coevally a distinctive bistability for cumulative positive freshwater fluxes to the North Atlantic. A reasonable distribution of MWP-1A to the Northern and Southern Hemisphere can therefore explain the continuance of the THC and the “delayed” onset of the YD at about 13 ka BP [Severinghaus and Brook, 1999]. Therefore, the THC bears the potential to react with a substantial long-term weakening in accordance with the YD. The end of this 1000 years lasting cold phase can be explained by a reduction of the deglacial melt water flow that caused a rapid amplification of the THC. Comprising we find that the interhemispheric temperature evolution as recorded in paleodata can be understood as an interplay of processes operating in both hemispheres that are connected via the Atlantic THC. Therefore, warming induced Southern Ocean changes are an integral part of the deglacial THC intensification [Knorr and Lohmann, 2003], since Southern Hemisphere warming can also evolve as a seesaw response to a meltwater reduced Atlantic THC in a deglacial global warming scenario.

References:

Alley, R. B., E. J. Brook, and S. Anandakrishnan (2002), A northern lead in the orbital band: north-south phasing of Ice-Age events, *Quaternary Science Reviews*, 21, 431-441.

Alley, R. B., and P. U. Clark (1999), The deglaciation of the northern hemisphere: A global perspective, *Annual Review of Earth and Planetary Sciences*, 27, 149-182.

Arz, H. W., J. Patzold, and G. Wefer (1999), The deglacial history of the western tropical Atlantic as inferred from high resolution stable isotope records off northeastern Brazil, *Earth and Planetary Science Letters*, 167, 105-117.

Bard, E., F. Rostek, J. L. Turon, and S. Gendreau (2000), Hydrological impact of Heinrich events in the subtropical northeast Atlantic, *Science*, 289, 1321-1324.

Bender, M., T. Sowers, and E. Brook (1997), Gases in ice cores, *Proceedings of the National Academy of Sciences of the United States of America*, 94, 8343-8349.

Bender, M., T. Sowers, M. L. Dickson, J. Orchardo, P. Grootes, P. A. Mayewski, and D. A. Meese (1994), Climate Correlations between Greenland and Antarctica During the Past 100,000 Years, *Nature*, 372, 663-666.

Bender, M. L., B. Malaize, J. Orchardo, T. Sowers, and J. Jouzel (1999), High Precision Correlations of Greenland and Antarctic Ice Core Records Over the Last 100 kyr, *Geophysical Monograph*, 112, 149-164.

Blunier, T., and E. J. Brook (2001), Timing of millennial-scale climate change in Antarctica and Greenland during the last glacial period, *Science*, 291, 109-112.

Blunier, T., J. Schwander, B. Stauffer, T. Stocker, A. Dällenbach, A. Indermühle, J. Tschumi, J. Chappellaz, D. Raynaud, and J.-M. Barnola (1997), Timing of temperature variations during the last deglaciation in Antarctica and the atmospheric CO2 increase with respect to the Younger Dryas event, *Geophysical Research Letters*, 24, 2683-2686.

Broecker, W. S. (1991), The great ocean conveyor, *Oceanography*, 4, 79-89.

Broecker, W. S., T.-H. Peng, J. Jouzel, and G. Russell (1990), The magnitude of global fresh-water transports of importance to ocean circulation, *Climate Dynamics*, 4, 73-79.

Broecker, W. S., D. M. Peteet, and D. Rind (1985), Does the ocean-atmosphere system have more than one stable mode of operation?, *Nature*, 315, 21-25.

Chappell, J. (2002), Sea level changes forced ice breakouts in the Last Glacial cycle: new results from coral terraces, *Quaternary Science Reviews*, 21, 1229-1240.

Charles, C. D., J. Lynch-Stieglitz, U. S. Ninnemann, and R. G. Fairbanks (1996), Climate connections between the hemisphere revealed by deep sea sediment core ice core correlations, *Earth and Planetary Science Letters*, 142, 19-27.

Clark, P. U., S. J. Marshall, G. K. C. Clarke, S. W. Hostetler, J. M. Licciardi, and J. T. Teller (2001), Freshwater forcing of abrupt climate change during the last glaciation, *Science*, 293, 283-287.

Clark, P. U., A. M. McCabe, A. C. Mix, and A. J. Weaver (2004), Rapid rise of sea level 19,000 years ago and its global implications, *Science*, 304, 1141-1144.

Clark, P. U., J. X. Mitrovica, G. A. Milne, and M. E. Tamisiea (2002), Sea-level fingerprinting as a direct test for the source of global meltwater pulse IA, *Science*, 295, 2438-2441.

Crowley, T. J. (1992), North Atlantic deep water cools the southern hemisphere, *Paleoceanography*, 7, 489-497.

Cuffey, K. M., G. D. Clow, R. B. Alley, M. Stuiver, E. D. Waddington, and R. W. Saltus (1995), Large Arctic Temperature-Change at the Wisconsin-Holocene Glacial Transition, *Science*, 270, 455-458.

Dansgaard, W., S. J. Johnsen, H. B. Clausen, D. Dahl-Jensen, N. Gundestrup, C. U. Hammer, and H. Oeschger, North Atlantic climatic oscillations revealed by deep Greenland ice cores. in *Climate Processes and Climate Sensitivity*, edited by Hansen, J. E. and T. Takahashi, pp. 288-298, Am. Geophys. Union, Washington, 1984.

Dokken, T. M., and E. Jansen (1999), Rapid changes in the mechanism of ocean convection during the last glacial period, *Nature*, 401, 458-461.

Fairbanks, R. G. (1989), A 17,000-Year Glacio-Eustatic Sea-Level Record - Influence of Glacial Melting Rates on the Younger Dryas Event and Deep-Ocean Circulation, *Nature*, 342, 637-642.

Ganopolski, A., and S. Rahmstorf (2001), Rapid changes of glacial climate simulated in a coupled climate model, *Nature*, 409, 153-158.

Ganopolski, A., and S. Rahmstorf (2002), Abrupt glacial climate changes due to stochastic resonance, *Physical Review Letters*, 88.

Gordon, A. L. (1986), Inter-Ocean Exchange of Thermocline Water, *Journal of Geophysical Research-Oceans*, 91, 5037-5046.

Gordon, A. L., R. F. Weiss, W. M. Smethie, and M. J. Warner (1992), Thermocline and Intermediate Water Communication between the South-Atlantic and Indian Oceans, *Journal of Geophysical Research-Oceans*, 97, 7223-7240.

Heinrich, H. (1988), Origin and Consequences of Cyclic Ice Rafting in the Northeast Atlantic-Ocean During the Past 130,000 Years, *Quaternary Research*, 29, 142-152.

Imbrie, J., and J. Z. Imbrie (1980), Modeling the Climatic Response to Orbital Variations, *Science*, 207, 943-953.

Johnsen, S. J., D. Dahljensen, W. Dansgaard, and N. Gundestrup (1995), Greenland Paleotemperatures Derived from Grip Bore Hole Temperature and Ice Core Isotope Profiles, *Tellus Series B-Chemical and Physical Meteorology*, 47, 624-629.

Jouzel, J., R. Vaikmae, J. R. Petit, M. Martin, Y. Duclos, M. Stievenard, C. Lorius, M. Toots, M. A. Melieres, L. H. Burckle, N. I. Barkov, and V. M. Kotlyakov (1995), The 2-Step Shape and Timing of the Last Deglaciation in Antarctica, *Climate Dynamics*, 11, 151-161.

Kapsner, W. R., R. B. Alley, C. A. Shuman, S. Anandakrishnan, and P. Grootes (1995), Dominant influenze of atmospheric circulation on snow accumulation in Greenland over the past 18,000 years, *Nature*, 373, 52-54.

Kim, J. H., R. R. Schneider, P. J. Muller, and G. Wefer (2002), Interhemispheric comparison of deglacial sea-surface temperature patterns in Atlantic eastern boundary currents (vol 194, pg 383, 2002), *Earth and Planetary Science Letters*, 203, 779-780.

Knorr, G., and G. Lohmann (2003), Southern Ocean Origin for the resumption of Atlantic thermohaline circulation during deglaciation, *Nature*, 424, 532-536.

Knorr, G., and G. Lohmann (2004), The Southern Ocean as the Flywheel of the Oceanic Conveyor Belt Circulation, *Pages News*, 12, 11-13.

Koc, N., E. Jansen, and H. Haflidason (1993), Paleoceanographic Reconstructions of Surface Ocean Conditions in the Greenland, Iceland and Norwegian Seas through the Last 14-Ka Based on Diatoms, *Quaternary Science Reviews*, 12, 115-140.

Lohmann, G. (1998), The influence of a near-bottom transport parameterization on the sensitivity of the thermohaline circulation, *Journal of Physical Oceanography*, 28, 2095-2103.

Lohmann, G., and S. Lorenz (2000), On the hydrological cycle under paleoclimatic conditions as derived from AGCM simulations, *Journal of Geophysical Research-Atmospheres*, 105, 17417-17436.

Lohmann, G., M. Butzin, K. Grosfeld, G. Knorr, A. Paul, M. Prange, V. Romanova, and S. Schubert, The Bremen Earth System Model of Intermediate Complexity (BREMIC) designed for long-term climate studies. Model description, climatology, and applications., University Bremen, Bremen, 2003.

Macdonald, A. M., and C. Wunsch (1996), An estimate of global ocean circulation and heat fluxes, *Nature*, 382, 436-439.

Maier-Reimer, E., U. Mikolajewicz, and K. Hasselmann (1993), Mean Circulation of the Hamburg Lsg Ogcm and Its Sensitivity to the Thermohaline Surface Forcing, *Journal of Physical Oceanography*, 23, 731-757.

Manabe, S., and R. J. Stouffer (1997), Coupled ocean-atmosphere model response to freshwater input: comparison to Younger Dryas event, *Paleoceanography*, 12, 321-336.

McCabe, A. M., and P. U. Clark (1998), Ice-sheet variability around the north Atlantic Ocean during the last deglaciation, *Nature*, 392, 373-377.

McManus, J. F., R. Francois, J. M. Gherardi, L. D. Keigwin, and S. Brown-Leger (2004), Collapse and rapid resumption of Atlantic meridional circulation linked to deglacial climate changes, *Nature*, 428, 834-837.

Milankovitch, M. (1941), Kanon der Erdbestrahlung, *Royal Serbian Acad. Spec. Publ. 132*, Sect. Math. Nat. Sci.

Petit, J. R., J. Jouzel, D. Raynaud, N. I. Barkov, J. M. Barnola, I. Basile, M. Bender, J. Chappellaz, M. Davis, G. Delaygue, M. Delmotte, V. M. Kotlyakov, M. Legrand, V. Y. Lipenkov, C. Lorius, L. Pepin, C. Ritz, E. Saltzman, and M. Stievenard (1999), Climate and atmospheric history of the past 420,000 years from the Vostok ice core, Antarctica, *Nature*, 399, 429-436.

Prange, M., G. Lohmann, and A. Paul (2003), Influence of vertical mixing on the thermohaline hysteresis: Analyses of an OGCM, *Journal of Physical Oceanography*, 33, 1707-1721.

Prange, M., V. Romanova, and G. Lohmann (2002), The glacial thermohaline circulation: Stable or unstable?, *Geophysical Research Letters*, 29, 2028, doi:2010.1029/2002LH015337.

Rahmstorf, S. (1996), On the freshwater forcing and transport of the Atlantic thermohaline circulation, *Climate Dynamics*, 12, 799-811.

Rahmstorf, S. (2003), Timing of abrupt climate change: A precise clock, *Geophys. Res. Lett.*, 30, 1510, doi:1510.1029/2003GL017115.

Rahmstorf, S., and J. Willebrand (1995), The role of temperature feedback in stabilising the thermohaline circulation, *Journal of Physical Oceanography*, 25, 787-805.

Rasmussen, T. L., D. Backstrom, J. Heinemeier, D. Klitgaard-Kristensen, P. C. Knutz, A. Kuijpers, S. Lassen, E. Thomsen, S. R. Troelstra, and T. C. E. van Weering (2002), The Faroe-Shetland Gateway: Late Quaternary water mass exchange between the Nordic seas and the northeastern Atlantic, *Marine Geology*, 188, 165-192.

Roeckner, E., and Coauthors, Simulation of the present-day climate with the ECHAM model: Impact of model physics and resolution, 171 pp., MPI-M, Hamburg, Germany, 1992.

Rohling, E. J., R. Marsh, N. C. Wells, M. Sidall, and N. R. Edwards (2004), Similar meltwater contributions to glacial sea level changes from Antarctic and northern ice sheest, *Nature*, 430, 1016-1021.

Romanova, V., M. Prange, and G. Lohmann (2004), Stability of the glacial thermohaline circulation and its dependence on the background hydrological cycle, *Climate Dynamics*, 22, 527-538.

Sachs, J. P., R. F. Anderson, and S. J. Lehman (2001), Glacial surface temperatures of the southeast Atlantic Ocean, *Science*, 293, 2077-2079.

Saravanan, R., and J. C. McWilliams (1995), Multiple Equilibria, Natural Variability, and Climate Transitions in an Idealized Ocean-Atmosphere Model, *Journal of Climate*, 8, 2296-2323.

Sarnthein, M., K. Winn, S. J. A. Jung, J. C. Duplessy, L. Labeyrie, H. Erlenkeuser, and G. Ganssen (1994), Changes in East Atlantic Deep-Water Circulation over the Last 30,000 Years - 8 Time Slice Reconstructions, *Paleoceanography*, 9, 209-267.

Schäfer-Neth, C., and A. Paul, Circulation of the glacial Atlantic: a synthesis og global and regional modeling. In *The northern North Atlantic: A changing environment*, edited by Schäfer, P., W. Ritzrau, M. Schlüter and J. Thiede, pp. 446-462, Springer-Verlag, Berlin, Heidelberg, 2001.

Schmidt, M. W., H. J. Spero, and D. W. Lea (2004), Links between salinity variation in the Caribbean and North Atlantic thermohaline circulation, *Nature*, 428, 160-163.

Schulz, M. (2002), On the 1470-year pacing of Dansgaard-Oeschger warm events, *Paleoceanography*, 17, doi: 10.1029/2000PA000571.

Schulz, M., A. Paul, and A. Timmermann (2002), Relaxation oscillators in concert: A framework for climate change at millenial timescales during the late Pleistocene, *Geophys. Res. Lett.*, 29, 2193, doi: 2110.1029/2002GL016144.

Severinghaus, J. P., and E. J. Brook (1999), Abrupt climate change at the end of the last glacial period inferred from trapped air in polar ice, *Science*, 286, 930-934.

Severinghaus, J. P., T. Sowers, E. J. Brook, R. B. Alley, and M. L. Bender (1998), Timing of abrupt climate change at the end of the Younger Dryas interval from thermally fractionated gases in polar ice, *Nature*, 391, 141-146.

Shackleton, N. J. (2000), The 100,000-year ice-age cycle identified and found to lag temperature, carbon dioxide, and orbital eccentricity, *Science*, 289, 1897-1902.

Shemesh, A., D. Hodell, X. Crosta, S. Kanfoush, C. Charles, and T. Guilderson (2002), Sequence of events during the last deglaciation in Southern Ocean sediments and Antarctic ice cores, *Paleoceanography*, 17.

Sowers, T., and M. Bender (1995), Climate Records Covering the Last Deglaciation, *Science*, 269, 210-214.

Stocker, T. (2003), South dials north, *Nature*, 524, 496-499.

Stocker, T. F. (1998), The seesaw effect, *Science*, 282, 61-62.

Stocker, T. F., and D. G. Wright (1991), Rapid transitions of the ocean's deep circulation induced by changes in surface water fluxes, *Nature*, 351, 729-732.

Stommel, H. (1961), Thermohaline convection with two stable regimes of flow, *Tellus*, 13, 224-230.

van Kreveld, S., M. Sarnthein, H. Erlenkeuser, P. Grootes, S. Jung, M. J. Nadeau, U. Pflaumann, and A. Voelker (2000), Potential links between surging ice sheets, circulation changes, and the Dansgaard-Oeschger cycles in the Irminger Sea, 60-18 kyr, *Paleoceanography*, 15, 425-442.

Weaver, A. J., O. A. Saenko, P. U. Clark, and J. X. Mitrovica (2003), Meltwater pulse 1A from Antarctica as a trigger of the Bølling-Allerød warm interval, *Science*, 299, 1709-1713.

Winton, M., Deep-decoupling oscillations of the oceanic thermohaline circulation. in *Ice in the climate system*, edited by Peltier, W. R., pp. 417-432, Springer Verlag, Berlin, 1993.

Wunsch, C. (2000), On sharp spectral lines in the climate record and the millennial peak, *Paleoceanography*, 15, 417-424.

Chapter 4

Interhemispheric teleconnections of the Atlantic thermohaline circulation: views obtained from conceptual and ocean general circulation models

Abstract

For the two most recent glacial terminations, different scenarios have been discussed referring to the initiation of deglacial warming in the Northern and Southern Hemisphere. These global scale climate transitions have been attributed to massive reorganizations in the Atlantic thermohaline circulation (THC). Applying an ocean general circulation model (OGCM) and a box model, we examine the sensitivity of the THC to different warming scenarios and meltwater fluxes associated with deglaciation. The OGCM experiments show that an amplification of the glacial THC can be achieved more effectively in the Southern Hemisphere in comparison to the Northern Hemisphere. This model response is substantiated by low order model studies of a density driven THC, which shows that a THC intensification can by achieved if warming and abrupt meltwater fluxes are applied to the Southern Hemisphere. The effect is related to the interactions of atmosphere and ocean heat transports that enable an effective interhemispheric mediation of a Southern Hemisphere warming induced THC amplification. The equivalent warming in the Northern Hemisphere leads to a less effective transmission to the Southern Hemisphere, since a weakening of the THC and broad scale upwelling in the global ocean reduces the contribution of the oceanic mediation.

4.1 Introduction

Proxy data from ice core [Petit et al., 1999; Blunier and Brook, 2001] and ocean sediment records [Sarnthein et al., 1994; Bard et al., 2000] indicate that various abrupt climate changes occurred during the last deglaciation, which are attributed to massive reorganisations of the thermohaline circulation (THC) and accompanying northward heat transport within the Atlantic [Rühlemann et al., 2004]. In particular, the climate sequence from the cold Heinrich-1 to the warm Bølling/Allerød (B/A) warm phase about 14.7 ka BP (thousand years before present) provides

evidence for a rapid climate transition with global effects, featuring an abrupt warming in Greenland ice cores [Grootes et al., 1993] and a cold reversal in Antarctica [Bender et al., 1994; Blunier and Brook, 2001]. Based on proxy data analyses from ice core and ocean sediment records, possible deglaciation scenarios have been discussed, referring to the progression of Northern and Southern Hemisphere warming [Sowers and Bender, 1995; Petit et al., 1999; Alley et al., 2002]. So far, the focus has been mostly on the North Atlantic realm to explain abrupt climate shifts. This is because North Atlantic deep water (NADW) formation sites and various sources of freshwater coexist around the North Atlantic that perturbs the THC during deglaciation. This approach is in accordance with the Milankovitch theory [Milankovitch, 1941]. A key element of this theory is that summer insolation at high latitudes of the Northern Hemisphere determines glacial-interglacial transition connected with the waxing and waning of large continental ice sheets [Imbrie and Imbrie, 1980]. However, there is considerable evidence that for the penultimate deglaciation Southern Hemisphere warming leads to ice-sheet melting as revealed by U/Th dating of marine bulk sediments [Henderson and Slowey, 2000]. This is possibly due to the direct Southern Hemisphere response to local Milankovitch forcing on the precessional period with corresponding response in sea ice cover [Kim et al., 1998] and due to changes in atmospheric CO_2, occurring nearly coincidentally with the warming of high southern latitudes as revealed by cross spectral analyses [Shackleton, 2000]. Besides the synchronous change in atmospheric CO_2 and Southern Hemisphere temperature, a delayed nutrient reorganization in the North Atlantic [Broecker and Henderson, 1998] suggests that changes in the Southern Ocean might have contributed to Northern Hemisphere deglaciation.

Recent modelling investigations have suggested that changes in the Southern Hemisphere are able to trigger a resumption of a meltwater induced stalled THC. In one scenario gradual warming and receding sea-ice cover around Antarctica leads to an abrupt amplification of the THC [Knorr and Lohmann, 2003] by increasing mass transport into the Atlantic Ocean via the warm and the cold water routes [Gordon, 1986] of the ocean conveyor belt circulation [Broecker, 1991]. Additionally, it has been reported that the injection of meltwater pulse 1A, possibly originating from Antarctica [Clark et al., 2002] may increase NADW formation by reducing the density of Antarctic intermediate and bottom waters [Weaver et al., 2003]. These mechanisms illuminate a potential influence of the Southern Ocean in deglacial climate changes [Stocker, 2003].

Motivated by the discussion of possible deglaciation scenarios and a possible influence of processes in the Southern Ocean for the B/A-onset, we examine the influence of different deglacial warming scenarios in the Northern and Southern Hemisphere on the Atlantic THC. For this purpose we use an ocean general circulation model (OGCM) and a box model, which extends a single hemispheric model type [Stommel, 1961; Prange et al., 1997] to cross-equatorial overturning flow in the Atlantic. The OGCM investigations are designed to understand the mechanisms that may amplify the Atlantic THC during deglaciation and to allow the spatial allocation of variations. The box model examinations focus on providing the most relevant processes, controlling the dynamics of the system by interpreting the sensitivity of the THC to changes in the radiative forcing. Furthermore, we will investigate the stability of the system to

abrupt and gradually increasing freshwater perturbations. Finally, the results of both model types will be compared to provide a deeper understanding of the essential physics behind Atlantic THC variations during deglaciation.

4.2 Methodology

4.2.1 The Ocean General Circulation Model

The three-dimensional ocean model is based on the large-scale geostrophic model LSG [Maier-Reimer et al., 1993], which is part of the Bremen Earth system model of intermediate complexity (BREMIC) [Lohmann et al., 2003]. The horizontal resolution is 3.5° on a semi-staggered grid (type 'E') with 11 levels in the vertical. It includes an enhanced advection scheme for temperature and salinity [Schäfer-Neth and Paul, 2001], and a parameterisation of overflow [Lohmann, 1998]. For glacial conditions the storage of water in ice sheets is taken into account by setting all ocean points with present-day water depth less than 120 m to land. This causes the Bering Strait to be closed and several shallow areas like the Arctic shelves to become land. To drive the ocean, monthly fields of wind stress, surface air temperature and freshwater fluxes are taken from a present-day and a Last Glacial Maximum (LGM) simulation of the atmospheric general circulation model ECHAM3/T42 [Roeckner et al., 1992; Lohmann and Lorenz, 2000]. In order to close the hydrological cycle, a runoff scheme transports freshwater from the continents to the ocean. We employ a modelling approach, which allows an adjustment of sea surface temperatures and salinity to changes in the ocean circulation, based on atmospheric energy balance considerations. The heat flux exchange Q at the ocean surface is formulated as suggested by Rahmstorf and Willebrand [1995]

$$Q = (\lambda_1 - \lambda_2 \nabla^2)\,(T_a - T_s)$$

where T_a is the prescribed air temperature, and T_s denotes the ocean surface temperature (λ_1 and λ_2 are chosen to be 15 W m^{-2} K^{-1} and 2 x 10^{12} W K^{-1}). The applied heat flux parameterisation has shown to be a suitable choice, allowing the simulation of observed sea surface temperatures and the maintenance of large-scale temperature anomalies in perturbation experiments [Prange et al., 2003]. The model set-up neglects feedbacks on atmospheric dynamics, hydrological cycle, vegetation, land-ice and sea-ice.

For the present-day state, we obtain an Atlantic Ocean circulation with a NADW-export of 14 Sv (1 Sv = 10^6 m^3 s^{-1}) at 30°S and maximum heat transport of 1.1 PW, which is in the range of observations [Macdonald and Wunsch, 1996]. For the LGM, our modelled ocean is characterized by a weaker circulation of about 7.5 Sv with convection sites shifted southward, compared to present-day sites [Prange et al., 2002]. NADW is formed in the sub-polar North Atlantic and the North Atlantic Current flows in zonal direction along the isopycnals, which is consistent with

reconstructions [Sarnthein et al., 1994]. A detailed description of the modern THC and hydrographic fields can be found elsewhere [Prange et al., 2003].

4.2.2 The box model

The ocean box model describes an interhemispheric ocean basin, which reaches meridionally from 60°S to 80°N and is 80° in width to crudely represent the Atlantic. The Atlantic is subdivided into four boxes, two representing the surface and deep water-layer in the tropics and two boxes are set up for the North and South Atlantic, respectively (Figure 4.1). The upper ocean is coupled to the atmosphere by heat and freshwater fluxes. Additionally, we introduce an ocean box that represents the "residual" global ocean. The temperature (T_5 = 5°C) and salinity (S_5 = 34.9 psu) of this huge reservoir are assumed to be constant.

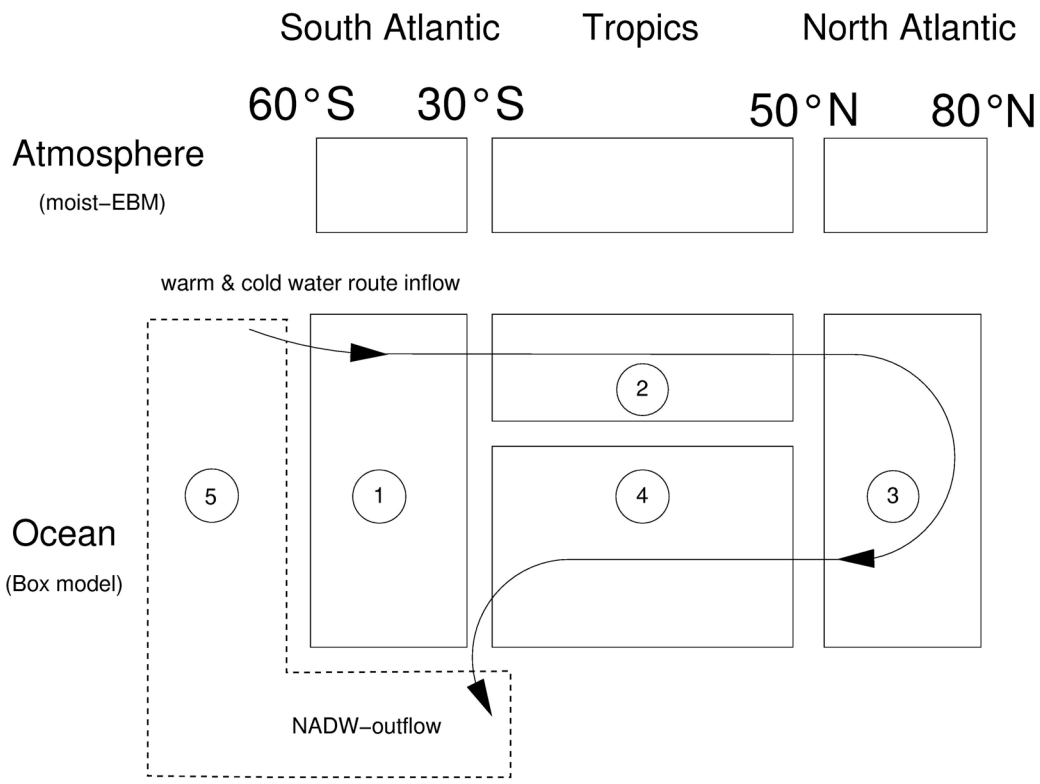

Figure 4.1: Simple diagram of the conceptual model of interhemispheric thermohaline flow. The flow is driven by different energy balances $R_{t,i}$ at the top of the atmosphere. Heat and salt are transported in the ocean by the THC with an overturning rate Φ, while the sensible (F_s) and latent heat fluxes (F_l) are poleward in the atmosphere. Atmosphere and ocean are coupled through heat $(F_{oa,i})$ and freshwater fluxes $(P\text{-}E)_i$.

The ocean boxes are advectively coupled to each other, and sinking in the northern high latitudes is considered, so that the prognostic equations for temperatures T_i and salinities S_i of the four boxes (i = 1, 2, 3, 4) are:

$$\frac{d}{dt}T_1 = \frac{\Phi}{V_1}(T_5 - T_1) + \frac{F_{oa,1}}{\rho_0 c_p \Delta h_1}, \quad (1)$$

$$\frac{d}{dt}T_2 = \frac{\Phi}{V_2}(T_1 - T_2) + \frac{F_{oa,2}}{\rho_0 c_p \Delta h_2}, \quad (2)$$

$$\frac{d}{dt}T_3 = \frac{\Phi}{V_3}(T_2 - T_3) + \frac{F_{oa,3}}{\rho_0 c_p \Delta h_1}, \quad (3)$$

$$\frac{d}{dt}T_4 = \frac{\Phi}{V_4}(T_3 - T_4), \quad (4)$$

$$\frac{d}{dt}S_1 = \frac{\Phi}{V_1}(S_5 - S_1) - \frac{S_0}{\Delta h_1}(P-E)_1, \quad (5)$$

$$\frac{d}{dt}S_2 = \frac{\Phi}{V_2}(S_1 - S_2) - \frac{S_0}{\Delta h_2}(P-E)_2, \quad (6)$$

$$\frac{d}{dt}S_3 = \frac{\Phi}{V_3}(S_2 - S_3) - \frac{S_0}{\Delta h_1}(P-E)_3, \quad (7)$$

$$\frac{d}{dt}S_4 = \frac{\Phi}{V_4}(S_3 - S_4), \quad (8)$$

where $F_{oa,i}$ denote the surface heat fluxes and V_i are the volumes of the four ocean boxes. S_0 is a reference salinity (34.9 psu), ρ_0 a reference density (1025 kg m^{-3}), and c_p the specific heat of water (4200 Jkg^{-1} °C^{-1}). $(P\text{-}E)_i$ denote the fresh water fluxes (precipitation minus evaporation) out of the low- and into the high-latitude boxes. The depths Δh_1 and Δh_2 of the ocean boxes amount to 4000 m and 200 m, respectively. The overturning rate Φ, i.e. the volume flux of the THC between two adjacent ocean boxes, is assumed to depend on the density difference between box 1 and 3:

$$\Phi = c[\rho(T_3, S_3) - \rho(T_1, S_1)], \quad (9)$$

where the densities (in kg m^{-3}) are calculated by a quadratic equation of state [Zhang et al., 1993]:

$$\rho(T_i, S_i) = 1003.0 + 0.77 S_i - 0.072 T_i (1 + 0.072 T_i). \quad (10)$$

The factor c in (9) is freely tuneable to adjust the strength of the thermohaline circulation. Neither convection nor diffusion is included in the model.

The ocean model is coupled to an atmospheric energy balance model (EBM) that includes variable air temperatures, as well as eddy heat and moisture transports and works with physical approximations of governing processes, where the transport terms are parameterised as diffusion. This approach is similar to the one described by Chen et al. [1995]. In our box model the atmosphere is subdivided into one low, and two high latitude boxes, which zonally span the whole circumference of the globe (Figure 4.1). The set-up with one box in the tropics, spanning the latitude belt from 30°S to 50°N represents an upper estimate for the interhemispheric exchange in the atmosphere. Assuming that both the sensible and the latent meridional heat fluxes vanish at the poles, the following prognostic equations determine the surface air temperatures $T_{a,i}$ (i = 1, 2, 3) of the atmospheric boxes:

$$\beta c_{p,a} \frac{dT_{a,1}}{dt} = \frac{\cos 30^\circ \cdot F_{30^\circ S}}{a(\sin 90^\circ - \sin 30^\circ)} + R_{t,1} - f_1 F_{oa,1}, \tag{11}$$

$$\beta c_{p,a} \frac{dT_{a,2}}{dt} = -\frac{\cos 30^\circ \cdot F_{30^\circ S} + \cos 50^\circ \cdot F_{50^\circ N}}{a(\sin 30^\circ + \sin 50^\circ)} + R_{t,2} - f_2 F_{oa,2}, \tag{12}$$

$$\beta c_{p,a} \frac{dT_{a,3}}{dt} = \frac{\cos 50^\circ \cdot F_{50^\circ N}}{a(\sin 90^\circ - \sin 50^\circ)} + R_{t,3} - f_3 F_{oa,3}, \tag{13}$$

where $c_{p,a}$ denotes specific heat of air (1004 J kg^{-1} °C), a the earth's radius (6.371 · 10^6 m), $F_{30°S}$ and $F_{50°N}$ the sum of sensible (16) and latent heat fluxes (17) from the mid-latitude to the high-latitude atmospheric boxes across the 30°S and 50°N latitude circle, respectively. $R_{t,i}$ represents the radiation balance at the top of the atmospheric boxes. Since the ocean surface occupies only a fraction of the total earth surface, the factors f_1, f_2 and f_3 are introduced. The factor $\beta c_{p,a}$ determines the time scale of atmospheric responses to the thermal forcings. Chen et al. [1995] found β to be 5300 kg m^{-2}. The radiation balance at the top of the atmosphere $R_{t,i}$ is expressed by:

$$R_{t,i} = R_{sol,i}(1 - \alpha_{p,i}) - I_i, \tag{14}$$

where $R_{sol,i}$ denotes the extraterrestrial solar insolation and $\alpha_{p,i}$ the planetary albedo. The outgoing infrared radiation I_i is formulated by a linear dependence on surface air temperature [Budyko, 1969]:

$$I_i = A + BT_{a,i}. \tag{15}$$

Chen et al. [1995] found the empirical constants A and B to be 213.35 W m^{-2} and 2.22 W m^{-2} °C^{-1}, respectively. Since atmospheric transports across the 30°S and the 50°N latitude circles are mainly

due to transient eddies [Oort and Peixoto, 1983], $F_{s,30°S}$ and $F_{s,50°N}$, as well as $F_{l,30°S}$ and $F_{l,50°N}$ can be parameterised in terms of the meridional surface air temperature gradient:

$$F_s = K_S \left| \frac{\partial T_a}{a \partial \phi} \right|, \tag{16}$$

$$F_l = K_l r_h \left(\frac{\partial q_s}{\partial T_a} \right) \cdot \left| \frac{\partial T_a}{a \partial \phi} \right|, \tag{17}$$

where K_s and K_l are tuned to reproduce observational values [e.g. Michaud and Derome, 1991]. The fixed relative humidity is r_h = 0.8 and $q_{s,i}$ denotes the temperature-dependent saturation specific humidity:

$$q_{s,i}(T_{a,i}) = \frac{0.622}{1000 \text{ mbar}} e_s(T_{a,i}). \tag{18}$$

The temperature-dependent saturation water vapour pressure e_s (in mbar) is formulated by:

$$e = 6.112 \exp \left[\frac{17.67\, T_{a,i}}{243.5 + T_{a,i}} \right]. \tag{19}$$

To determine the temperature at 30°S and 50°N we assume that the latitudinal profile of the zonal mean surface air temperature can be approximated in a linear fashion.

For the coupling of atmosphere and ocean by surface freshwater fluxes we assume that net freshwater fluxes poleward of 60°S and 80°N vanish. The freshwater fluxes are then calculated diagnostically by:

$$(P-E)_1 = \frac{1}{L_v \rho_w} \cdot \frac{\cos 30^\circ \cdot F_{l,30^\circ S}}{a(\sin 60^\circ - \sin 30^\circ)}, \tag{20}$$

$$(P-E)_2 = -\frac{1}{L_v \rho_w} \cdot \frac{\cos 30^\circ \cdot F_{l,30^\circ S} + \cos 50^\circ \cdot F_{l,50^\circ N}}{a(\sin 30^\circ + \sin 50^\circ)}, \tag{21}$$

$$(P-E)_3 = \frac{1}{L_v \rho_w} \cdot \frac{\cos 50^\circ \cdot F_{l,50^\circ N}}{a(\sin 80^\circ - \sin 50^\circ)}, \tag{22}$$

where L_v denotes the latent heat of vaporisation (2.5 10^6 J kg^{-1}) and ρ_w the density of freshwater. The net surface heat flux is parameterised by:

$$F_{oa,i} = Q_{1,i} - Q_{2,i}(T_i - T_{a,i}), \tag{23}$$

with $Q_{1,i}$ and $Q_{2,i}$ being constants. Haney [1971] calculated the zonal averages of the net upward flux of the sum of longwave radiation, latent heat, and sensible heat, per °C of the ocean - atmosphere temperature difference. He found that this value varies only by 20 % in latitude. Therefore $Q_{2,i}$ is taken to be constant at a value of 50.0 Wm^{-2}. To reproduce the present climatology the following constants have been chosen for $Q_{1,i}$ in the style of Haney [1971]: $Q_{1,1}$ = 10.0 Wm^{-2}, $Q_{1,2}$ = 70.0 Wm^{-2}, $Q_{1,3}$ = 20 Wm^{-2}.

The tuning parameters required to reproduce the current climate are shown in Table I, and the obtained climatological values are listed in Table II. Integration of the system of coupled ordinary differential equations in the following investigations is performed by an Euler forward scheme with a time step of 3.65 days. In this study equilibrium states without deep-water formation in the North Atlantic are not investigated.

Table I: Parameters used in the conceptual coupled ocean-atmosphere model.

Parameter	**Units**	**Value**
c	$m^9 s^{-1} kg^{-2}$	2.0×10^{10}
K_s	$W\ °C^{-1}$	1.3×10^{13}
K_l	W	5.1×10^{17}
$R_{sol,1}$	$W\ m^{-2}$	320.00
$R_{sol,2}$	$W\ m^{-2}$	380.00
$R_{sol,3}$	$W\ m^{-2}$	205.00
$\alpha_{p,1}$	-	0.40
$\alpha_{p,2}$	-	0.22
$\alpha_{p,3}$	-	0.45

Table II: The different climate equilibrium states

Variable	**Units**	**Present climate**	**Colder Climate**	**Climate differences**
$T_{a,1}$	(°C)	4.91	2.37	-2.54
$T_{a,2}$	(°C)	22.04	20.23	-1.81
$T_{a,3}$	(°C)	1.02	-1.87	-2.89
T_1	(°C)	5.11	2.56	-2.55
T_2	(°C)	23.08	21.28	-1.80
$T_3 = T_4$	(°C)	3.39	0.46	-2.93
S_1	(psu)	34.53	34.53	0.0
S_2	(psu)	36.03	36.07	0.04
$S_3 = S_4$	(psu)	34.90	34.90	0.0
Φ	(Sv)	10.37	9.58	-0.79
oceanic heat transport:	(PW)	0.85	0.83	-0.02
atmospheric heat transports:				
Northern Hemisphere				
sensible	(PW)	2.76	2.90	0.14
latent	(PW)	1.47	1.24	-0.23
Southern Hemisphere				
sensible	(PW)	2.33	2.43	0.10
latent	(PW)	2.20	1.92	-0.28

4.3 Ocean General Circulation Model investigations

4.3.1 Experiments

In order to study the influence of deglacial warming on the THC, we perform different idealized deglaciation experiments with the OGCM. The experiments are equivalent to those described in Knorr and Lohmann [Knorr and Lohmann, 2003] and the supplemental material therein. Therefore, we have chosen the same notation for the experiments. For modern and glacial conditions we have performed the control runs PD and LGM_CTRL_ICE, respectively.

Starting from the glacial equilibrium, we have applied Southern Ocean warming south of 30°S and Northern Hemisphere warming north of 30°N. The respective simulations are referred to as LGM_SH and LGM_NH. The deglacial warming is simulated by an initial transition from glacial to interglacial background climate conditions in air temperature, sea ice and wind stress. In all OGCM experiments changes in sea ice cover have been prescribed globally.

4.3.2 Model results

Southern Ocean warming in experiment LGM_SH increases the overturning strength to about 14 Sv, almost reaching interglacial values (Figure 4.2a). Along with an intensified NADW overturning circulation in the Atlantic (Figure 4.2b) the maximum northward heat transport in the Atlantic Ocean increases from 0.8 PW in our glacial simulation to 1.2 PW in experiment LGM_SH. This causes an upper ocean temperature rise of about 2°C in the North Atlantic (Figure 4.2c). Knorr and Lohmann [2003] pointed out that the THC intensification is linked to enhanced volume transport of near surface waters into the South Atlantic via the warm and the cold water routes [Gordon, 1986] of the global ocean circulation, affecting the salt balance within the Atlantic. In the North Atlantic northward transport of water masses also increases, providing relatively salty and hence, dense surface waters to the North Atlantic (Figure 4.2d), which favours deepwater formation (Figure 4.2a). Moreover, the model response has been analysed with respect to wind and temperature effects, showing that the imposed temperature and sea ice changes in the Southern Hemisphere are the primary factors in changing the THC. Alterations in wind stress are of minor importance as shown in the supplemental material of Knorr and Lohmann [2003].

To test the potential of Northern Hemisphere warming to induce deglacial THC changes we have conducted experiment LGM_NH. Due to warming and reduced sea ice cover in the North Atlantic the deep-water formation sites are shifted northward, compared to the glacial state. Hence, the sinking branch of the NADW overturning cell is located between 55°N and 70°N (Figure 4.3), with contributions of the Nordic Seas to NADW. Nevertheless, the model response is relatively weak (Figure 4.2a) compared to LGM_SH. The NADW-outflow in LGM_NH increases only by about 1.5 Sv, since local warming at the North Atlantic surface causes a density reduction in the

formation regions of NADW. The glacial climate conditions in the Southern Ocean constrain the inter-ocean exchange between the Atlantic basin and the Indian and Pacific Ocean to a glacial flow regime.

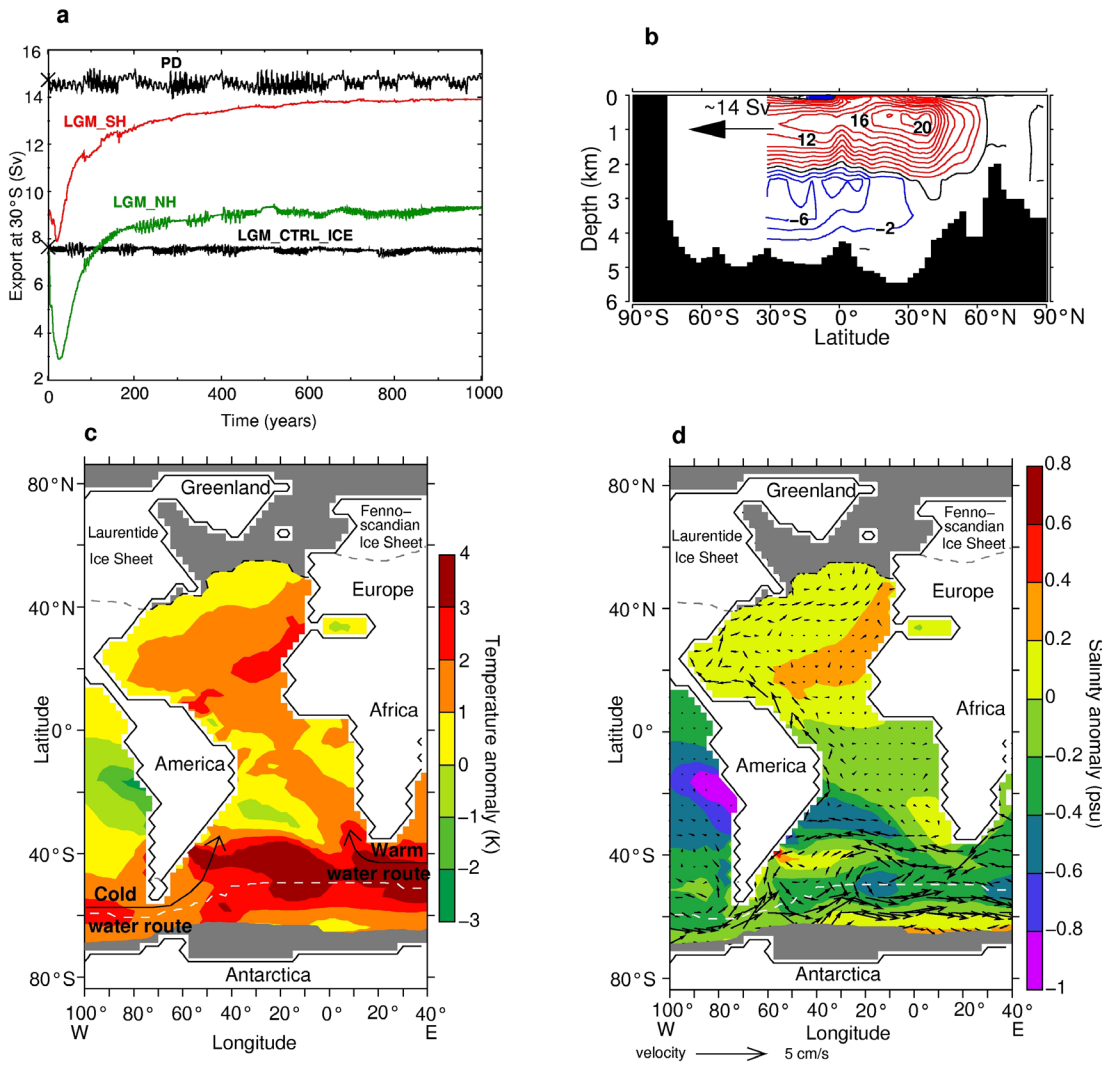

Figure 4.2: Changes in the Atlantic overturning circulation, and differences between LGM_SH and LGM_CTRL_ICE after 1000 model years. (a) Present-day (PD) and glacial (LGM_CTRL_ICE) reference states are indicated by the black curves and crosses. In experiment LGM_SH (red curve) modern temperature, sea ice and wind stress is applied south of 30°S, while in LGM_NH (green curve) the respective climate background has been changed north 30°N. Both experiments have been started from the LGM reference state. (b) Meridional stream function of the Atlantic overturning circulation (Sv) in experiment LGM_SH. The NADW cell is indicated by the blue lines and the AABW cell by the red lines. (c) Annual mean temperature difference between LGM_SH and LGM_CTRL_ICE, averaged for the upper 800 m; schematically overlaid with the main pathways of water import to the Atlantic Ocean at 30°S. The gray shaded area indicates the sea ice extent related to the area, which is covered six months by ice for LGM_SH. The white-dashed line shows the corresponding LGM sea ice extent in the Southern Ocean. (d) annual mean salinity (psu) and horizontal velocity (cm s^{-1}) differences between LGM_SH and LGM_CTRL_ICE; average over the upper 800 m in the Atlantic Ocean. Sea ice margins and continental ice sheets as in panel (c).

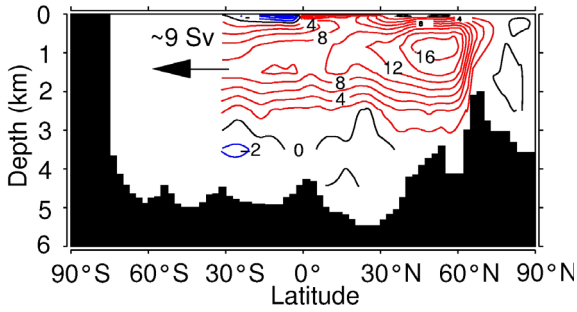

Figure 4.3: Meridional overturning stream function (Sv) in the Atlantic in experiment LGM_NH. The NADW cell is indicated by the red lines and the Antarctic Bottom Water cell by the blue lines.

The global switch to modern climate background conditions in temperature, sea ice cover and wind stress lead to an overturning augmentation to about 13 Sv (not shown). This amplification of the NADW cell is weaker than in experiment LGM_SH, which can be attributed to the warm interglacial temperatures in the formation regions of NADW that reduce the density at the ocean surface. The same effect restricted the strength of the NADW cell in LGM_NH. Therefore, the strongest NADW response occurs in experiment LGM_SH, while NADW outflow changes at 30°S in LGM_NH are negligible.

4.4 Sensitivity experiments with the low-order model

4.4.1 Thermohaline circulation in different climates

This section is aimed to test and deepen the physical understanding evolving from the OGCM experiments, using a low-order model of the ocean-atmosphere system (Figure 4.1). The present-day control run is characterized by an overturning strength of about 10.37 Sv and a northward oceanic heat transport of 0.86 PW. The globally averaged atmosphere temperature amounts to 15.30 °C. For the given choice of tuning parameters in Table I both, the thermal and haline density-components induce deep-water formation in the North Atlantic, indicating a so-called thermohaline flow regime. For meltwater perturbations to the North Atlantic, larger than about 0.18 Sv the circulation becomes unstable and collapses (Figure 4.4).

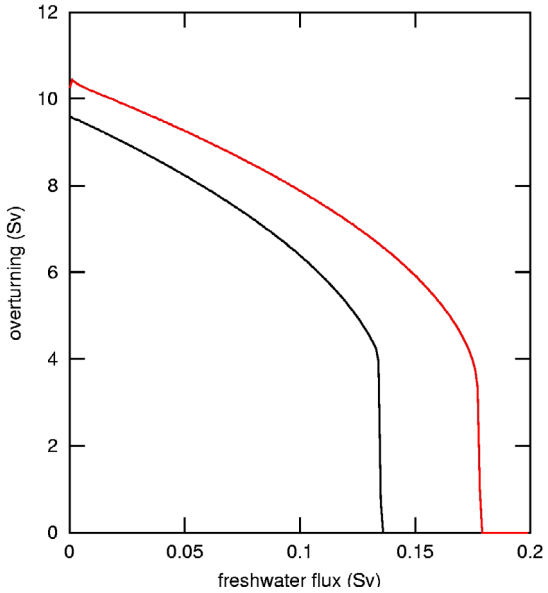

Figure 4.4: Temporal changes of the Atlantic overturning circulation in response to gradual increasing freshwater perturbations to the North Atlantic of the box model. The stability curves represent the modern climate (red) and a colder climate (black).

In the following set of experiments we explore the effect of different warming scenarios on the THC of a colder climate. The colder climate is generated by altering the radiation balance at the top of the atmosphere. The effect of atmospheric greenhouse gases can be simulated by varying the parameterisation for the long-wave emission I_i in (15) by multiplication with a factor γ that depends on greenhouse gas concentration [Budyko, 1977]. The coefficient γ should not differ too much from 1.0 in a box model since the tuning is based on present-day climatology and important physical processes might be neglected, such as prominent changes of sea ice distributions that strongly influence surface heat fluxes, and hence, the stability of the THC [Lohmann et al., 1996; Prange et al., 1997]. To account for this limitation, γ is set to 1.02 for the simulation of the colder (glacial) climate. In addition to the change of γ, the temperature of the "residual" ocean box 5 is decreased by 2.5°C, which is in accordance with glacial deep ocean temperature reconstructions in the Pacific, using pore fluid measurements of chloride concentrations and oxygen isotope composition of marine bulk sediments [Adkins et al., 2002], as well as with recent model simulations [Otto-Bliesner et al., 2005].

In the colder climate state, whose variables are listed in Table II, the global atmospheric temperature averages to a value of 13.18°C. Alterations in net radiation at the top of the atmosphere amount to $\Delta R_{t,1}$ = 1.28 Wm^{-2}, $\Delta R_{t,2}$ = -1.14 Wm^{-2}, $\Delta R_{t,3}$ = 2.22 Wm^{-2}. In a steady state the radiative changes are balanced by meridional transports in the atmosphere-ocean system and the total heat transports decreases in the colder climate, albeit the pole to equator temperature gradients ($\Delta(T_{a,2} - T_{a,1})$ = 0.73°C; $\Delta(T_{a,2} - T_{a,3})$ = 1.08°C) increase, and therefore sensible heat

fluxes. The increase in sensible heat flux is overbalanced by decreasing latent heat fluxes, due to decreased moisture capacity of the cooled atmosphere.

Although, the meridional north-south ocean temperature gradient increases in the colder climate ($\Delta(T_1 - T_3) = 0.38°C$) a weakening of the THC is detected, which can be related to the temperature dependence of the thermal expansion coefficient of seawater $\partial\rho_i / \partial T_i$. This coefficient increases linearly with temperature according to (10). This effect is reinforced by decreased northward oceanic salt transport from the tropics to the North Atlantic box. The density in the South Atlantic increases, while the North Atlantic density remains almost constant and the overturning circulation weakens to a value of 9.59 Sv, due to a reduced north–south density contrast ($\Delta(\rho_3 - \rho_1) = -0.024$ kg m^{-3}).

4.4.2 Warming impact on the thermohaline circulation

Starting from the colder climate two different warming scenarios are conducted in which the equivalent to a global radiation surplus of 1 Wm^{-2} is applied. In experiment SH_WARM, local warming is applied in the southern high latitudes, whereas local northern high latitude warming is applied in experiment NH_WARM. The alteration of the radiation (14) by an additional radiation surplus of 8.55 Wm^{-2} in the North and 4.0 Wm^{-2} in the South are applied after 400 model years.

Southern Hemisphere warming in experiment SH_WARM induces an increase in South Atlantic atmosphere and ocean temperatures (Figure 4.5a, b), which intensifies the Atlantic THC (Figure 4.5c) and increases the northward oceanic heat transport by 0.08 PW. Thus, the North Atlantic realm warms (Figure 4.5a, b). The atmospheric moisture transports in both Hemispheres and the accompanying surface freshwater fluxes increase (Figure 4.5d), due to the increased moisture capacity of the warmer air. Contrary, the sensible heat transports from the tropics to the Southern and Northern high latitudes decrease, because the temperature in the tropics remains nearly constant and the respective temperature gradients in both hemispheres decrease. However, the total poleward heat transport of the coupled atmosphere-ocean system increases in the Northern Hemisphere (Figure 4.5e). The combined effect of a stronger THC and increased oceanic northward heat transport, together with the augmentation in atmospheric latent heat transport raises the temperatures by 0.56°C and 0.40°C in the North Atlantic and the respective atmospheric box (Figure 4.5a, b).

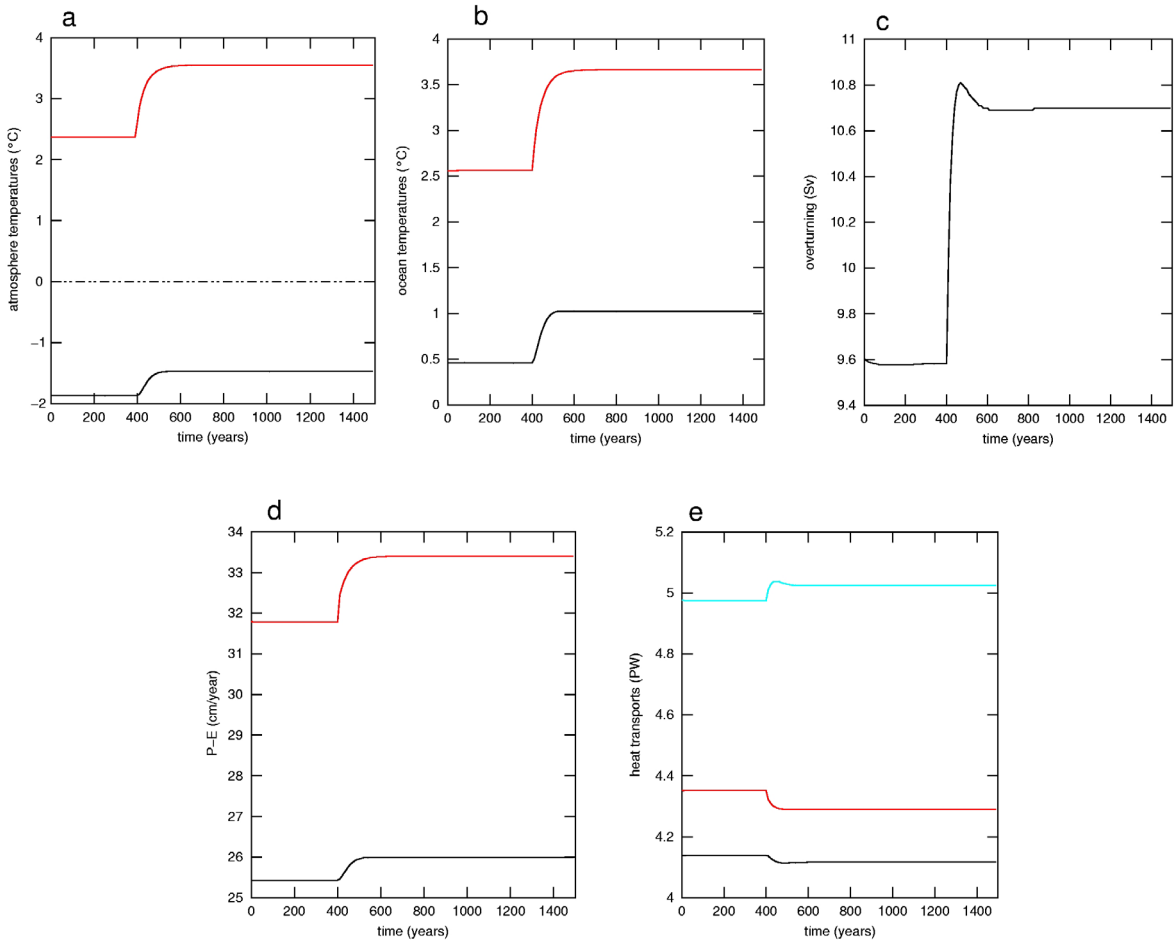

Figure 4.5: Temporal changes in experiment SH_WARM: atmosphere (a) and ocean (b) temperatures, as well as overturning strength (c), and surface freshwater fluxes (d). The respective values of the Southern Hemisphere are indicated by red curves and in Northern Hemisphere by black curves. This notation will be applied in this and all following figures. The heat transports (e) contain the southward (red) and northward (black) atmospheric transports, as well as the overall equator to pole heat flux in the Northern Hemisphere (turquoise).

In experiment NH_WARM the radiation change causes an increase of atmosphere and ocean temperatures in the North Atlantic (Figure 4.6a, b). Consequently, a decline of the overturning strength is detected (Figure 4.6c). The accompanying reduction of oceanic heat transport by 0.15 PW leads to additional warming in the tropics that amounts to 0.28°C and 0.33°C in the atmosphere and the ocean, respectively. The temperature in the South Atlantic and the overlying atmosphere increase by 0.11°C (Figure 4.6a, b). The temperature increase of all atmospheric boxes leads to a stronger pole-ward moisture transport and hence, surface freshwater fluxes in both hemispheres (Figure 4.6d). The temperature gradient and the atmospheric sensible heat transport in the Southern Hemisphere remain almost constant, contrary to a reduced sensible heat transport in the Northern Hemisphere, owing to a reduced pole to equator temperature gradient. The response

of the combined sensible and latent heat transports in both hemispheres is vice versa, with an augmentation in the Southern Hemisphere and an abatement in the Northern Hemisphere (Figure 4.6e). The overall northward heat transport of the coupled system in the Northern Hemisphere decreases by about 0.2 PW (Figure 4.6e) that counteract the initial warming in the North. The resulting warming of the North Atlantic and the overlying atmosphere amounts to 1.49°C and 1.85°C, respectively.

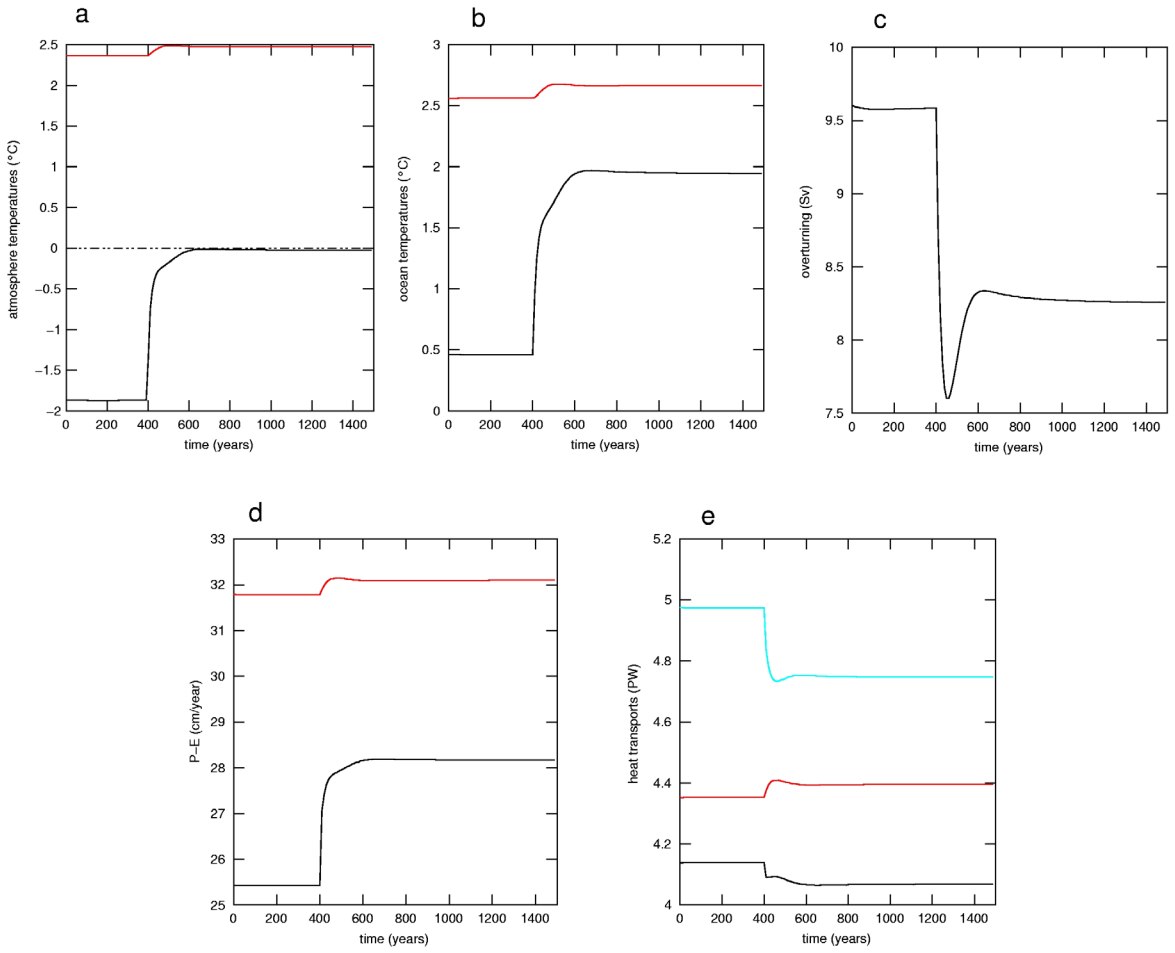

Figure 4.6: Temporal changes in experiment NH_WARM: atmosphere (a) and ocean (b) temperatures, as well as overturning strength (c), surface freshwater fluxes (d), and different heat transports (e). The colours are chosen as in the previous Figure 4.5.

A global radiation change by 1 Wm^{-2} leads to a THC amplification of 0.13 Sv (not shown). This model THC response to global warming is relatively weak compared to the THC amplification of 1.1 Sv in experiment SH_WARM. The engagement of the hydrological cycle to the glacial equilibrium strength leads to slightly different model responses in our experiments. The variations are less than 5 % and the general trends prevail. The relatively weak impact of the hydrological

cycles in the warming experiments is directly apparent from the changes in surface freshwater fluxes (Figure 4.5e, 4.6e) that increase in both experiments and hemispheres and therefore almost cancel its overall effect on the interhemispheric density gradient.

4.4.3 Meltwater impacts

So far we have seen that the presented low order model of the interhemispheric Atlantic THC is sensitive to changes in the long wave emission. The next section is aimed to examine the sensitivity of the glacial THC to different freshwater perturbations, which mimic the effect of deglacial meltwater discharge. In experiment FWF_GRAD we perform a stability analyses of the THC in the colder climate, with regards to a gradual increasing freshwater-flux perturbation to the North Atlantic for the glacial climate state. For this purpose a slowly increasing freshwater flux with a rate of 0.01 Sv per 1000 years is applied to ocean box 3. In experiment FWF_NH and FWF_SH we investigate the THC response to a meltwater pulse of 0.2 Sv to the North and South Atlantic, respectively. The meltwater discharge is applied between model year 400 and 500.

With increasing freshwater flux to the North Atlantic in FWF_GRAD the salinity is effectively reduced in the deep-water formation box (Figure 4.7a), which reduces the north-south density contrast and therefore the overturning strength (Figure 4.4). The gradual weakening of the THC causes a temperature decrease in the North Atlantic, and a temperature increase in the tropics and the South Atlantic (Figure 4.7b, c), which is linked to a reduced oceanic heat transport (Figure 4.7d). The declined oceanic heat transport also leads to a cooling of air temperatures in the North, while the tropics and the atmosphere in the Southern Hemisphere warms. The resulting alteration of atmospheric temperature gradient intensifies the atmospheric sensible heat transport in the Northern Hemisphere. Freshwater transports depend on both the meridional temperature gradient and the absolute temperature (17). Therefore, the temperature decrease in the North Atlantic is accompanied by decreasing latent heat transport and surface freshwater fluxes (Figure 4.7e). The sum of both atmospheric transports in the Northern Hemisphere increases with increasing freshwater discharge to the North Atlantic (Figure 4.7d). In the Southern Hemisphere, the poleward sensible heat transport decreases due to a declined atmospheric temperature gradient. Contrary, the latent heat transport and hence the surface freshwater flux to the South Atlantic is augmented due to increasing temperatures in the tropics and the South Atlantic (Figure 4.7e). The increase in latent heat transport dominates the decrease in the sensible heat transport and the combined atmospheric transport increases in the Southern Hemisphere (Figure 4.7d).

The gradual increase of freshwater discharge to the North Atlantic leads to a shift in the THC flow regime. For perturbations larger than 0.11 Sv the THC state is purely thermally driven, since the salinity in the South Atlantic becomes larger than in the North Atlantic (Figure 4.7a). For freshwater fluxes greater than about 0.14 Sv to the North Atlantic, a threshold is reached and the THC with sinking in the North Atlantic collapses (Figure 4.7b).

The present-day overturning circulation is less sensitive to North Atlantic freshwater discharge (Figure 4.4), because of the stronger equilibrium overturning circulation and a strengthened feedback between heat transport and meridional density gradient, owing to increased thermal expansion coefficients according to (10). Fixed equilibrium atmospheric moisture transports decrease the stability of the THC, since an increase of surface freshwater fluxes in the South and a decrease in the North is inhibited as response to a weakening in the overturning strength. Both surface freshwater fluxes tend to maintain the density difference between the northern and southern high latitude boxes (Figure 4.7e).

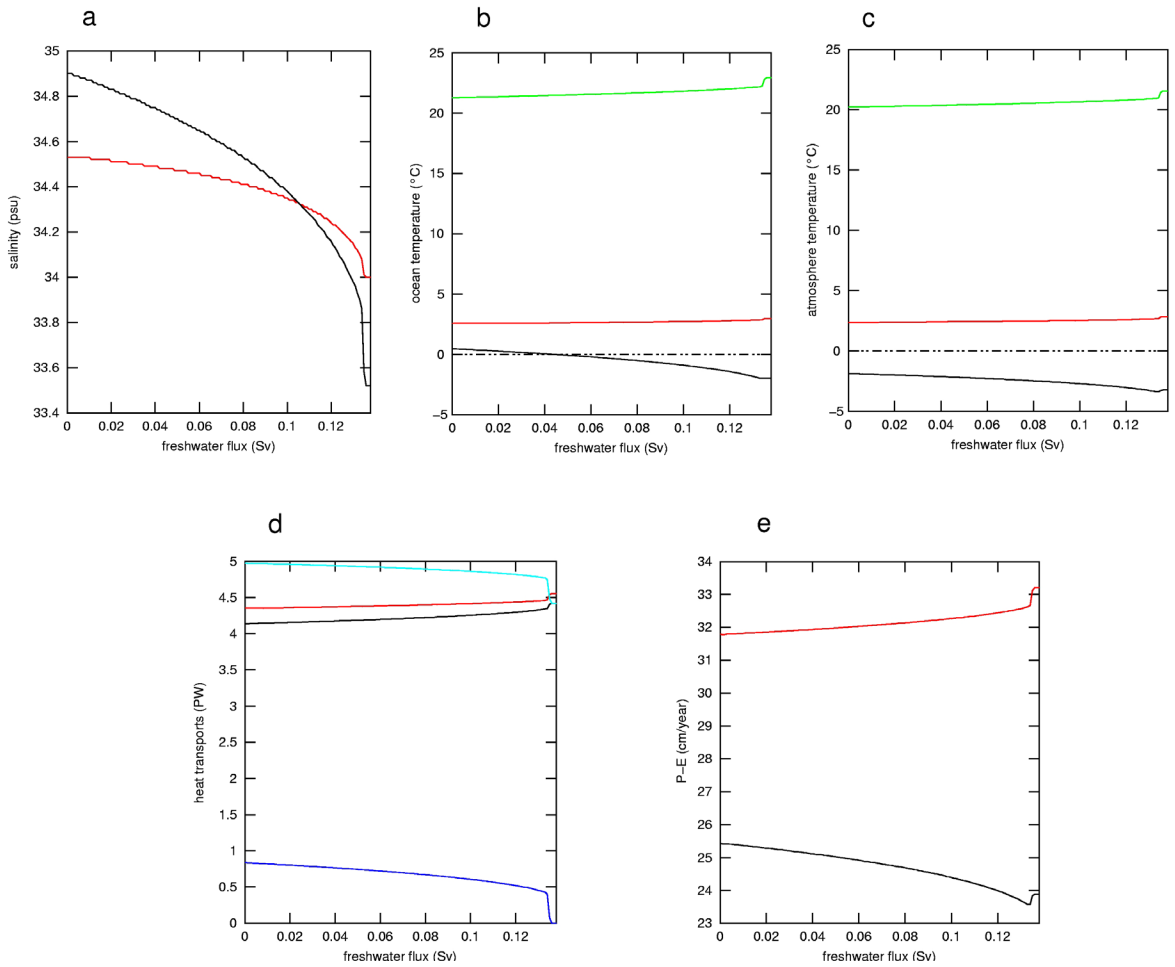

Figure 4.7: Temporal changes in experiment FWF_GRAD: salinities (a), ocean (b) and atmosphere (c) temperatures, as well as heat-transports in the ocean atmosphere system (d) and atmospheric freshwater transports (e). Additional to the colour scheme in the previous figures, temperature changes in the tropics are displayed in green (a, b) and the ocean heat transport in blue (d).

In experiment FWF_NH, the injection of an abrupt meltwater pulse of 0.2 Sv with a duration of 100 years initially reduces the North Atlantic salinity (Figure 4.8a) and the overturning strength to less than half of its equilibrium strength within about 100 years (Figure 4.8b). The THC recovers within the next 100 years to its initial strength. The oceanic overturning drop leads to a temperature decrease in the northern high latitudes, while the atmosphere and ocean temperatures in the tropics (not shown) and the Southern Hemisphere increase (Figure 4.8c, d). This “seesaw” pattern is attributed to decreased oceanic heat transport, which overbalances the increase in northward atmospheric heat transport (Figure 4.8e), due to an increased temperature gradient between the tropics and the northern high latitudes. The latent northward heat transport and the respective freshwater fluxes decrease in the Northern Hemisphere and increase in the Southern Hemisphere (Figure 4.8f).

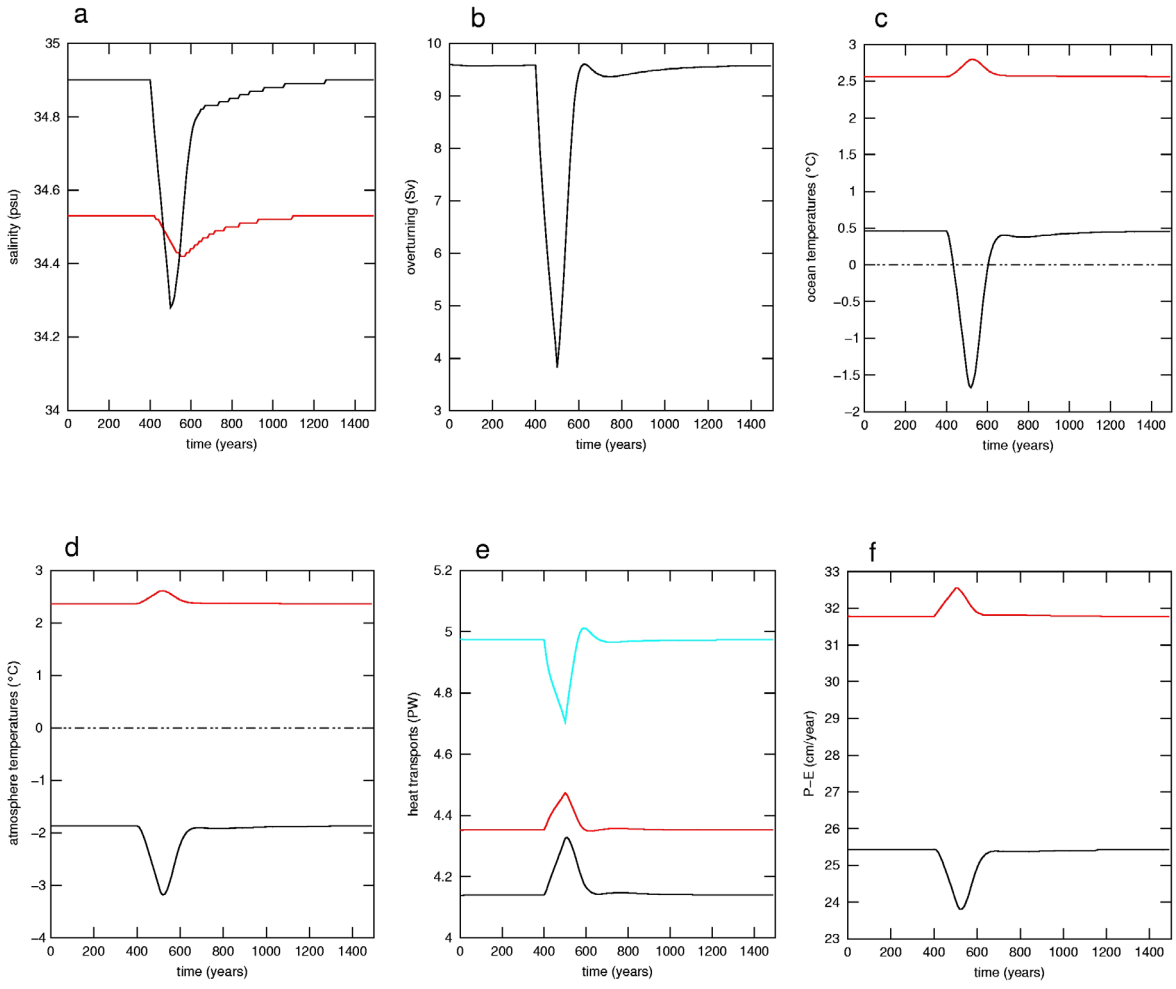

Figure 4.8: Temporal changes in experiment FWF_NH: salinities (a), overturning strength (b), ocean (c), and atmosphere temperatures (d), as well the atmospheric heat transports and the total northward heat transport (e), and surface freshwater fluxes (f). Colours are chosen as in Figure 4.5.

The influence of freshwater perturbations to the South Atlantic in experiment FWF_SH leads to an abrupt decrease of South Atlantic salinities (Figure 4.9a) and therefore, to an acceleration of the density driven Atlantic THC (Figure 4.9b). After the freshwater flux ceases the THC switches back to nearly the initial strength within 100 years. As a consequence of increased oceanic heat transport the ocean and atmosphere temperatures of the North Atlantic rise, while South Atlantic temperatures decrease temporarily (Figure 4.9c, d). Compared to the changes in FWF_NH the variations in the overturning circulation in FWF_SH are relatively small, since the overall increase of the total northward heat transport of the coupled ocean-atmosphere system warms the North Atlantic (Figure 4.9e). Moreover, increased northward moisture transport and decreased southward moisture export from the tropics (Figure 4.9f) directly counteract an amplification of the density driven meridional overturning circulation in the Atlantic.

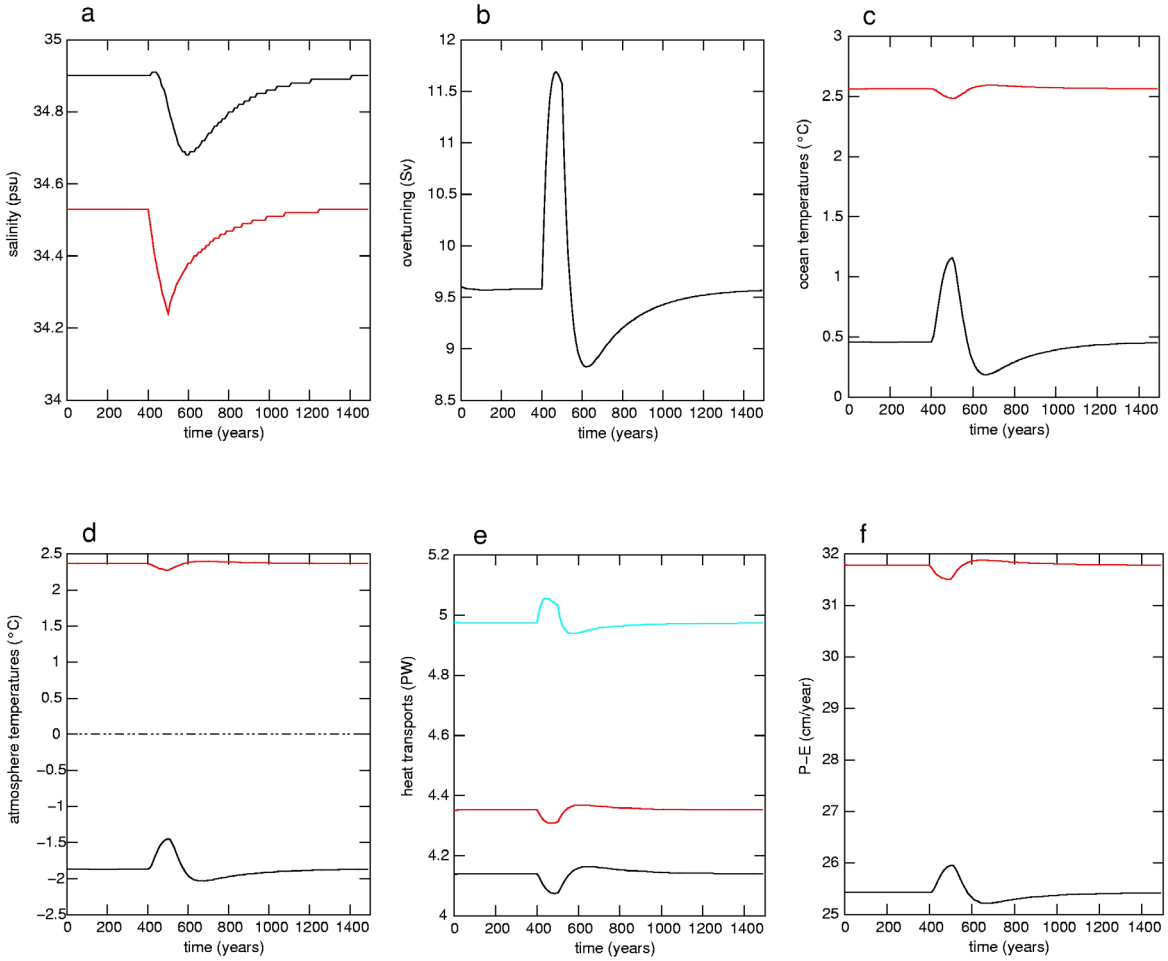

Figure 4.9: Temporal changes in experiment FWF_SH: salinities (a), overturning strength (b), ocean (c), and atmosphere temperatures (d), as well the atmospheric heat transports and the total northward heat transport (e), and surface freshwater fluxes (f). Colours are chosen as in Figure 4. 5.

4.5 Discussion and Conclusions

In the present study we have investigated the effect of different deglacial warming scenarios on the strength of the Atlantic THC, using an OGCM and a conceptual model. In prior work a conceptual single hemispheric model type [Stommel, 1961] has been independently extended to interhemispheric flow [Rooth, 1982]. Later, this model type was applied to the steady state pole-to-pole circulation [e.g. Rahmstorf, 1996]. However, these model studies employ ad hoc formulations for the atmospheric surface fluxes to simplify the coupled climate system, i.e. a temperature restoring condition with fixed freshwater-fluxes at the ocean surface. Different studies have shown that atmosphere-ocean interactions may have a strong effect on the stability properties of the THC [Nakamura et al., 1994; Marotzke and Stone, 1995; Lohmann et al., 1996; Prange et al., 1997; Scott et al., 1999]. In our interhemispheric THC model the impact of changes in the hydrological cycle have shown to be of minor importance compared to the respective changes in the freshwater scenarios, since the representation of the tropical atmosphere as one box enables a strong transmission between both hemispheres. As a result, the freshwater fluxes in both Hemispheres increase in each of the warming experiments, which decrease the respective densities in the northern and southern high latitudes. Therefore, the overall effect on the THC strength is of minor importance. In this context it is necessary to point out that the influence of the hydrological cycle on the THC stability is strongly dependent from the latitude belt at which the transition between the tropics and the high latitudes has been chosen [cf. Prange et al., 1997].

Our conceptual model has shown to capture major features of interhemispheric coupling via the Atlantic THC. Thereto belong, the reduction of the THC to meltwater events in the North Atlantic and an accompanying thermal “seesaw” [Broecker, 1998; Stocker, 1998] between the North and South Atlantic. In a colder climate the ocean circulation in the box model system is characterised by a weaker circulation, since the thermal expansions coefficient of seawater decreases with temperature [cf. Prange et al., 1997]. A strengthening of the THC in the colder climate is achieved if Southern Hemisphere and global warming are applied, while warming in the Northern Hemisphere leads to a THC decline. The different responses are related to the warming impact that increases temperature and hence, decreases density of the respective ocean boxes. The amplification of the THC in the Southern Hemisphere warming scenario warms the North Atlantic effectively, since the heat surplus is transported northward by ocean and atmospheric heat transports. In the Northern Hemisphere warming scenario the additional energy is transmitted to the South via an interhemispheric atmospheric bridge, since the NADW overturning cell is closed by broad scale upwelling to the surface ocean including the low latitudes of the global oceans that has been estimated to about 40 %, based on revisited energy requirements to sustain deep water formation [Webb and Suginohara, 2001]. According to this approach the other 60 % of NADW upwelling are accomplished by Ekman pumping along the Antarctic divergence [Toggweiler and Samuels, 1995], which occurs circumpolar and therefore, not only influences the South Atlantic. The different routes, characterizing the transmission of an anomalous local high-latitude warming in the Southern and Northern Hemisphere, suggest a classification in direct (active) and indirect

(passive) interhemispheric mediation, with respect to oceanic heat transport. The latter way of mediation accounts for the effect of heat storing in the South by a Northern Hemisphere warming induced THC slow down.

In the second approach, based on our OGCM experiments, it has been shown that Southern Ocean warming leads to a more efficient amplification of the glacial THC than global and Northern Hemisphere warming. These different THC model responses can be explained by warmer surface temperatures in the North Atlantic that arise as a direct response in the two latter scenarios. The resulting decrease of the surface density in the formation regions of NADW counteracts an augmentation of the Atlantic THC. The strongest THC amplification in the Southern Hemisphere warming scenario emphasises the key role of warming conditioned import changes to the South Atlantic via an enhanced warm and cold water route that endorse deep water formation in the North Atlantic. As in our conceptual model, Southern Hemisphere warming leads to an active heat transmission to the North Atlantic by increased northward oceanic heat transport.

Our OGCM experiments suggest that in particular the warming conditional increased import of near surface waters to the South Atlantic via the warm and the cold water route are important for deglacial climate changes. This is an alternative approach to interpretations of an Antarctic Bottom Water - NADW [Mikolajewicz, 1998] or Antarctic Intermediate Water - NADW [Weaver et al., 2003] balanced interhemispheric circulation within the Atlantic Ocean, which is based on model simulations applying freshwater perturbations to the Southern Ocean and thereby affecting the densities of the respective water masses. Although the THC responses in the conceptual model can explain much of the THC alterations simulated in the OGCM experiments, it does not account for climate shifts that are associated with vertical and horizontal convection changes in the North Atlantic. Moreover, zonal transports are not represented. In the OGCM the contribution of northward shifted convection sites is mainly responsible for the slight THC intensification detected in the Northern Hemisphere warming scenario. Furthermore, the import dynamics to the South Atlantic, which are linked to the cold (Pacific Ocean) and warm (Indian Ocean) water route of the global ocean circulation [Gordon, 1986], are not resolved. Model studies suggest that the thermohaline properties of the upper branch of the overturning circulation in the Atlantic control the buoyancy flux and eventually NADW formation [Gordon et al., 1992; Weijer et al., 2002]. Therefore, the relative contributions of the cold and warm water routes are important for the THC and its variation may exert a substantial influence on the entire climate system [Gordon, 2003].

The examinations of the present work have been motivated by a debate about possible termination-I and II scenarios concerning the deglacial initiation of warming in the Northern and Southern Hemispheres [Sowers and Bender, 1995; Bender et al., 1999; Petit et al., 1999; Alley et al., 2002], as well as a possible influence of processes in the Southern Ocean for the deglacial amplification of the THC [Knorr and Lohmann, 2003; Weaver et al., 2003]. The weaker THC in the glacial climate in both model approaches is in qualitative agreement with analyses of benthic $\delta^{13}C$ data [Sarnthein et al., 1994] and $^{231}Pa/^{230}Th$ data of marine bulk sediments [McManus et al., 2004]. In the conceptual model the equilibrium overturning strength is associated with a reduced stability of

the THC with respect to gradual North Atlantic freshwater discharge, consistent with analyses using more complex model approaches [Ganopolski and Rahmstorf, 2001; Prange et al., 2002; Knorr and Lohmann, 2003]. The localised warming scenarios are of course rather idealized, since during the last two terminations increasing atmospheric CO_2 concentration contributed to global deglacial warming [Bender et al., 1997]. Furthermore it has been proposed that different feedbacks, involving e.g. ice albedo and greenhouse-gas effects, caused regional to global synchronization of deglaciation [Alley and Clark, 1999]. During the penultimate deglaciation, these effects might have amplified radiation changes in the Southern Hemisphere due to variations in the Milankovitch forcing on the precessional period with a corresponding response in sea ice cover [Kim et al., 1998]. Despite the different approaches and interpretations that have been designed to understand THC alterations and climate shifts during deglaciation, increasingly a picture emerges that highlights the importance of the Southern Ocean as a potential "Flywheel" for an augmentation of the THC.

References:

Adkins, J. F., K. McIntyre, and D. P. Schrag (2002), The salinity, temperature, and $\delta^{18}O$ of the glacial deep ocean, *Science*, 298, 1769-1773.

Alley, R. B., and P. U. Clark (1999), The deglaciation of the northern hemisphere: A global perspective, *Annual Review of Earth and Planetary Sciences*, 27, 149-182.

Alley, R. B., E. J. Brook, and S. Anandakrishnan (2002), A northern lead in the orbital band: north-south phasing of Ice-Age events, *Quaternary Science Reviews*, 21, 431-441.

Bard, E., F. Rostek, J. L. Turon, and S. Gendreau (2000), Hydrological impact of Heinrich events in the subtropical northeast Atlantic, *Science*, 289, 1321-1324.

Bender, M., T. Sowers, M. L. Dickson, J. Orchardo, P. Grootes, P. A. Mayewski, and D. A. Meese (1994), Climate Correlations between Greenland and Antarctica During the Past 100,000 Years, *Nature*, 372, 663-666.

Bender, M., T. Sowers, and E. Brook (1997), Gases in ice cores, *Proceedings of the National Academy of Sciences of the United States of America*, 94, 8343-8349.

Bender, M. L., B. Malaize, J. Orchardo, T. Sowers, and J. Jouzel (1999), High Precision Correlations of Greenland and Antarctic Ice Core Records Over the Last 100 kyr, *Geophysical Monograph*, 112, 149-164.

Blunier, T., and E. J. Brook (2001), Timing of millennial-scale climate change in Antarctica and Greenland during the last glacial period, *Science*, 291, 109-112.

Broecker, W., and G. Henderson (1998), The sequence of events surrounding Termination II and their implications for the cause of glacial-interglacial CO_2 changes, *Paleoceanography*, 13, 353-364.

Broecker, W. S. (1991), The great ocean conveyor, *Oceanography*, 4, 79-89.

Broecker, W. S. (1998), Paleocean circulation during the last deglaciation: a bipolar seesaw?, *Paleoceanogr.*, 13, 119-121.

Budyko, M. I. (1969), The effect of solar radiation variations on the climate of the earth, *Tellus*, 21, 611-619.

Budyko, M. I. (1977), *Climatic Changes*, Washington, D.C., American Geophysical Union, 244 pp.

Chen, D. L., R. Gerdes, and G. Lohmann (1995), A 1-D atmospheric energy balance model developed for ocean modelling, *Theoretical and Applied Climatology*, 51, 25-38.

Clark, P. U., J. X. Mitrovica, G. A. Milne, and M. E. Tamisiea (2002), Sea-level fingerprinting as a direct test for the source of global meltwater pulse IA, *Science*, 295, 2438-2441.

Ganopolski, A., and S. Rahmstorf (2001), Rapid changes of glacial climate simulated in a coupled climate model, *Nature*, 409, 153-158.

Gordon, A. L. (1986), Interocean exchange of thermocline water, *Journal of Geophysical Research*, 91, 5037-5046.

Gordon, A. L., R. F. Weiss, W. M. Smethie, and M. J. Warner (1992), Thermocline and intermediate water communication between the South-Atlantic and Indian Oceans, *Journal of Geophysical Research-Oceans*, 97, 7223-7240.

Gordon, A. L. (2003), Oceanography - The brawniest retroflection, *Nature*, 421, 904-905.

Grootes, P., M. Stuiver, J. W. C. White, S. J. Johnsen, and J. Jouzel (1993), Comparison of oxygen isotope records from GISP2 Greenland ice cores, *Nature*, 366.

Haney, R. L. (1971), Surface thermal boundary condition for ocean circulation models., *Journal of Physical Oceanography*, 1, 241-248.

Henderson, G., and N. Slowey (2000), Evidence against northern-hemisphere forcing of the penultimate deglaciation, *Nature*, 402, 61-66.

Imbrie, J., and J. Z. Imbrie (1980), Modeling the climatic response to orbital variations, *Science*, 207, 943-953.

Kim, S. J., T. J. Crowley, and A. Stössel (1998), Local orbital forcing of Antarctic climate change during the last interglacial, *Science*, 280, 728-730.

Knorr, G., and G. Lohmann (2003), Southern Ocean Origin for the resumption of Atlantic thermohaline circulation during deglaciation, *Nature*, 424, 532-536.

Lohmann, G., R. Gerdes, and D. L. Chen (1996), Stability of the thermohaline circulation in a simple coupled model, *Tellus Series a-Dynamic Meteorology and Oceanography*, 48, 465-476.

Lohmann, G. (1998), The influence of a near-bottom transport parameterization on the sensitivity of the thermohaline circulation, *Journal of Physical Oceanography*, 28, 2095-2103.

Lohmann, G., and S. Lorenz (2000), On the hydrological cycle under paleoclimatic conditions as derived from AGCM simulations, *Journal of Geophysical Research-Atmospheres*, 105, 17417-17436.

Lohmann, G., M. Butzin, K. Grosfeld, G. Knorr, A. Paul, M. Prange, V. Romanova, and S. Schubert (2003), The Bremen Earth System Model of Intermediate Complexity (BREMIC) designed for long-term climate studies, model description, climatology, and applications, *Technical Report*, University Bremen.

Macdonald, A. M., and C. Wunsch (1996), An estimate of global ocean circulation and heat fluxes, *Nature*, 382, 436-439.

Maier-Reimer, E., U. Mikolajewicz, and K. Hasselmann (1993), Mean Circulation of the Hamburg LSG OGCM and its Sensitivity to the Thermohaline Surface Forcing, *Journal of Physical Oceanography*, 23, 731-757.

Marotzke, J., and P. H. Stone (1995), Atmospheric transports, the thermohaline circulation, and flux adjustments in a simple coupled model, *Journal of Physical Oceanography*, 25, 1350-1364.

McManus, J. F., R. Francois, J. M. Gherardi, L. D. Keigwin, and S. Brown-Leger (2004), Collapse and rapid resumption of Atlantic meridional circulation linked to deglacial climate changes, *Nature*, 428, 834-837.

Michaud, R., and J. Derome (1991), On the mean meridional transport of energy in the atmosphere and oceans as derived from six years of ECMWF analyses, *Tellus*, 43a, 1-14.

Mikolajewicz, U. (1998), Effect of meltwater input from the Antarctic ice sheet on the thermohaline circulation, *Annals of Glaciology*, 27, 311-316.

Milankovitch, M. (1941), Kanon der Erdbestrahlung, *Royal Serbian Acad. Spec. Publ. 132*, Sect. Math. Nat. Sci.

Nakamura, M., P. H. Stone, and J. Marotzke (1994), Destabilization of the thermohaline circulation by atmospheric eddy transports, *Journal of Climate*, 7, 1870-1882.

Oort, A. H., and J. P. Peixoto (1983), Global angular momentum and energy balance requirements from observations, *Advances in Geophysics*, 355-490.

Otto-Bliesner, B., E. C. Brady, G. Clauzet, R. A. Tomas, S. Levis, and Z. Kothavala (2005), Last Glacial Maximum and Holocene Climate in CCSM3, *Climate Dynamics*, submitted.

Petit, J. R., J. Jouzel, D. Raynaud, N. I. Barkov, J. M. Barnola, I. Basile, M. Bender, J. Chappellaz, M. Davis, G. Delaygue, M. Delmotte, V. M. Kotlyakov, M. Legrand, V. Y. Lipenkov, C. Lorius, L. Pepin, C. Ritz, E. Saltzman, and M. Stievenard (1999), Climate and atmospheric history of the past 420,000 years from the Vostok ice core, Antarctica, *Nature*, 399, 429-436.

Prange, M., G. Lohmann, and R. Gerdes (1997), Sensitivity of the thermohaline circulation for different Climates - investigations with a simple atmosphere-ocean model, *Paleoclimates*, 2, 71-97.

Prange, M., V. Romanova, and G. Lohmann (2002), The glacial thermohaline circulation: Stable or unstable?, *Geophysical Research Letters*, 29, 2028, doi:2010.1029/2002LH015337.

Prange, M., G. Lohmann, and A. Paul (2003), Influence of vertical mixing on the thermohaline hysteresis: Analyses of an OGCM, *Journal of Physical Oceanography*, 33, 1707-1721.

Rahmstorf, S., and J. Willebrand (1995), The role of temperature feedback in stabilising the thermohaline circulation, *Journal of Physical Oceanography*, 25, 787-805.

Rahmstorf, S. (1996), On the freshwater forcing and transport of the Atlantic thermohaline circulation, *Climate Dynamics*, 12, 799-811.

Roeckner, E., K. Arpe, L. Bengtsson, S. Brinkop, L. Dümenil, M. Esch, E. Kirk, F. Lunkeit, M. Ponater, B. Rockel, R. Sausen, U. Schlese, S. Schubert, and M. Windelband (1992), Simulation of the present-day climate with the ECHAM model: Impact of model physics and resolution, *MPI Rep.*, MPI-M Hamburg, Germany, 171 pp.

Rooth, C. (1982), Hydrology and ocean circulation, *Progress in Oceanography*, 11, 131-149.

Rühlemann, C., S. Mulitza, G. Lohmann, A. Paul, M. Prange, and G. Wefer (2004), Intermediate depth warming in the tropical Atlantic related to weakened thermohaline circulation: Combining paleoclimate data and modeling results for the last deglaciation, *Paleoceanography*, 19, PA1025, Doi:10.1029/2003PA000948.

Sarnthein, M., K. Winn, S. J. A. Jung, J. C. Duplessy, L. Labeyrie, H. Erlenkeuser, and G. Ganssen (1994), Changes in East Atlantic Deep-Water Circulation over the Last 30,000 Years - 8 Time Slice Reconstructions, *Paleoceanography*, 9, 209-267.

Schäfer-Neth, C., and A. Paul, Circulation of the glacial Atlantic: a synthesis of global and regional modeling. in *The northern North Atlantic: A changing environment*, edited by Schäfer, P., W. Ritzrau, M. Schlüter and J. Thiede, pp. 446-462, Springer-Verlag, Berlin, Heidelberg, 2001.

Scott, J. R., J. Marotzke, and P. H. Stone (1999), Interhemispheric thermohaline circulation in a coupled box model, *Journal of Physical Oceanography*, 29, 351-365.

Shackleton, N. J. (2000), The 100,000-year ice-age cycle identified and found to lag temperature, carbon dioxide, and orbital eccentricity, *Science*, 289, 1897-1902.

Sowers, T., and M. Bender (1995), Climate Records Covering the Last Deglaciation, *Science*, 269, 210-214.

Stocker, T. (2003), South dials north, *Nature*, 524, 496-499.

Stocker, T. F. (1998), The seesaw effect, *Science*, 282, 61-62.

Stommel, H. (1961), Thermohaline convection with two stable regimes of flow, *Tellus*, 13, 224-230.

Toggweiler, J. R., and B. Samuels (1995), Effect of Drake Passage on the global thermohaline circulation, *Deep-Sea Research I*, 42, 477-500.

Weaver, A. J., O. A. Saenko, P. U. Clark, and J. X. Mitrovica (2003), Meltwater pulse 1A from Antarctica as a trigger of the Bølling-Allerød warm interval, *Science*, 299, 1709-1713.

Webb, D. J., and N. Suginohara (2001), Oceanography - Vertical mixing in the ocean, *Nature*, 409, 37-37.

Weijer, W., W. de Ruijter, A. Sterl, and S. Drijfhout (2002), Response of the Atlantic overturning circulation to South Atlantic sources of buoyancy, *Global Planetary Change*, 34, 293-311.

Zhang, S., R. J. Greatbatch, and C. A. Lin (1993), A reexamination of the polar halocline catastrophe and implications for coupled ocean-atmosphere modelling, *Journal of Physical Oceanography*, 23, 287-299.

Chapter 5

Atmospheric responses to abrupt changes in the thermohaline circulation during deglaciation

Abstract

Using a three-dimensional atmosphere circulation model, we have analyzed circulation changes that arise in response to a deglacial reduction and amplification of the thermohaline circulation (THC). Caused by a meltwater-induced slowdown of the THC, the atmosphere exhibits cooling in large parts of the Northern Hemisphere and an intensified subtropical North Atlantic high. Opposite temperature and pressure trends evolve in the South Atlantic. Contrary, the abrupt deglacial amplification of the THC results in North Atlantic warming and a reduction of the subtropical high, with again opposite trends in the South Atlantic. Interestingly, the northwestern Pacific region exhibits a warming parallel to Greenland stadials and vice versa during interstadials. This inter-ocean anti-phasing is linked to changes in the strength of the Aleutian low, associated with variations in the advection of warmer Pacific air. Furthermore, this temperature pattern is shown to be sensitive on the climate background conditions, such as the glacial orography.

5.1 Introduction

The last deglaciation between 20 ka BP (thousand years before present) and 10 ka BP has been punctuated by a series of abrupt climate sequences as documented in ice core [e.g. Blunier and Brook, 2001] and marine sediment records [e.g. Bard et al., 2000]. These deglacial climate shifts have been linked to changes in the Atlantic thermohaline circulation (THC). Data from marine sediment cores suggest that meltwater discharge and enhanced abundances of ice-rafted debris in the North Atlantic, known as Heinrich Events [Heinrich, 1988; Bond et al., 1992] were associated with shutdowns of the THC and cold climate conditions in the North Atlantic realm [Broecker and Hemming, 2001; Clark et al., 2002]. Subsequently, sea surface temperatures (SST) in the North Atlantic almost reached interglacial values during the Bølling-Allerød (B/A), consistent with active North Atlantic deepwater (NADW) formation, as corroborated by benthic $\delta^{13}C$ data [Sarnthein et al., 1994]. Recently, it has been shown with the aid of model investigations that the

Atlantic THC can be restarted from a meltwater induced THC “off-mode” by Southern Ocean [Knorr and Lohmann, 2003] or global deglacial warming [Knorr and Lohmann, 2005]. In these scenarios, rising sea surface temperatures and receding sea-ice cover around Antarctica increase the volume transport into the Atlantic via the warm and the cold water route [Gordon, 1986] of the global ocean circulation. The regaining influence of the warm water route favours convective activity in the North Atlantic by the import of relatively salty water from the Indian Ocean. Combined with increased advection of salty water from the tropics the surface density in the regions of NADW formation increases and leads to a rapid switch-on of the Atlantic THC after a threshold density is reached.

In the present study we apply a three-dimensional atmosphere general circulation model (AGCM) of intermediate complexity, which is driven by monthly SST fields taken from a global deglacial model simulation with an ocean general circulation model (OGCM) [Knorr and Lohmann, 2005]. This one-way ocean-atmosphere coupling enables a first estimation of dynamical atmospheric responses to abrupt changes of the THC during deglaciation. The present study is aimed to simulate and analyze changes in the spatial temperature, pressure and precipitation pattern in the atmosphere, as response to the 19 ka meltwater pulse (MWP) [Clark et al., 2004] and an abrupt amplification of the THC, associated with the onset of the B/A.

5.2 The atmospheric model

The Portable University Model of the Atmosphere (PUMA) is derived from the Reading multi-level spectral model described by Hoskins and Simmons [1975]. The model is based on the moist primitive equations formulated in terms of the vertical component of absolute vorticity, the horizontal divergence, the temperature, the logarithm of the surface pressure and the specific humidity. The equations are solved using the spectral transform method [Orszag, 1970; Eliasen et al., 1970] with terrain following coordinates in the vertical. Belonging to models of intermediate complexity [Claussen et al., 2002], PUMA is completed by comparatively simple parameterization schemes for climate relevant processes like radiation, boundary layer fluxes, cloud formation, as well as convective and stratiform precipitation [Fraedrich et al., 1998; http://puma.dkrz.de/planet]. PUMA is integrated in T21/L5 spectral resolution. Recent applications of PUMA investigate simulations of glacial climate [Romanova et al., 2005a], as well as extreme “Snowball earth” scenarios [Romanova et al., 2005b].

To simulate the climate state under glacial conditions, we prescribe specific static boundary conditions like glacial orography, land-sea and glacier distributions according to Peltier [1994]. The atmospheric CO_2 concentration is fixed at 200 ppm according to reconstructions [Barnola et al., 1987; Keeling et al., 1996]. Orbital parameters Earth's obliquity, orbital eccentricity and vernal equinox mean longitude of perihelion are calculated for the year 21.000 years BP according to Berger [1978]. A detailed description of the glacial background climate, as represented in PUMA simulations can be found in Romanova et al. [2005a, b].

5.3 The atmospheric forcing fields

The atmospheric model is driven by monthly SST fields taken from a deglacial model simulation with the OGCM LSG [Maier-Reimer et al., 1993; Lohmann et al., 2003], which has been used for various paleoclimatic applications [e.g., Prange et al., 2002; Knorr and Lohmann 2003; Romanova et al., 2004]. For a detailed description of the modeled deglaciation scenario with the OGCM we would like to refer to experiment B2 in Knorr and Lohmann [2005]. This ocean model run represents a transient simulation of the deglacial climate sequence starting from the Last Glacial Maximum (LGM) until 13 ka BP, which contains the Heinrich I sequence and the onset of the B/A. To simulate a deglacial warming in the ocean model, the climatological background fields in temperature, sea ice and wind stress were linearly interpolated between preindustrial and glacial climate conditions (Figure 5.1a), which have been provided by model simulations with the atmospheric model ECHAM3/T42 [Roeckner et al., 1992; Lohmann and Lorenz, 2000]. In the deglacial OGCM experiment the atmospheric freshwater fluxes remain in the glacial state as modelled in Lohmann and Lorenz [2000]. Additional to the changed background climate, freshwater flux perturbations have been induced to the North Atlantic to mimic the effect of melting ice from the great Northern Hemisphere ice sheets. The 19 ka MWP is simulated by a freshwater magnitude of 0.25 Sv (1 Sv = 10^6 kg m^{-3}) and a duration of 200 years (Figure 5.1b), which is motivated by geological data from the Irish Sea [Clark et al., 2004] and sea level reconstructions [Chappell, 2002]. The meltwater inflow to the Atlantic Ocean has been uniformly applied between 20°N and 50°N, according to deglacial meltwater routes via the Mississippi, St. Lawrence and Hudson River, respectively [Clark et al., 2001].

Deepwater formation in the North Atlantic is reduced immediately in response to the 19 ka MWP (Figure 5.1c), linked to decreased salinities (Figure 5.1d) and hence, reduced density in the near-surface North Atlantic. As response to the 19 ka MWP, the SST decrease by about 1°C in large parts of the North Atlantic (Figure 5.1d). After the meltwater inflow ceases the THC recovers, but the subsequent meltwater spikes centred at 2.5 and 3.5 ka (Figure 5.1b) lead to a THC collapse until the abrupt THC amplification after 6000 model years (Figure 5.1c), which can be related to the onset of the B/A. As a result North Atlantic SST increase by about 2°C, while temperatures in the South Atlantic decrease. In the Labrador Sea the temperature increase reaches a maximum, exceeding 10°C [Knorr and Lohmann, 2005].

To investigate the dynamical atmospheric responses to the 19 ka MWP and the abrupt reactivation of the THC we apply the AGCM. All static boundary conditions in the atmospheric model, including orbital parameters and CO_2 are kept constant for the different experiments at levels of the LGM. Along with SST changes, sea ice distribution is calculated with a thermodynamic sea ice model according to SST conditions predicted by the ocean model.

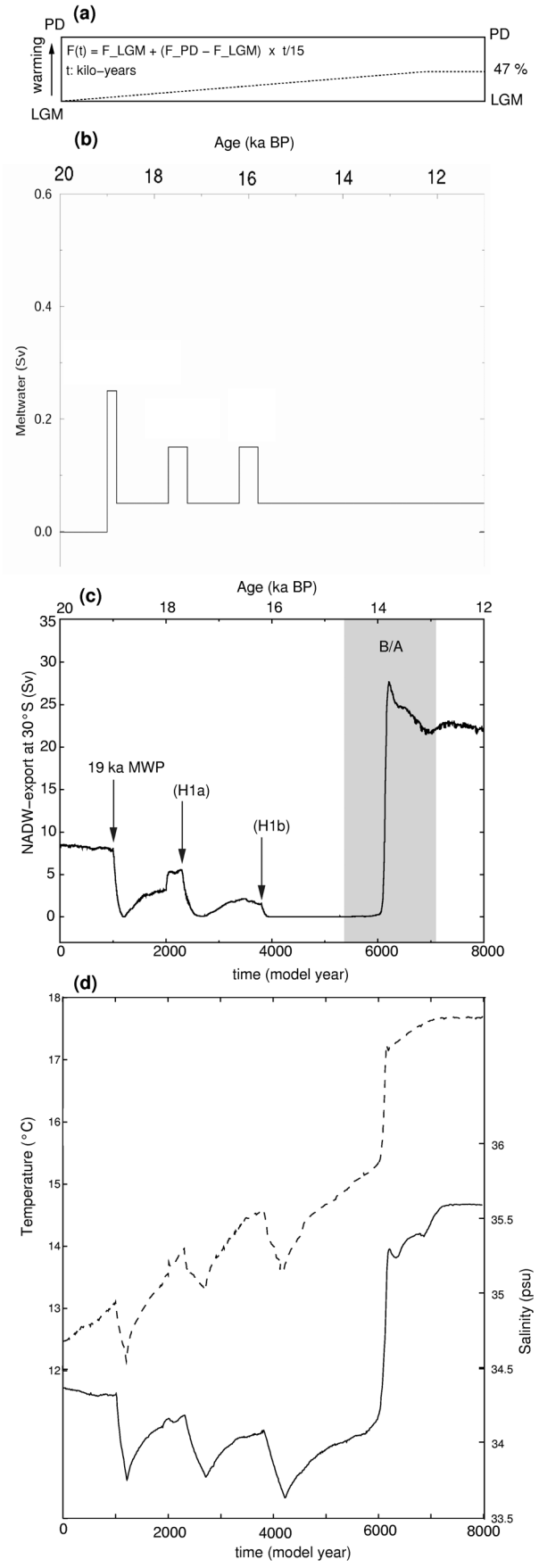

Figure 5.1: Illustration of temporal changes in the background climate of the ocean model experiment [Knorr and Lohmann, 2005] that forms the basis of the surface temperature field of the atmospheric model runs with PUMA. F is a climatological field. The subscripts "LGM" and "PD" denote Last Glacial Maximum and present-day conditions correspondingly, and t is the time from the beginning of the transient experiment expressed in kilo-years. Hence, the analyses with the PUMA are related to about 1/15 and 6/15 of the total deglacial warming (a); the meltwater scenario of the whole run (b); the NADW export at 30°S (c), and annual changes of temperature (°C, dashed line) and salinity (psu, solid line) averaged in the North Atlantic realm between 35-45°N and 55-65°W (d). The abbreviation 19 ka MWP indicates the meltwater pulse at 19 ka BP [Clark et al., 2004]; the meltwater pulses associated with the Heinrich events H1a and H1b [Bard et al., 2000] are not focus of the present study. The grey shaded area indicates the temporal classification of the B/A warm phase. Panel (a), (c) and (d) are taken from Knorr and Lohmann [2005].

5.4 Results

5.4.1 The 19 ka meltwater pulse

In the first experiment, referred to as LGM_MWP, we investigated the atmospheric model response to the 19 ka MWP that nearly causes a shut down of the overturning circulation in the Atlantic (Figure 5.1c). The corresponding surface air temperatures (ST) in LGM_MWP (Figure 5.2a) reacts with a general cooling of the North Atlantic, reaching up to 1.5°C along the East-American coast and up to 1°C in the eastern tropical North Atlantic. The South Atlantic experiences a general warming of about 0.75°C along the Argentinean coast and 0.5°C at the coast off Angola and Namibia. The cooling of the North Atlantic leads to a simultaneous cooling of eastern Europe and south-eastern Asia, especially in the Himalayan region. In contrast to this, the north Siberian and North American regions get warmer, possibly a result of a slight strengthening of the Aleutian low associated with advection of warmer Pacific temperatures (Figure 5.2b). The anomalous pressure pattern shows a seesaw between the North and South Atlantic, with higher pressure over the colder North Atlantic and accompanied intensified stronger westerlies. On the other hand, advection of cold and dry air from the northeastern Atlantic to the north-western tropical Atlantic supports the generally anticyclonic gyre transport of the North Atlantic. In the Northern Hemisphere pressure increases in the Atlantic–Eurasian region, while pressure decreases over the Pacific and North America. The cooling of the North Atlantic has also implications for the hydrological cycle. Figure 5.2c shows the anomalous P-E pattern for LGM_MWP. The net precipitation rate (Figure 5.2c) generally amplifies over the colder North Atlantic. The north-western tropics show increased evaporation, while net precipitation is increased south of the equator.

5.4.2 The Bølling-Allerød transition

In the second experiment, named LGM_BA, we examine the atmospheric effect of a conveyor start up at the onset of the B/A. As a response the North Atlantic gets warmer, especially in the downstream region of the Labrador Sea. Here, warming of up to 8°C in ST initiates an extensive warming over the North Atlantic realm (Figure 5.3a). Besides the neighboured regions of Greenland and north-east America, the warming extends far over Europe with rates of more than 3°C at the west Siberian coast. Whole northern Europe and huge parts of Asia become warmer. Contrary, the South Atlantic gets colder, with highest amplitudes along the Argentinean coast. The resumption of the THC in the Atlantic has only marginal impact on the Pacific Ocean, which shows no significant changes in the anomalous ST field for the B/A event.

The strong temperature increase in the North Atlantic influences the atmospheric circulation in the Northern Hemisphere and leads to a negative pressure anomaly in the SLP field of the North Atlantic (Figure 5.3b), inducing a weakening of the westerlies. This yields to sustain the warm anomaly in the North Atlantic, which is generally advected to the east with the mean westerly

flow. The South Atlantic experiences a pressure increase. The Aleutian low is also reduced and the global pressure distribution shows a generally opposite behaviour compared to the 19 ka MWP event. Evaporation increases over the western North Atlantic, possibly contributing to the resumption of the THC in this area. Downstream to the east, increased precipitation occurs along with the mean westerly flow. In the tropics, an opposite picture to the 19 ka MWP is visible.

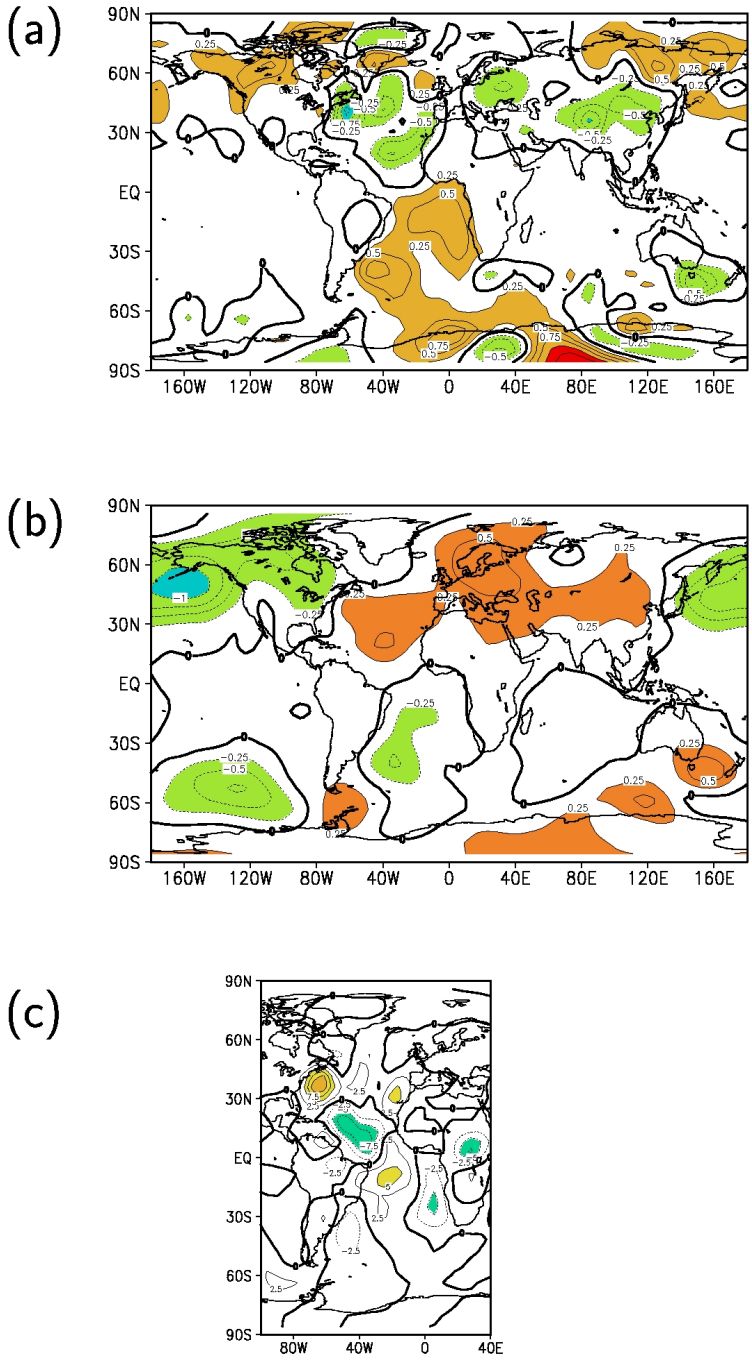

Figure 5.2: Annual mean differences in (a) surface temperature (°C); (b) sea level pressure (hPa), and (c) P-E (mm/month) patterns for the 19 ka MWP event, as simulated with PUMA in LGM_MWP. The changes are given by the difference between model year 1000 and 1200, respectively. Values greater/lower than +/-0.25°C in (a), +/-0.25 hPa in (b), and +/-5 mm/month in (c) are shaded orange-red/green-blue, respectively.

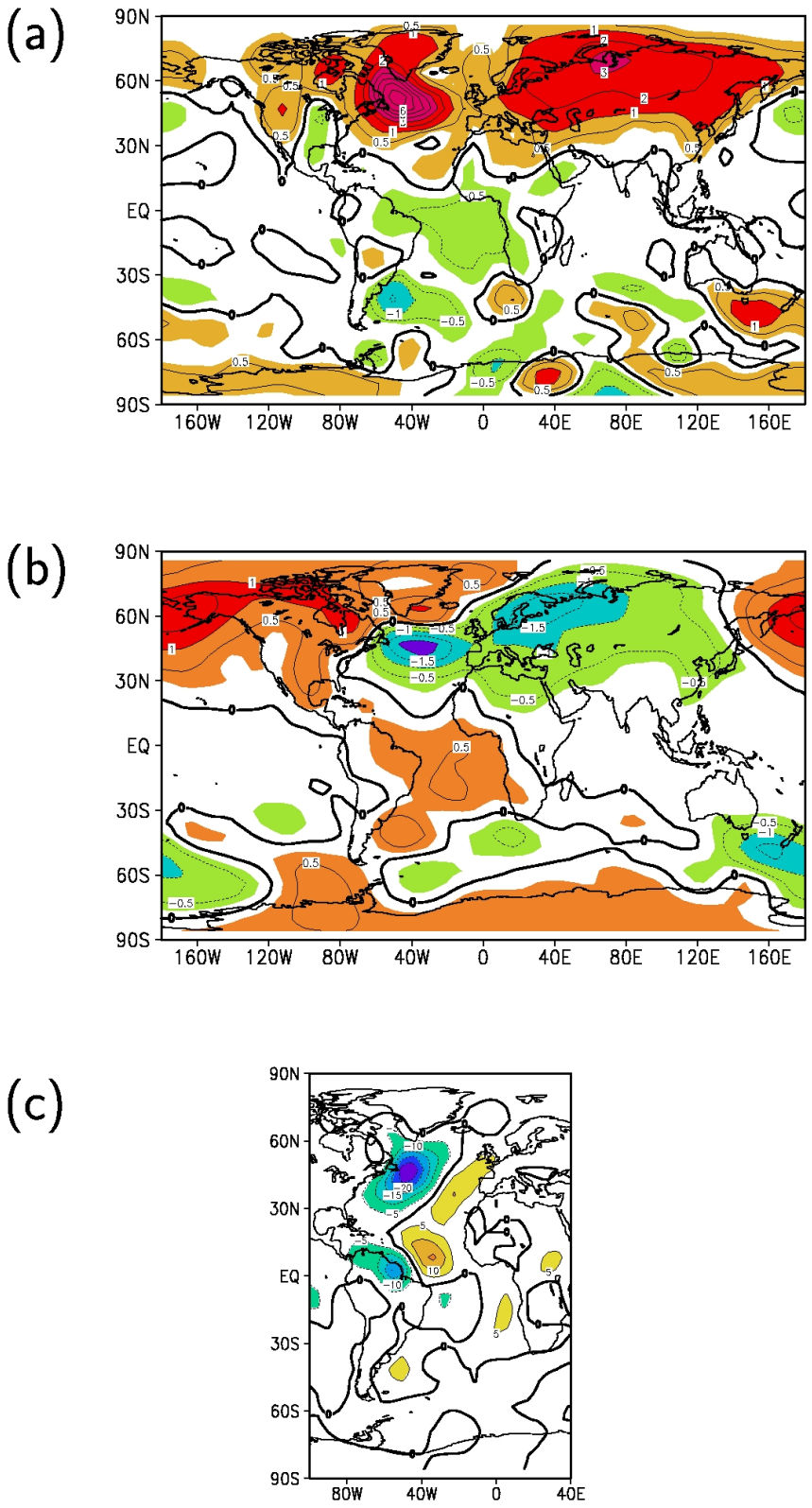

Figure 5.3: Annual mean differences in (a) surface temperature (°C); (b) sea level pressure (hPa), and (c) P-E (mm/month) patterns for the B/A transition, as simulated in LGM_BA. The changes are given by the difference between 6170 and 6000 model years. The colouring is chosen as in Figure 5.2.

5.4.3 Sensitivity study on background climate conditions

Contrary to the observed cooling in large parts of the Northern Hemisphere in response to the 19 ka MWP, our results in LGM_MWP exhibit a warming in the high latitudes of the northwest Pacific. On first sight this contrasts with atmospheric heat transfer, expected to produce quasi-coeval signals across the Hemisphere. To evaluate possible reasons for this inter-oceanic phasing, we rerun LGM_MWP with the same set-up, but altering the glacial background conditions in that we exchange the glacial orography with present-day conditions in LGM_BC (BC: background climate). The glacier mask is further on taken for glacial conditions to account for identical albedo feedbacks. This aims to investigate the role of exact background climate conditions, because earlier studies perform meltwater experiments that are mostly based on present-day set-ups.

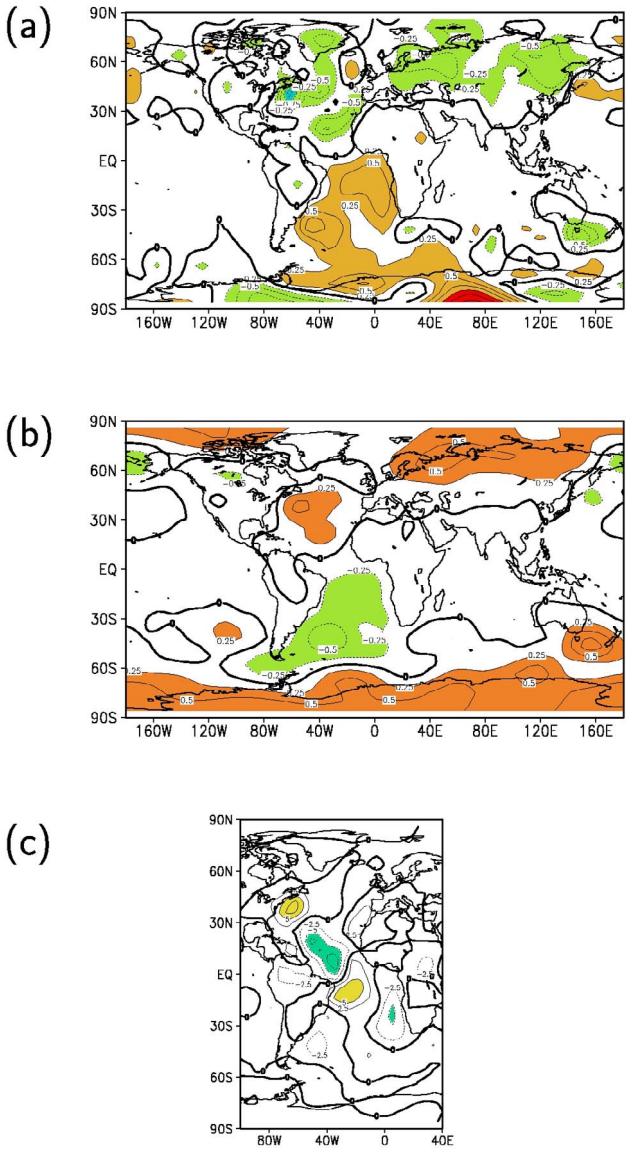

Figure 5.4: Annual mean differences in (a) surface temperature (°C); (b) sea level pressure (hPa), and (c) P-E (mm/month) patterns for the 19 ka MWP event, but with present-day orography, as simulated in LGM_BC. The changes are given by the difference between model year 1200 and 1000, respectively. The colouring is chosen as in Figure 5.2.

Compared to Figure 5.2, the changed orography shows colder ST over North America and Siberia, along with a slight warming in Europe and Asia (Figure 5.4a). The reason is given through the changed pressure field over the ice sheets, weakening the anomalous Aleutian low and changing the wavelike deflected flow regime to a more westerly circulation (Figure 5.4b). The water vapour transport over the North Atlantic is less influenced due to the identical boundary conditions over the ocean (Figure 5.4c). Only over North America and Europe, net precipitation changes to an evaporative regime, however, with no significant amplitudes.

5.5 Discussion and Conclusion

In the present study we have applied an AGCM of intermediate complexity, which is driven by monthly SST fields taken from a global deglacial model simulation [Knorr and Lohmann, 2005]. This one-way coupling approach is limited in the model response since the ocean neither accounts for changes in atmospheric circulation, nor for the temperature anomalies transport by atmospheric circulation itself. Only over the continents and sea ice the atmospheric temperature is relatively free to respond to changes in atmospheric circulation. The one-way ocean-atmosphere coupling enables a first estimation of dynamical atmospheric responses to abrupt changes of the THC in response to the 19 ka MWP (LGM_MWP), as well as an abrupt amplification of the THC that can be linked to the onset of the B/A (LGM_BA). Moreover, we examined the sensitivity of the Northern Hemisphere inter-ocean temperature signature in dependence of the background climate conditions (LGM_BC). The main findings to the abrupt deglacial THC changes have been:

(i) The global climate impact and the interhemispheric temperature and pressure seesaw in the Atlantic by large scale temperature advection

(ii) The North Atlantic - North Pacific inter-ocean temperature seesaw in dependence of the glacial background conditions

5.5.1 The global climate impact and the interhemispheric temperature and pressure seesaw in the Atlantic

Due to the coupling between the ocean and atmosphere the adjacent continental areas around the Atlantic are directly influenced by changes in the THC and associated northward heat transport. The results also show a strong response of atmospheric processes that might be important to transmit abrupt Atlantic climate signals to other regions. The spatial patterns of atmospheric ST, SLP and P-E changes in LGM_MWP suggest that the climate impact has been global. The general spatial signature of associated temperature variations in the Atlantic can be compared with those of Heinrich events [Bond et al., 1992] and the model response is qualitatively consistent with proxy reconstructions that indicate a spaciously Northern Hemisphere cooling and Southern Hemisphere

warming during stadial phases [Voelker et al., 2002]. In the continental Americas along a Pole-Equator-Pole transect, reconstructed climatic changes for the last glacial termination exhibit similar responses [Markgraf et al., 2000]. Furthermore, ice core records from Greenland and Antarctica suggest the start of a prolonged cooling in the North Atlantic realm (the Oldest Dryas) [Grootes et al., 1993], while a progressive deglacial warming has been documented over Antarctica [Petit et al., 1999; Blunier and Brook, 2001]. The most sensitive regions to detect the respective cooling are along the East-American coast, as well as the locations off the north west coast of Africa and the Iberian Peninsula. Based on alkenone data, typical cooling rates of 3-6°C have been estimated to be a typical feature of Heinrich events off the Portuguese coast [Bard et al. 2000; Pailler and Bard, 2002]. Compared to these temperature variations the simulated temperature variations of 1-1.5°C in LGM_MWP are relatively small, which can be explained by the background warming and the short duration of the 19 ka MWP that leads to a strongly reduced but not stalled THC in LGM_MWP. The temperature differences are also dependent on the modelled equilibrium state. For instance the SST variations in meltwater scenario with modern boundary conditions, detected in a coupled atmosphere-ocean examination [Knutti et al., 2004] are reported to exceed 3°C, which can be largely attributed to the relatively strong equilibrium overturning.

In the South Atlantic, the regions off the Argentinean and Namibian coasts exhibit a pronounced warming. Both regional features have also been found in a coupled atmosphere-ocean study [Lohmann, 2003]. The strong warming off Argentina is associated with an anomalous southward flow along the coast of South America. The pronounced warming off Namibia can be linked to a reduced northward flow along the conveyor belt circulation and suppressed upwelling. Moreover, the general warming in South Atlantic, also detected in marine sediment cores [e.g., Charles et al., 1996; Vidal et al., 1999; Kim et al., 2002], might have contributed to the sea ice melt back as reported for a marine core site south of the present-day subpolar front [Shemesh et al., 2002] at 19 ka BP.

The SLP alterations can be largely linked to the temperature changes. The anomalous cold subtropical North Atlantic generates an atmospheric high pressure-system. We speculate that the amplification of the pressure difference between the subtropical and the northern North Atlantic might have generated stronger eastward winds that effectively transported the cold air to Europe. The detected precipitation increase in the North Atlantic might have provided a positive feedback on the meltwater induced THC reduction. In the tropics, the detected pattern of increased evaporation in the north-western part and increased net precipitation south of the equator, is similar to investigations performed with a coupled atmosphere-ocean model [Lohmann, 2003], and might be a result of the southward shift of Hadley cells in combination with a migration of the thermal equator. This is in accordance with an alteration from dry LGM conditions to relatively wet climate conditions in south-east Brasilia as revealed by modern pollen analogues in marine sediment cores during deglaciation [Behling et al., 2000]. In the Pacific, the amplified Aleutian low provokes an increased moisture transport to the East, causing increased precipitation and sustaining growth of the Laurentide Ice Sheet.

The THC amplification in LGM_BA, simulating the B/A transition, causes different atmospheric responses, which exhibit with respect to temperature opposite trends to LGM_MWP. The general

warming in large parts of the Northern Hemisphere and the accompanying cooling in the Southern Hemisphere with a cold reversal in Antarctica is in agreement with proxy reconstructions for the B/A transition as reflected in ice core records [e.g., Grootes et al., 1993; Dansgaard et al., 1993; Blunier and Brook, 2001]. Furthermore, the climate over Britain shifts to warmer and wetter conditions [Atkinson, 1987]. The reduction of the Northern Atlantic temperature gradient and the resulting strengthening of the pressure gradient might have sustained the warm anomaly that is generally advected to the east with the mean westerly flow. The warming of the North Atlantic also influenced the hydrological cycle and the evaporation increase over the western North Atlantic could have additionally increased the salinity of the surface layers. This might have provided a positive feedback for the amplification of the THC at the onset of the B/A.

5.5.2 The North Atlantic-North Pacific inter-ocean temperature seesaw

Rest on foraminifera-based SST, Kiefer et al. [2001] has claimed that the northwest Pacific warms parallel to cold stadials and vice versa during warm interstadials. In previous studies this North Atlantic – Pacific seesaw has been linked to either dominant atmospheric [Lohmann, 2003] or oceanic forcing [Kiefer et al., 2001]. In the latter explanation the THC initiates a shutdown of cold Pacific deepwater upwelling as NADW formation ceases in response to North Atlantic meltwater discharge. Since our model studies do not indicate a significant warming in the North Pacific, but a slight warming over northern North America and East Siberia, we attribute this effect to the amplification of the Aleutian low and the corresponding changes in atmospheric circulation. The sensitivity study LGM_BC reveals that the northwest Pacific warming is conditional on the correct background climate conditions, such as a glacial orography. Without ice sheet over North America, the North Pacific surrounding continental regions (Eurasia and the north-west America) show substantial cooling. The representation of the glacial orography however, induces a deflection of the wave trains and leads to a slight warming of the high latitudes around the North Pacific. In contrast, an investigation using a coupled atmosphere-ocean general circulation model (OAGCM) [Mikolajewicz et al., 1997] shows that an intensification of the Aleutian low amplifies in-phase responses with the North Atlantic, which has been attributed to an augmentation of upwelling in the subpolar Pacific due to a stronger cyclonic atmosphere circulation. This interaction is not represented in our model approach. The same in-phase relation between the high latitude North Atlantic and the North Pacific was also found in different previous studies concerning the impact of THC changes on climate, performed with different OAGCM's, however, based on modern boundary conditions [e.g., Manabe and Stouffer, 1997; Mikolajewicz et al., 1997, Wood et al. 1999; Knutti et al., 2004]. Alternatively to the sensitivity of the North Atlantic – North Pacific phase relation on the background climate, the discrepancy between the present and previous works might be related to the missing eastward transport of temperature anomalies from the North Atlantic via atmosphere circulation in the experiment by Knorr and Lohmann [2005].

Summarizing the present study clearly demonstrates that variations in atmospheric circulation and precipitation pattern, in response to deglacial changes in the THC, exert a profound contribution to the regional and global transmission of abrupt climate shifts in the Atlantic. It is also possible that

changes in the hydrological cycle might have provided a positive feedback on a deglacial reduction and amplification of the Atlantic THC. Besides, these atmospheric impacts we would like to highlight the role of adequate climate background conditions in order to simulate abrupt climate changes during the last glacial and termination-I. In the future deeper insights concerning the relevance of atmospheric processes, oceanic thresholds and their coupling must be gathered in deglacial simulations with fully coupled models of the atmosphere-ocean-cryosphere system.

References:

Atkinson, T. C., K. R. Briffa, and G. R. Coope (1987), Seasonal temperatures in Britain during the past 22,000years, reconstructed using beetle remains, *Nature*, 325, 587-592.

Bard, E., R. Rostek, J. L. Turon, and S. Gendreau (2000), Hydrological impact of Heinrich events in the subtropical northeast Atlantic, *Science*, 289, 1321-1324.

Barnola, J. M., D. Raynauld, Y. S. Korotkevich, and C. Lorius (1987), Vostok ice core provides 160,000 year record of atmospheric CO_2, *Nature*, 329, 408-414.

Behling, H., W. H. Arz, J. Pätzold, and G. Wefer (2000), Late Quaternary vegetational and climate dynamics in northeastern Brazil, inferences from marine core GeoB 3104-1, *Quaternary Science Reviews*, 19, 981-994.

Berger, A. L. (1978), Long term variations of daily insolation and quaternary climate changes, *J. Atmos. Sci.*, 35(12), 2362-2367.

Blunier, T., and E. J. Brook (2001), Timing of millennial-scale climate change in Antarctica and Greenland during the last glacial period, *Science*, 291, 109-112.

Bond, G., H. Heinrich, W. Broecker, L. Labeyrie, J. McManus, J. Andrews, S. Huon, R. Jantschik, S. Clasen, C. Simet, K. Tedesco, M. Klas, G. Bonani, and S. Ivy (1992), Evidence for massive discharges of icebergs into the North Atlantic ocean during the last glacial period, *Nature*, 360, 245-249.

Broecker, W. S., and S. Hemming (2001), Climate swings come into focus, *Science*, 294, 2308-2309.

Chappell, J. (2002), Sea level changes forced ice breakouts in the Last Glacial cycle: new results from coral terraces, *Quaternary Science Reviews*, 21, 1229-1240.

Charles, C. D., J. Lynch-Stieglitz, U. S. Ninnemann, and R. G. Fairbanks (1996), Climate connections between the hemispheres revealed by deep sea sediment core/ice core correlations, *Earth and Planetary Science Lett.*, 142, 19-27.

Clark, P. U., S. J. Marshall, G. K. C. Clarke, S. W. Hostetler, J. M. Licciardi, and J. T. Teller (2001), Freshwater forcing of abrupt climate change during the last glaciation, *Science*, 293, 283-287.

Clark P. U., N. G. Pisias, T.F. Stocker, and A.J. Weaver (2002), The role of the thermohaline circulation in abrupt climate change, *Nature*, 415, 863-869.

Clark, P. U., A. M. McCabe, A. C. Mix, and A. J. Weaver (2004), Rapid rise of sea level 19,000 years ago and its global implications, *Science*, 304, 1141-1144.

Claussen, M., L. A. Mysak, A. J. Weaver, M. Crucifix, T. Fichefet, M.-F. Loutre, S. L.Weber, J. Alcamo, V A. Alexeev, A. Berger, R. Calov, A. Ganopolski, , H. Goosse, G. Lohmann, F. Lunkeit, I. I. Mokhov, V. Petoukhov, P. Stone, and Z. Wang (2002), Earth System models of intermediate complexity: Closing the gap in the spectrum of climate system models, *Clim. Dyn.*, 18, 579-586.

Dansgaard, W., S. J. Johnsen, H. B. Clausen, D. Dahl-Jensen, N. S. Gundestrup, C. U. Hammer, C. S. Hvidberg, J. P. Steffenson, A. E. Sveinbjörnsdottir, J. Jouzel, and G. Bond (1993), Evidence for general instability of past climate from a 250-kyr ice-core record, *Nature*, 364, 218–220.

Eliasen, E., B. Machenhauer, and E. Rasmussen (1970), On a numerical method for integration of the hydrodynamical equations with a spectral representation of the horizontal fields, *Inst. of Theor. Met., 2*, Univ. of Copenhagen, 37pp.

Fraedrich, K., E. Kirk, and F. Lunkeit (1998), Portable University Model of the Atmosphere. Deutsches Klimarechenzentrum, *Tech. Rep., 16*, 37pp, [online at http:/www/dkrz.de/forschung/reports.html].

Gordon, A.L. (1986), Interocean exchange of thermocline water. *J. Geophys. Res.*, 91, 5037-5046.

Grootes, P.M., M. Stuiver, J. W. C. White, S. Johnsen, and J. Jouzel (1993), Comparison of oxygen isotope records from the GISP2 and GRIP Greenland ice cores, *Nature*, 366, 552–554.

Heinrich, H. (1988), Origin and consequences of cyclic ice rafting in the northeast Atlantic Ocean during the past 130,000 years, *Quat. Res.*, 29, 142-152.

Hoskins, B. J., and A. J. Simmons (1975), A multi-layer spectral model and the semi-implicit method, *Q. J. R. Meteorol. Soc.*, 101, 637-655.

Keeling, C. D., J. F. S Chin, and T. P. Whorf (1996), Increased activity of northern vegetation inferred from atmospheric CO_2 measurements, *Nature*, 382, 146-149.

Kim, J. H., R. R. Schneider, P. J. Müller, and G. Wefer (2002), Interhemispheric comparison of deglacial sea-surface temperature patterns in Atlantic eastern boundary currents, *Earth and Planetary Science Letters*, 194, 383-393.

Kiefer, T., M. Sarnthein, H. Erkenheuser, P. M. Grootes, and A. P. Roberts (2001), North Pacific response to millenial-scale schnges in ocean circulation over the last 60 kyr. Paleoceanogr., 16(2), 179-189.

Knorr, G., and G. Lohmann (2003), Southern ocean origin for resumption of Atlantic thermohaline corculation during glaciation, *Nature*, 424, 532-536.

Knorr, G., and G. Lohmann (2005), Transitions in the Atlantic thermohaline circulation by global deglacial warming and meltwater pulses, submitted to *Paleoceanography*.

Knutti, R., J. Flückiger, T. F. Stocker, and A. Timmermann (2004), Strong hemispheric coupling of glacial climate through freshwater discharge and ocean circulation, *Nature*, 430, 851-856.

Lohmann, G. (2003), Atmospheric and oceanic freshwater transport during weak Atlantic overturning circulation, *Tellus, 55A*, 438-449.

Lohmann, G., and S. Lorenz (2000), On the hydrological cycle under paleoclimatic conditions as derived from AGCM simulations. Journal of Geophysical Research, 105, (13), 17,417-436.

Lohmann, G., M. Butzin, K. Grosfeld, G. Knorr, A. Paul, M. Prange, V. Romanova, and S. Schubert (2003), The Bremen Earth System Model of Intermediate Complexity (BREMIC) designed for long-term climate studies. Model description, climatology, and applications. *Technical Report, Bremen University, Bremen, Germany*. (available at http://www.palmod.uni-bremen.de).

Maier-Reimer, E., U. Mikolajewicz, and K. Hasselmann (1993), Mean circulation of the Hamburg LSG OGCM and its sensitivity to the thermohaline surface forcing. Journal of Physical Oceanography, 23, 731-757.

Manabe, S. and R. J. Stouffer (1997), Coupled ocean-atmosphere model response to freshwater input: comparison to the Younger Dryas event, *Paleoceanography*, 12, 321-336.

Markgraf, V., T. R. Baumgartner, J. P. Bradbury, H. F. Diaz, R. B. Dunbar, B. H. Luckman, G. O. Seltzer, T. W. Swetman, and R. Villalba (2000), Paleoclimate reconstruction along the Pole-Equator-Pole transect of the Americas (PEP I), *Quaternary Science Reviews, 19*, 125–140.

Mikolajewicz, U., T. J. Crowley, A. Schiller and R. Voss (1997), Modelling teleconnections between the North Atlantic and North Pacific during the Younger Dryas, *Nature*, 387, 384-387.

Orszag, S. A. (1970), Transform method for calculation of vector coupled sums: Application to the spectral form of the vorticity equation, *J. Atmos. Sci.*, 27, 890-895.

Peltier, W.R. (1994), Ice age paleotopography, *18(3)*, 5058, (doi:10.1029/2002PA000783).

Petit, J. R., D. Raynaud, N. I. Barkov, J. M. Barnola, M. Basile, M. Bender, J. Chappellaz, M. Davis, G. Delaygue, M. Delmotte, V. M. Kotlyakov, M. Legrand, V. Y. Lipenkov, C. Lorius, L. Pepin, C. Ritz, E. Saltzman, and M. Stievenard (1999), Climate and atmospheric history of the past 420,000 years from the Vostok ice core, Antarctica. *Nature*, 399, 429-436.

Prange, M., V. Romanova, and G. Lohmann (2002), The glacial thermohaline circulation: stable or unstable? Geophysical Research Letters Vol. 29, No. 21, 2028, doi:10.1029/2002GL015337.

Roeckner, E., K. Arpe, L. Bengtsson, S. Brinkop, L. Dümenil, M. Esch, E. Kirk, F. Lunkeit, M. Ponater, B. Rockel, R. Sausen, U. Schlese, S. Schubert, and M. Windelband (1992), Simulation of present-day climate with the ECHAM model: Impact of model physics and resolution. MPI Report No. 93, ISSN 0937-1060, Max-Planck-Institut für Meteorologie, Hamburg, Germany, 171 pp.

Romanova, V., M. Prange and G. Lohmann (2004), The stability of the glacial thermohaline circulation and its dependence on the background hydrological cycle, *Climate Dynamics*, 22, 527-538.

Romanova, V., G. Lohmann, K. Grosfeld, and M. Butzin (2005a), The relative role of oceanic heat transport and orography on glacial climate, *Quaternary Science Reviews*, (submitted).

Romanova, V., G. Lohmann, and K. Grosfeld (2005b), Simulation of extreme climates: effect of land albedo, CO_2, orography, and oceanic heat transport, *Global and Planetary Change*, (submitted).

Sarnthein, M., Winn, K., Jung, S. J. A., Duplessy, J. C., Labeyrie, L., Erlenkreuser, H., and Ganssen, (1994): Changes in east Atlantic deepwater circulation over the last 30,000 years: Eight time slice reconstructions. *Paleoceanography*, 9, 209-267.

Shemesh, A., D. Hodell, X. Crosta, S. Kanfoush, C. D. Charles, and T. Guilderson (2002), Sequence of events during the last deglaciation in Southern Ocean sediments and Antarctic ice cores, *Paleoceanography 17*, 1056, doi: 10.1029/2000PA000599.

Voelker, A. H. L., and workshop participants (2002), Global distribution if centennial-scale records for Marine Isotope Stage (MIS) 3: a database, *Quaternary Science Reviews*, 21, 1185-1212.

Vidal, L., R. R. Schneider, T. Marchal, T. Bickert, T. F. Stocker, and G. Wefer (1999), Link between the North and South Atlantic during the Heinrich events of the last glacial period, *Climate Dynamics*, 15, 909-919.

Wood, R. A., A. B. Keen, J. F. B. Mitchell, and J. M. Gregory (1999), Changing spatial structure of the thermohaline circulation in response to atmospheric CO_2 forcing in a climate model, *Nature*, 399, 572-575.

Chapter 6

Synopsis

6.1 Summary and Conclusions

The present study was aimed to an understanding of the climate dynamics during deglaciation with emphasis on deglacial climate variations and interhemispheric teleconnections as detected in paleodata, e.g. ice core and ocean sediment records. Different proxy data and modelling studies indicate that the last deglaciation is characterized by a transition from a weak glacial to a strong interglacial Atlantic THC. During the B/A warm period the sea surface temperatures (SST) in the North Atlantic almost reached interglacial values, consistent with active deep-water formation as endorsed by benthic $\delta^{13}C$ data [Sarnthein et al., 1994]. Other proxy data, based on Pa/Th [McManus et al., 2004] and Neodymium isotope ratios [Piotrowski et al., 2004] in marine bulk sediments, and modelling results [Ganopolski and Rahmstorf, 2001; Prange et al., 2002] also indicate a weak glacial and a strong interglacial ocean circulation. Previous model studies have also shown that the stability of this circulation is limited [Manabe and Stouffer, 1993; Stocker and Schmittner, 1997] and that changes in the surface salinity can trigger major reorganizations of the THC. Therefore, the impact of different deglacial warming and meltwater scenarios on the THC has been investigated, using models of different complexity, including the OGCM LSG [Maier-Reimer et al., 1993; Lohmann et al., 2003] and the AGCM PUMA [Fraedrich et al., 1998; Fraedrich et al., 2003; Fraedrich et al., 2005]. These models of intermediate complexity [Claussen et al., 2002] resolve most of the dynamical processes in the ocean and the atmosphere, respectively. Complementary, a low order model in that most of the dynamical processes are parameterised, has been designed to examine the essential physics of an interhemispheric density driven THC. The comprehensive contemplation of the different model results and the comparison with the available paleodata and model studies gives rise to the four major questions that motivated the present work:

(1) *What is the reason that gradual deglacial warming over Antarctica preceded a rapid temperature increase in Greenland at the onset of the B/A by more than 1000 years?*

Different deglacial simulations have shown that a preceding gradual warming trend in the Southern Ocean and Antarctica, relatively to temperatures in the North Atlantic realm, can be attributed to either Southern Ocean warming [Knorr and Lohmann, 2003b] or gradual

global warming [Knorr and Lohmann, 2005], superposed by an oceanic "seesaw-effect". This effect can arise in response to realistic deglacial meltwater fluxes to the North Atlantic that weakened the THC and the accompanying northward heat transport in the Atlantic [Knorr and Lohmann, 2005; Knorr et al., 2005b]. These alterations also have global atmospheric implications with cooling in large parts of the Northern Hemisphere and an intensified subtropical high in the North Atlantic. Opposite temperature and pressure trends evolve in the South Atlantic [Knorr et al., 2005a]. The global deglaciation scenario probably better characterises the interhemispheric temperature evolution during deglaciation, since increasing atmospheric CO_2 concentration contributed to global deglacial warming [Bender et al., 1997; Petit et al., 1999]. Moreover, it has been suggested that different feedbacks, involving e.g. ice albedo and greenhouse-gas effects, caused regional to global synchronization of deglaciation [Alley and Clark, 1999]. During the penultimate deglaciation, these effects might have amplified radiation changes in the Southern Hemisphere due to variations in the Milankovitch forcing on the precessional period with a corresponding response in sea ice cover [Kim et al., 1998].

(2) *What caused the abrupt warming in the north at the onset of the B/A that involved a transition from a weak glacial to a strong interglacial THC in presence of deglacial meltwater discharge to the North Atlantic, characterising the H1 cold sequence?*

Various deglacial model examinations have revealed that gradual global and Southern Ocean warming can trigger a rapid transition from a weak glacial to strong interglacial ocean circulation [Knorr and Lohmann, 2003b; Knorr and Lohmann, 2005]. In both scenarios warming induced changes in the Southern Ocean are an integral part of the deglacial THC amplification. Slowly increasing sea surface temperatures and receding sea ice cover in the Southern Ocean lead to enhanced volume transport of near surface waters into the South Atlantic via the warm (Indian Ocean) and the cold water (Pacific Ocean) routes [Gordon, 1986] of the global ocean circulation, affecting the salt balance within the Atlantic. In addition, increased northward advection of salty waters from the tropics increase the density in the regions of NADW formation and lead to a "kick-start" of the THC and meridional heat transport in the Atlantic. The initiation of new convection sites in formerly ice-covered parts of the northern North Atlantic also involves heat release from deeper layers of the North Atlantic to the colder overlying atmosphere, which in turn reinforces the THC amplification temporarily. As a consequence, sea surface temperatures in the North Atlantic increase by more than 6 – 10ºC within a few decades [Knorr and Lohmann, 2003b; Knorr and Lohmann, 2005]. The atmospheric model responds with a warming and a reduction of the subtropical high in the North Atlantic [Knorr et al., 2005a]. The amplitude and rapidity of the event compare well with the paleoclimatic record [Severinghaus et al., 1998; Severinghaus and Brook, 1999]. Different melt water

scenarios have shown that the abrupt resumption of the Atlantic THC via global and Southern Ocean warming prevails over the destabilizing impact of melt water discharge to the North Atlantic during the H1 sequence. Contrary, Northern Hemisphere warming is not sufficient to cause a reactivation of the THC from the "off-mode" in presence of reasonable melt water fluxes to the North Atlantic.
The THC amplification via global and Southern Ocean warming represents an alternative explanation to the suggestion that melt water from Antarctica retracts Antarctic Bottom Water formation, leading to a switch-on of the THC at a critical threshold [Mikolajewicz, 1998; Weaver et al., 2003], an effect that would amplify the mechanism proposed here [Knorr and Lohmann, 2005].

(3) How is it possible that the largest deglacial meltwater pulse 1A (MWP-1A) occurs more than 1,000 years before the next significant change in the THC associated with the Younger Dryas cold interval?

The warming induced import changes to the South Atlantic cause a THC flow regime, which is stronger and bistable [Knorr and Lohmann, 2003b; Knorr and Lohmann, 2005]. The bistable flow regime is driven by heat loss, whereas freshwater tends to reduce the overturning strength [Stommel, 1961]. Therefore, the interglacial THC associated with the B/A warm phase possesses a strong insensitivity with respect to deglacial melt water pulses to the North Atlantic and coincidentally a pronounced bistability in the hysteresis curve for cumulative freshwater perturbations to the North Atlantic [Knorr and Lohmann, 2005]. It has been proposed that MWP-1A largely originated from the Antarctic Ice Sheet, where its effect on the THC would be reduced considerably [Clark et al., 2002]. The presented model studies support this explanation, since a reasonable deglacial melt water spreading to the Northern and Southern Hemisphere [Rohling et al., 2004] would weaken but does not stop NADW formation [Knorr and Lohmann, 2005; Knorr et al., 2005b]. This might explain the delayed long term weakening of the THC and the accompanying YD cold phase, 1000 years after the occurrence of MWP-1A [Severinghaus et al., 1998].

(4) Where are the centres of activity responsible for the abrupt deglacial changes in the THC?

As yet, the research focus has been mainly on the northern high latitudes, since the THC is known to be susceptible to pulses of melt water into the North Atlantic, where NADW is generated. During deglaciation, the North Atlantic was exposed to large meltwater discharge from the melting Laurentide and Fennoscandian ice sheets. This continuous freshwater release on the order of about 0.1 Sv [Marshall and Clarke, 1999; Chappell, 2002] posed a constant threat to the "Achilles Heel" of the oceanic conveyor belt

circulation [Broecker, 1991], located in the North Atlantic (schematic picture in Figure 6.1). Therefore, degalcial melt water and background noise in the North Atlantic can trigger instabilities that weaken or even shut down the THC [Broecker, 1997; Ganopolski and Rahmstorf, 2001]. As a result global impacts by the operation of the oceanic “seesaw-effect” are possible.

Based on evidence of a weak glacial conveyor belt, it is natural to ask about the “Flywheel” of the ocean circulation, which might have initiated the transition to a strong interglacial ocean circulation. Given the collective results of this thesis it seems however, that the reactivation from a weaker glacial ocean circulation to a stronger interglacial THC may originate from events in the far south, since warming induced import changes to the South Atlantic are an integral part of deglacial climate change [Knorr and Lohmann, 2003b]. Especially insofar, as Southern Ocean warming can also arise as “seesaw” response to a reduced THC by melt water fluxes to the North Atlantic in a global warming scenario [Knorr et al., 2005a; Knorr and Lohmann, 2005]. These insights based on the OGCM and AGCM studies are in line with the low order model results. In the conceptual model of an interhemispheric density driven THC the deglacial key players, warming and freshwater, reduce the Atlantic overturning if applied in the North and strengthen the circulation if applied in the South [Knorr et al., 2005b]. The involved mechanisms are consistent with the phase offsets between Southern and Northern Hemisphere climate change on glacial – interglacial time scales and provide a natural link between processes operating on scales of thousands of years with faster changes in the THC.

Comprising it can be suggested that the "Achilles Heel" [Broecker, 1991] and the "Flywheel" of the Atlantic overturning circulation on paleoclimate timescales are located in the North Atlantic and the Southern Ocean, respectively (Figure 6.1). Like the “conveyor belt” metaphor [Broecker, 1991; Brünning and Lohmann, 1999] the “Flywheel” metaphor illuminates the basic idea that the Southern Ocean can be understood as the engine for the oceanic transport system at glacial-interglacial timescales [Knorr and Lohmann, 2003a; Knorr and Lohmann, 2003b; Knorr and Lohmann, 2004]. A zone of special interest is the area around the Cape of Good Hope because it represents an import route of relatively warm and saline water from the Indian Ocean (Figure 6.1 c) that is thought to precondition NADW formation [Gordon et al., 1992]. Berger and Wefer [1996] surmise that this narrow portal is directly related to the position of the sub-tropical convergence zone. Therefore, a northward displacement of this front could reduce [Gersonde et al., 2003; Paul and Schäfer-Neht, 2003] or even pinch off access, leading to speculation that the reopening of the Agulhas gap at the end of the last ice age may have played a role in restarting the Atlantic THC [Berger and Wefer, 1996].

Which conclusions can be drawn for future anthropogenic climate change? Generally, the deglaciation history suggests that the climate system is sensitive to warming and freshwater forcing in both hemispheres and responds in nonlinear ways, including the potential for strong amplifiers. Although much progress has been made in modelling these mechanisms, it is difficult

to predict the response of the THC to anthropogenic increase in CO_2. Hence, the possibility of nonlinear responses in the ocean-atmosphere system adds uncertainty to our assessment of future climate changes, which is a cause for caution.

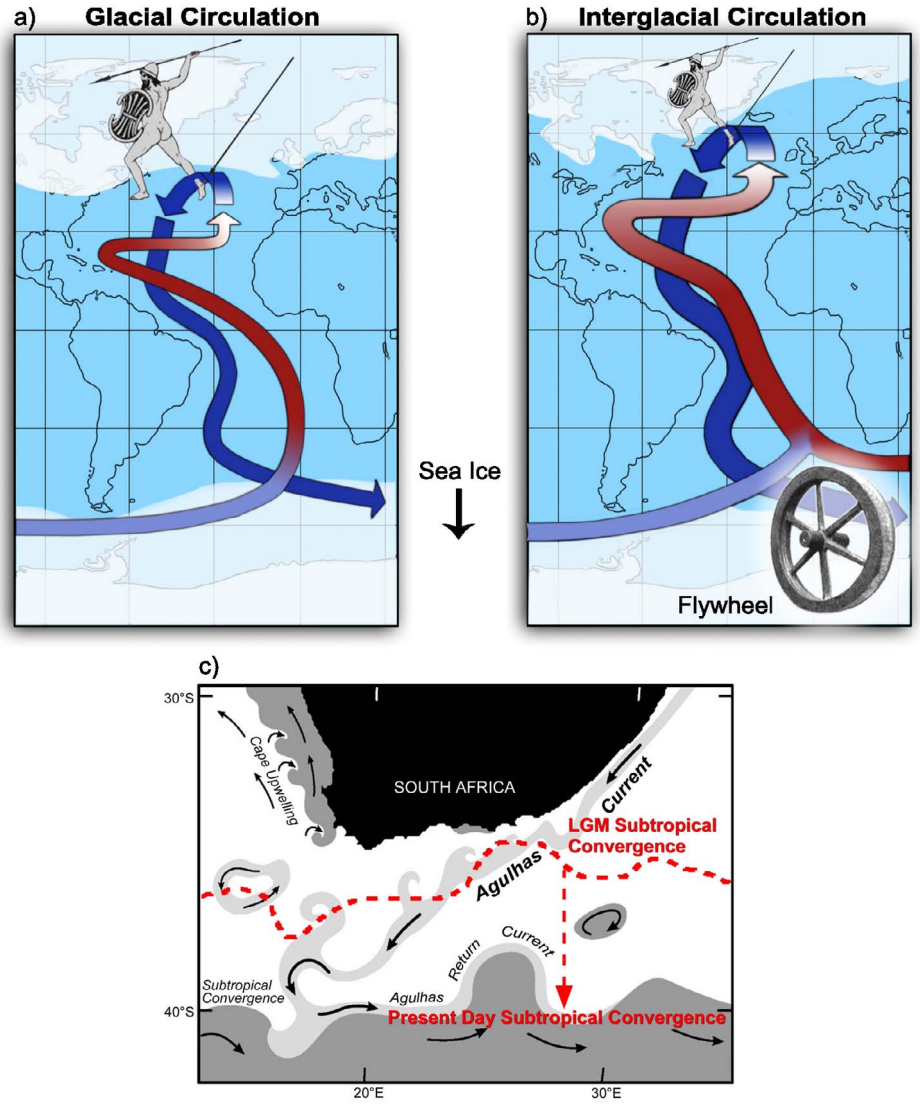

Figure 6.1 Schematic representation of the differences between the glacial and the restarted interglacial ocean circulation, and a conceptual diagram of the Agulhas Current system [taken from Knorr and Lohmann, 2004].(a) Glacial circulation is characterized by a weaker mode without a warm water route that is activated by Southern Hemisphere warming (b), operating as a pathway for relatively warm and saline water from the Indian Ocean in the interglacial mode. Moreover, the Antarctic circumpolar current accelerates and increases volume transport from the Pacific Ocean via the cold-water route into the South Atlantic. (c) Conceptual diagram of the southern Agulhas Current system [adapted from Lutjeharms, 1981], summarizing the main circulation features and a potential northward displacement (red line) of about 2°-4° of latitude of the glacial subtropical convergence zone [Brathauer and Abelmann, 1999; Gersonde et al., 2003] that might cause a reduction or a "switch-off" of the warm water route.

6.2 Outlook

The climate model approaches utilized in the presented examinations are comparatively simplified ones, but are efficient for investigating oceanic processes and atmospheric responses, associated with deep-ocean circulation and its long adjustment time.

However, the coarse resolution and the neglected non-linear terms in the oceanic momentum balance restrict studies to spatial scales larger than 1000 kilometres. Since the South Atlantic is characterized by a number of unique dynamical features, such as the large Agulhas Rings [Schouten et al., 2002] that form a key link in the THC, it is of interest to investigate the "Flywheel" and its respective energy source, using high-resolution models of the South Atlantic, to obtain a more detailed view of this region. Another limitation of the presented model approaches is related to the non-interactive coupling between the AGCM and the OGCM. Therefore, the temperature changes over the ocean are essentially determined by the OGCM simulation, which neither accounts for changes in atmospheric circulation, nor for the temperature anomalies transported by atmospheric circulation itself. Thus, essential atmosphere-ocean feedbacks are disregarded, which might attenuate or amplify the processes described in the thesis. Complementary, the application of a biogeochemical model component with a sediment module might allow to simulate directly changes of various proxies in marine sediment deposits and artificial sediment cores.

Besides these basic questions, it will be of interest to investigate the origin of Southern Hemisphere warming. Possible aspirants for Southern Hemisphere warming are the local response to Milankovitch forcing on the precessional period [Kim et al., 1998] or the result of tropical SST anomalies that transmitted from the tropical Pacific to the Antarctic region [Lea et al., 2000; Koutavas et al., 2002].

Another future objective will be to examine the role of the Southern Ocean with respect to abrupt climate change during the last glacial period. This approach seems to be promising, since a similar temporal shape as for the B/A onset is detected at other abrupt stadial (cold) to interstadial (warm) transitions, named Dansgaard-Oeschger (DO) events of the last glacial period [Dansgaard et al., 1984]. A Southern Hemisphere trigger for DO events might represent an alternative theory to the approach that climate changes in the Northern Hemisphere trigger a response in the Southern Hemisphere. Model experiments [Toggweiler and Samuels, 1995; Knorr and Lohmann, 2003b; Weaver et al., 2003] and ocean sediment-core data [Ninnemann and Charles, 2002; Peeters et al., 2004] suggest that different processes in the Southern Hemisphere might have generated changes in the THC. These include changes in the strength of westerly winds and the circumpolar current; changes in Southern Ocean density structure; and gradual warming and receding sea-ice cover around Antarctica that increased the mass transport into the South Atlantic via the warm (Indian Ocean) and cold water route (Pacific Ocean) of the ocean conveyor belt circulation. So far, the notion of a Southern Hemisphere trigger for climate changes is an interesting theory that lacks a conceptual model able to explain all the observations from Antarctica and Greenland [Dokken and Nisancioglu, 2004]. At present the necessary data from the northern and southern

oceans are missing to put paleoceanographic constraints on the past history of THC shifts from a Southern Ocean perspective.

To address these questions in the future, investigations should be performed utilizing more comprehensive approaches with fully coupled atmosphere-ocean, vegetation and sea ice compartments. Several climate models now also incorporate continental ice sheets, and such models can reproduce irregular ice sheet surges. However, the interactions of the ice sheet with shelf ice and the ocean are currently only included in regional and process models, but not in global climate models. Hence these models do not yet contain the mechanism for triggering and/or synchronizing ice sheet surges via sea level changes. Another limitation is that the location, timing and amplitude of melt water events are still poorly known, despite their importance for the response of the ocean circulation and, hence the climate record in the high latitudes.

Although recently the focus has moved away from the North Atlantic to consider the influence of other regions on global climatic change more high-resolution climate reconstructions from the Southern Hemisphere are required to make more progress toward a unified view of the climate system.

References:

Alley, R. B., and P. U. Clark (1999), The deglaciation of the northern hemisphere: A global perspective, *Annual Review of Earth and Planetary Sciences*, 27, 149-182.

Bender, M., T. Sowers, and E. Brook (1997), Gases in ice cores, *Proceedings of the National Academy of Sciences of the United States of America*, 94, 8343-8349.

Berger, W. H., and G. Wefer, *Expeditions into the Past: Paleoceanographic Studies in the South Atlantic*, 644 pp., Springer-Verlag, Berlin Heidelberg, 1996.

Brathauer, U., and A. Abelmann (1999), Late Quaternary variations in sea surface temperatures and their relationship to orbital forcing recorded in the Southern Ocean (Atlantic sector), *Paleoceanography*, 14, 135-148.

Broecker, W. S. (1991), The great ocean conveyor, *Oceanography*, 4, 79-89.

Broecker, W. S. (1997), Thermohaline circulation, the Achilles heel of our climate system: will man-made CO_2 upset the current balance?, *Science*, 278, 1582-1588.

Brünning, R., and G. Lohmann (1999), Charles S. Peirce on creative metaphor: A case study of the conveyor belt metaphor in Oceanography. Special Issue for Scientific Discovery and Creativity., *Foundations of Science*, 4, 389-403.

Chappell, J. (2002), Sea level changes forced ice breakouts in the last glacial cycle: new results from coral terraces, *Quaternary Science Reviews*, 21, 1229-1240.

Clark, P. U., J. X. Mitrovica, G. A. Milne, and M. E. Tamisiea (2002), Sea-level fingerprinting as a direct test for the source of global meltwater pulse IA, *Science*, 295, 2438-2441.

Claussen, M., L. A. Mysak, A. J. Weaver, M. Crucifix, T. Fichefet, M. F. Loutre, S. L. Weber, J. Alcamo, V. A. Alexeev, A. Berger, R. Calov, A. Ganopolski, H. Goosse, G. Lohmann, F. Lunkeit, Mokhov, II, V. Petoukhov, P. Stone, and Z. Wang (2002), Earth system models of intermediate complexity: closing the gap in the spectrum of climate system models, *Climate Dynamics*, 18, 579-586.

Dansgaard, W., S. J. Johnsen, H. B. Clausen, D. Dahl-Jensen, N. Gundestrup, C. U. Hammer, and H. Oeschger, North Atlantic climatic oscillations revealed by deep Greenland ice cores. in *Climate Processes and Climate Sensitivity*, edited by Hansen, J. E. and T. Takahashi, pp. 288-298, Am. Geophys. Union, Washington, 1984.

Dokken, T. M., and K. H. Nisancioglu (2004), Fresh angle on the polar seesaw, *Nature*, 430, 842-843.

Fraedrich, K., E. Kirk, and F. Lunkeit (1998), Portable University Model of the Atmosphere. Deutsches Klimarechenzentrum, *Technical Report*, 16, 37 pp.

Fraedrich, K., E. Kirk, U. Luksch, and F. Lunkeit (2003), Ein Zirkulationsmodell für Forschung und Lehre, *Promet*, 29, 34-48.

Fraedrich, K., H. Jansen, E. Kirk, A. Kleidon, U. Luksch, and F. Lunkeit (2005), The Planet Simulator: Model description and application, *Meteorologische Zeitschrift*, submitted.

Ganopolski, A., and S. Rahmstorf (2001), Rapid changes of glacial climate simulated in a coupled climate model, *Nature*, 409, 153-158.

Gersonde, R., A. Abelmann, U. Brathauer, S. Becquey, C. Bianchi, G. Cortese, H. Grobe, G. Kuhn, H. S. Niebler, M. Segl, R. Sieger, U. Zielinski, and D. K. Fütterer (2003), Last glacial sea surface temperatures and sea-ice extent in the Southern Ocean (Atlantic-Indian sector): A multi proxy approach, *Paleoceanography*, 18, doi: 10.10292002PA10000808.

Gordon, A. L. (1986), Inter-Ocean Exchange of Thermocline Water, *Journal of Geophysical Research-Oceans*, 91, 5037-5046.

Gordon, A. L., R. F. Weiss, W. M. Smethie, and M. J. Warner (1992), Thermocline and Intermediate Water Communication between the South-Atlantic and Indian Oceans, *Journal of Geophysical Research-Oceans*, 97, 7223-7240.

Kim, S. J., T. J. Crowley, and A. Stössel (1998), Local orbital forcing of Antarctic climate change during the last interglacial, *Science*, 280, 728-730.

Knorr, G., and G. Lohmann (2003a), Interhemisphärische Telekonnektionen der atlantischen thermohalinen Zirkulation: Evidenzen von Daten und Ozeanmodellen, *Terra Nostra*, 2003/6, 250-254.

Knorr, G., and G. Lohmann (2003b), Southern Ocean Origin for the resumption of Atlantic thermohaline circulation during deglaciation, *Nature*, 424, 532-536.

Knorr, G., and G. Lohmann (2004), The Southern Ocean as the Flywheel of the Oceanic Conveyor Belt Circulation, *Pages News*, 12, 11-13.

Knorr, G., K. Grosfeld, G. Lohmann, F. Lunkeit, and K. Fraedrich (2005a), Atmospheric responses to abrupt changes in the thermohaline circulation during deglaciation, *Geochemistry Geophysics Geosystems*, accepted.

Knorr, G., and G. Lohmann (2005), Transitions in the Atlantic thermohaline circulation by global deglacial warming and meltwater pulses, *Paleoceanography*, submitted.

Knorr, G., G. Lohmann, and M. Prange (2005b), Interhemispheric teleconnections of the Atlantic thermohaline circulation: views obtained from a conceptual and an ocean general circulation model, *Climate Dynamics*, in preparation.

Koutavas, A., J. Lynch-Stieglitz, T. M. Marchitto, and J. P. Sachs (2002), El Ninio-like pattern in ice age tropical Pacific sea surface temperature, *Science*, 297, 226-230.

Lea, D. W., D. K. Pak, and H. J. Spero (2000), Climate impact of late Quaternary equatorial Pacific sea surface temperature variations, *Science*, 289, 1719-1724.

Lohmann, G., M. Butzin, K. Grosfeld, G. Knorr, A. Paul, M. Prange, V. Romanova, and S. Schubert (2003), The Bremen Earth System Model of Intermediate Complexity (BREMIC) designed for long-term climate studies, Model description, climatology, and applications, *Technical Report*, University Bremen.

Lutjeharms, J. R. E. (1981), Spatial scales and intensities of circulation in the ocean areas adjacent to South Africa, *Deep Sea Research Part A*, 28, 1289-1302.

Maier-Reimer, E., U. Mikolajewicz, and K. Hasselmann (1993), Mean Circulation of the Hamburg LSG OGCM and its Sensitivity to the Thermohaline Surface Forcing, *Journal of Physical Oceanography*, 23, 731-757.

Manabe, S., and R. J. Stouffer (1993), Century-scale effects of increased atmospheric CO_2 on the ocean-atmosphere system, *Nature*, 364, 215-218.

Marshall, S. J., and G. K. C. Clarke (1999), Modeling North Atlantic freshwater runoff through the last glacial cycle, *Quaternary Research*.

McManus, J. F., R. Francois, J. M. Gherardi, L. D. Keigwin, and S. Brown-Leger (2004), Collapse and rapid resumption of Atlantic meridional circulation linked to deglacial climate changes, *Nature*, 428, 834-837.

Mikolajewicz, U. (1998), Effect of meltwater input from the Antarctic ice sheet on the thermohaline circulation, *Annals of Glaciology*, 27, 311-316.

Ninnemann, U., and C. D. Charles (2002), Changes in the mode of Southern Ocean circulation over the last glacial cycle revealed by foraminiferal stable isotopic variability, *Earth and Planetary Science Letters*, 201, 383-396.

Paul, A., and C. Schäfer-Neht (2003), Modeling the water masses of the Atlantic Ocean at the Last Glacial Maximum, *Paleoceanography*, 18, doi: 10.1029/20027PA000783.

Peeters, F. J. C., R. Acheson, G. J. A. Brummer, W. de Ruijter, R. R. Schneider, G. Ganssen, E. Ufkes, and D. Kroon (2004), Vigorous exchange between the Indian and Atlantic oceans at the end of the past five glacial periods, *Nature*, 430, 661-665.

Petit, J. R., J. Jouzel, D. Raynaud, N. I. Barkov, J. M. Barnola, I. Basile, M. Bender, J. Chappellaz, M. Davis, G. Delaygue, M. Delmotte, V. M. Kotlyakov, M. Legrand, V. Y. Lipenkov, C. Lorius, L. Pepin, C. Ritz, E. Saltzman, and M. Stievenard (1999), Climate and atmospheric history of the past 420,000 years from the Vostok ice core, Antarctica, *Nature*, 399, 429-436.

Piotrowski, A. M., S. L. Goldstein, S. R. Hemming, and R. G. Fairbanks (2004), Intensification and variability of ocean thermohaline circulation through the last deglaciation, *Earth and Planetary Science Letters*, 225, 205-220.

Prange, M., V. Romanova, and G. Lohmann (2002), The glacial thermohaline circulation: Stable or unstable?, *Geophysical Research Letters*, 29, 2028, doi:2010.1029/2002LH015337.

Rohling, E. J., R. Marsh, N. C. Wells, M. Sidall, and N. R. Edwards (2004), Similar meltwater contributions to glacial sea level changes from Antarctic and northern ice sheest, *Nature*, 430, 1016-1021.

Sarnthein, M., K. Winn, S. J. A. Jung, J. C. Duplessy, L. Labeyrie, H. Erlenkeuser, and G. Ganssen (1994), Changes in East Atlantic Deep-Water Circulation over the Last 30,000 Years - 8 Time Slice Reconstructions, *Paleoceanography*, 9, 209-267.

Schouten, M. W., W. de Ruijter, and P. J. van Leeuwen (2002), Upstream control of Agulhas Ring shedding, *Journal of Geophysical Research*, 107, 1707-1721.

Severinghaus, J. P., T. Sowers, E. J. Brook, R. B. Alley, and M. L. Bender (1998), Timing of abrupt climate change at the end of the Younger Dryas interval from thermally fractionated gases in polar ice, *Nature*, 391, 141-146.

Severinghaus, J. P., and E. J. Brook (1999), Abrupt climate change at the end of the last glacial period inferred from trapped air in polar ice, *Science*, 286, 930-934.

Stocker, T. F., and A. Schmittner (1997), Influence of CO_2 emission rates on the stability of the thermohaline circulation, *Nature*, 388, 862-865.

Stommel, H. (1961), Thermohaline convection with two stable regimes of flow, *Tellus*, 13, 224-230.

Toggweiler, J. R., and B. Samuels (1995), Effect of Drake Passage on the global thermohaline circulation, *Deep-Sea Research I*, 42, 477-500.

Weaver, A. J., O. A. Saenko, P. U. Clark, and J. X. Mitrovica (2003), Meltwater pulse 1A from Antarctica as a trigger of the Bølling-Allerød warm interval, *Science*, 299, 1709-1713.

Danksagung

Zum Gelingen der Arbeit haben viele Kollegen und Freunde beigetragen.

Insbesondere möchte ich mich bedanken bei:

Herrn Prof. Dr. Gerrit Lohmann für das spannende Thema und die Betreuung während meiner Arbeit. Sein Vertrauen, die persönliche Unterstützung und konkrete wissenschaftliche Beratung in schweren Phasen kombiniert mit einer großen Freiheit in wissenschaftlicher Ausrichtung und Arbeitsweise, haben die Zusammenarbeit geprägt und entscheidend zum Erfolg der Arbeit beigetragen. Danke für die gemeinsame Zeit!

Herrn Prof. Dr. Klaus Fraedrich danke ich für sein Interesse an meiner Arbeit und seine Bereitschaft, die Begutachtung der Dissertation zu übernehmen. Außerdem möchte ich ihm dafür danken, dass ich in der theoretischen Meteorologie ein sehr kreatives und angenehmes Arbeitsumfeld erleben durfte.

Herrn Prof. Kay-Christian Emeis, Dr. Frank Lunkeit und Dr. Joachim Segschneider danke ich für die Teilnahme im Prüfungsausschuss. Herrn Prof. Dr. Thomas Stocker danke ich für die Erstellung eines externen Gutachtens. Den Mitarbeitern der theoretischen Abteilung des Meteorologischen Instituts möchte ich für viele Anregungen und die Unterstützung in technischen Fragen danken. Simon Blessing und Torben Kunz danke ich für humorvolle Gesellschaft und die Bereitschaft zu kritischer Diskussion. Nicht zuletzt möchte ich meinen Freunden für ihr Interesse, ihr Verständnis und die Unterstützung danken. Ganz besonderer Dank gilt meiner Familie.

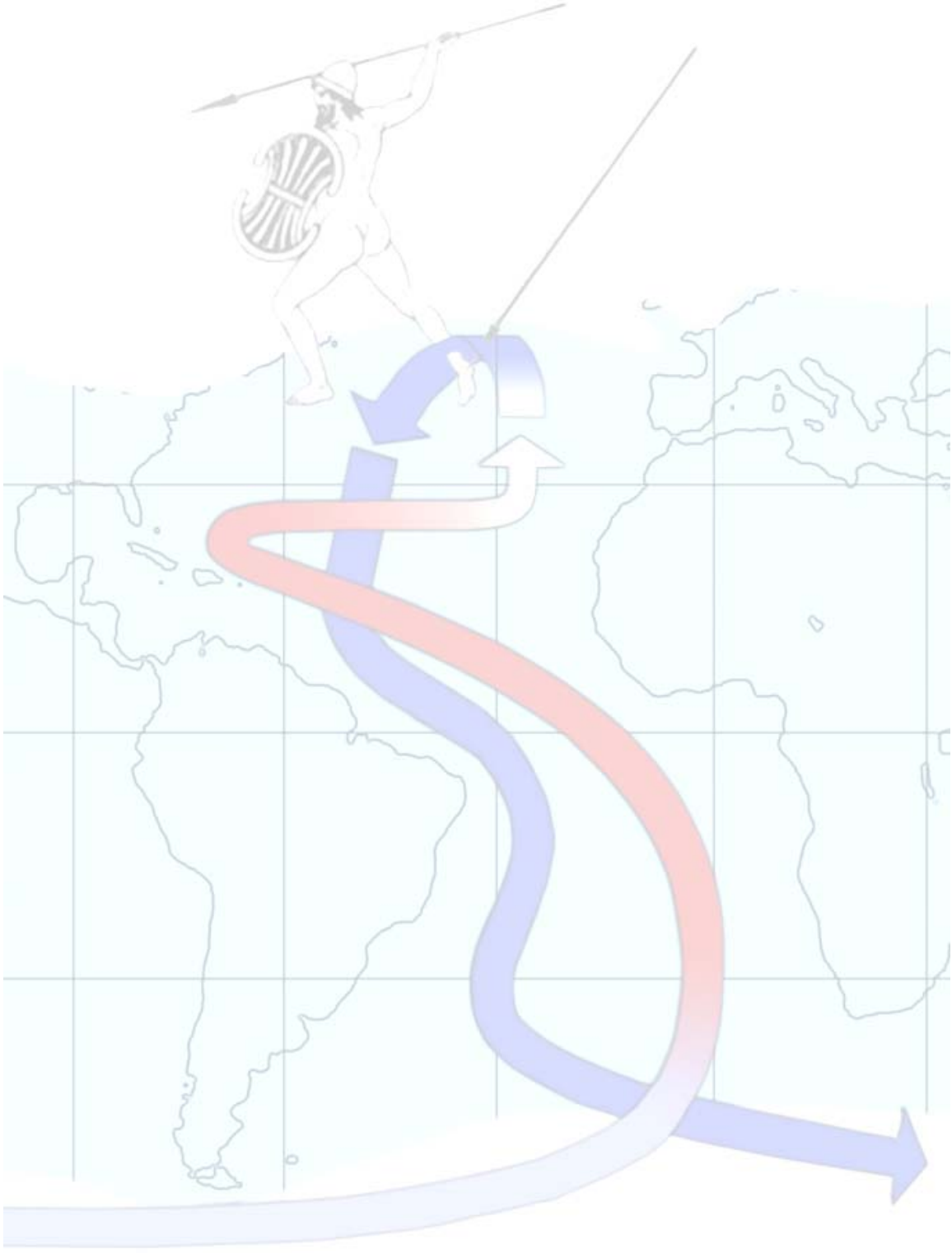

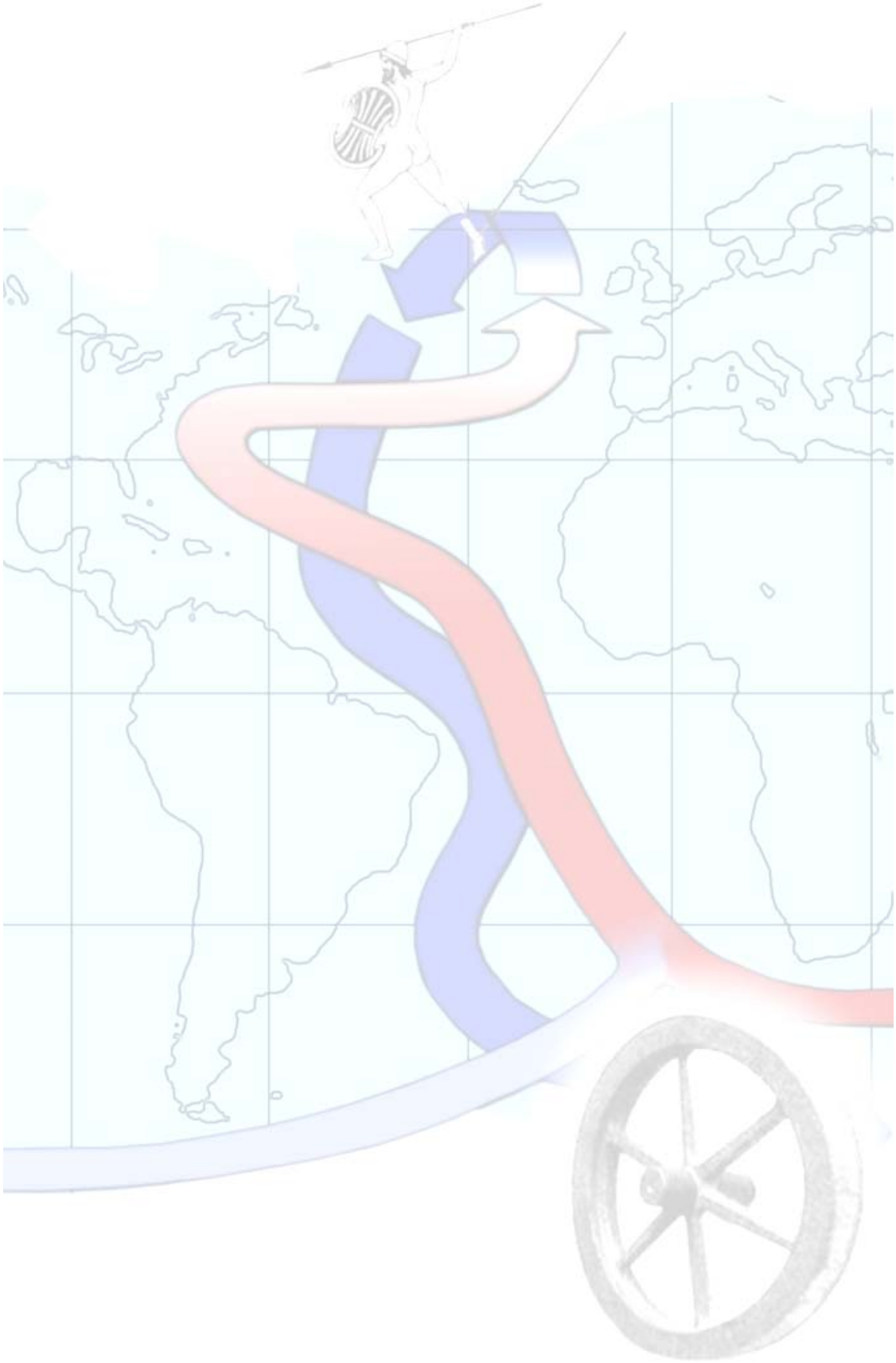

Graphic designed by Lisa Könnecke.